

2016

Hapln1a-ECM mediates Cx43 dependent skeletal phenotypes during zebrafish fin regeneration

Jayalakshmi Govindan
Lehigh University

Follow this and additional works at: <http://preserve.lehigh.edu/etd>



Part of the [Molecular Biology Commons](#)

Recommended Citation

Govindan, Jayalakshmi, "Hapln1a-ECM mediates Cx43 dependent skeletal phenotypes during zebrafish fin regeneration" (2016).
Theses and Dissertations. 2612.
<http://preserve.lehigh.edu/etd/2612>

This Dissertation is brought to you for free and open access by Lehigh Preserve. It has been accepted for inclusion in Theses and Dissertations by an authorized administrator of Lehigh Preserve. For more information, please contact preserve@lehigh.edu.

Hapln1a-ECM mediates Cx43 dependent skeletal phenotypes during
zebrafish fin regeneration

by

Jayalakshmi Govindan

A Dissertation

Presented to the Graduate and Research Committee

of Lehigh University

in Candidacy for the Degree of

Doctor of Philosophy

in

Cell and Molecular Biology

Lehigh University

January 2016

Copyright © 2015

Jayalakshmi Govindan

Approved and recommended for acceptance as a dissertation in partial fulfillment of the requirements for the degree of Doctor of Philosophy

Jayalakshmi Govindan

Hapln1a-ECM mediates Cx43 dependent skeletal phenotypes during zebrafish fin regeneration.

08/18/2015

Defense Date

Approved Date

M. Kathryn Iovine, Ph.D.
(Dissertation Director)

Committee Members

Michael R. Kuchka, Ph.D.

Lynne Cassimeris, Ph.D.

Linda J. Lowe-Krentz, Ph.D.

Caroline N. Dealy, Ph.D.

ACKNOWLEDGEMENTS

It is a humbling experience to acknowledge those people who have helped along the journey of my PhD. I am indebted to so many for their encouragement and support. First, I would like to extend my deepest and sincere gratitude to my mentor and thesis advisor, Dr. Kathy Iovine for letting me to complete my doctoral research in her lab. I don't have enough words to thank her for immediately accepting me as her student without any hesitation when I had to suddenly switch labs in the midst of my graduate career. She did not even take a few moments before saying a "yes", when I approached her to accept me into her lab. This belief that she had in me has been my greatest motivation to pursue my degree after the unexpected twist of events. She has always given her time, ideas and continuous focus to push forward and advance our shared research goals. This dissertation has been possible only because of her constant encouragement, guidance and her enthusiasm and excitement for science. Apart from being my research mentor, she has been a very approachable person, and has always been there when I needed her. For being a wonderful mentor and for many other personal reasons...., thank you so much Kathy!

I am grateful to my committee members, Dr. Caroline Dealy, Dr. Linda J. Lowe-Krentz, Dr. Lynne Cassimeris and Dr. Michael Kuchka for their continued support, suggestions and honest critiques over the past few years. Thank you all, for providing me with proper guidance for the successful completion of my doctorate degree. Thankyou Dr. Dealy for sharing some of your lab protocols; especially, the antigen retrieval protocol has helped all our lab members. Thank you Dr. Cassimeris and Dr. Lowe-Krentz and Dr. Kuchka for providing me with constructive feedback after every single presentation, which has always helped me to improve and become a better researcher.

Also, I would like to extend my special thanks and deepest gratitude to Dr. Kuchka. He is a great example of a dedicated teacher and I thoroughly enjoyed his discussion class on Molecular genetics and I feel lucky to have had that opportunity. Another instance that I enjoyed, learned and can never forget is the period during which I worked as his teaching assistant for the molecular genetics lab course. He is an extremely professional yet an approachable person and “What else can I say Dr. Kuchka, if there is something that I am going to miss terribly after graduating from Lehigh, that would be our daily basis non-science talks, exchanging and sharing life experiences in your office during my coffee breaks, that has always refreshed my mind”. And most of all thank you Dr. Kuchka for always caring, encouraging, and believing in me.

I would also like to thank Dr. Vassie Ware for her support throughout my graduate career. My experience in her lab as a rotation student was wonderful. Personally, she has been a great inspiration to me. Her energy, motivation, and her commitment to her profession and family cannot be expressed through words and she has been a great example to me in several ways.

I would like to thank the Department of Biological Sciences and all the faculty members for providing a wonderful and challenging environment and their dedication and commitment to research and graduate education. Special thanks to Dr. Falk and his lab members for sharing reagents and letting me to use their “EndNote” software whenever needed. My sincere thanks to Vicki Ruggiero and Heather Sohara for their administrative support and Maria Brace for her technical assistance and many other help that has facilitated my study. My sincere thanks to Lee Graham for always being there to provide assistance with instrumental facilities. He has saved my experiments several times and his readiness to help any day, any time is beyond admirable.

A special thanks to past Lehigh members, Dr. Michael Kearse, Dr. Joe Comber, Dr. Soumya Rudra, and Dr. Christina Sie for their support inside and outside of the lab and have always offered input and advice. Mike and Joe, your tremendous support and your willingness to share your knowledge and experience during my initial days at Lehigh will always be appreciated. I would also like to thank Dr. Amy Camp for her mentorship during my time in her lab and Dr. Jutta Marzillier for her encouragement and support.

A big thank you note to all the students of Biological Sciences Department for contributing to a very helpful, collaborative and a happy environment. I would also like to thank Tia Kowal, Rachael Andrews, Charles Fischer, Brett Gershman, Catherine Mageeney, Jessica Leung, Sara Lynn Farwell and Michael McQuillan for their friendship and support. A special thanks to Jeremy Brozek for his friendship, for the many shared coffee breaks, contagious excitement and enthusiasm for nature and science, for scientific input, for exchanging information about our cultures and for temporarily sharing some of his pets with my daughter. I wish good luck to all the graduate students with their future endeavors.

My sincere thanks to all the present and past members of the Iovine lab. Success in a program is not possible without a supportive, encouraging and a peaceful work atmosphere and I would like to thank Joyita Bhadra, Rajeswari Banerji, and Rebecca Bowman for providing that. I would also like to thank the undergraduates Francesca Oniyuke, Kyaw Min Tun, Samuel Flores, Harneel Riar and Jasmine Singh for contributing to advance my research work. My sincere thanks to the past members Dr. Quynh Ton and Dr. Diane Jones for helping me get started in the lab.

Over the years I have been privileged to get to know a number of amazing people. A special acknowledgement to my friend Balaji Raj, whom I have known for more than 15 years. Thank you for all your support, encouragement, care and relentless help with editing whenever

I asked for it and for making me think by asking several questions about my research. I have always enjoyed our science conversations. I would like to extend my thanks to my best friend Cynthia for her continued support throughout my time at Lehigh. More than getting a degree, I am feeling happy and grateful for getting a lifetime friend. My heartfelt gratitude to my wonderful friend Ashok Manicka Kumar and I am always indebted to his unrelenting support for listening to anything that I said without complaining and always being there to discuss any issues and supporting me through my difficult times and instilling enthusiasm in me whenever I lacked it. My sincere thanks to my childhood friend Anupama, Amudha and my cousin Manju for their moral support and always having faith in my abilities. I would like to thank my family friends in NJ (Shanmuga Priya, Lakshmi, Rathi, Shylaja, Dhanashree, Kalpana, Gayathri, Lavanya and Radhika) who have become an important part of my life after my coming to US and I cannot imagine a social life without you all. Thank you for all the support you have shown to me and my family over the past 9 years and I am extremely excited to return to NJ.

To my family, I am grateful to my parents Ananthalakshmi and Govindan for encouraging me in all of my pursuits and inspiring me to follow my dreams. My mom has always provided us with a loving, caring and nurturing environment and my father has been a role model in several ways and especially showing what hard work means. Together they have instilled in me high personal and moral values and they knew it would be a long and sometimes bumpy road, but nevertheless always encouraged and supported me along the way. Their unlimited best wishes and everything that they have done for me, I cannot ask for anything more. Special thanks to my late grandmother Balalakshmi for her unconditional support and love and providing me with everlasting childhood memories. Everything happens for a reason and I am lucky enough to have my sister next to me in this country and my brother in Canada. I would like to thank my beautiful and amazing sister Priya and my brother in-law Sathish for

their support and for introducing Lehigh University to me when I was planning on getting back into grad school. Without them I might have missed this awesome place. I would like to thank my brother Radhakrishnan and my sister in-law Thamaraiselvi for their constant support and always being there with a word of encouragement or listening ear. My sincere thanks to my in-laws, Maheshwari, Anantharaman, Sangeetha, Madhan, Harikrishnan and Mangai for happily accepting me into their family and for supporting and reassuring me that everything will be fine.

To my loving daughter Priyanka, who has made my life meaningful and she has been the life's best teacher and made me realize what true happiness is all about. I started when she was 3 years old and she will be turning 8 in a few months and I can't believe how fast time can fly. Having my daughter before starting my PhD, has made me a pro with my organizational skills and time management and I am thankful for that. I love her more than anything and I appreciate all her patience and support during mommy's PhD.

To my loving husband Narayanan, whose unconditional love, patience, and continual support of my academic endeavors over the past several years have enabled me to complete this thesis. He has sacrificed a lot in several ways and especially career wise to help me achieve my career goals. Getting back into school after a break of 7 years in itself was hard and that too with a kid was even tougher, but it has become possible for me, only because of him and his sincere support for the past years and sharing all the responsibilities. During all my tough times he has been there beside me, to remind me of what is more important in life and enjoy the present moment. I am thankful for everything that he has done for me and I am sure future has many wonderful things in store for us to explore together.

Last but not least, to, all the unmentioned people whom I know have helped me at some point of my life; I may not have mentioned their names, but my sincere and heartfelt thanks for all the timely help.

Table of contents

Acknowledgements	iv
Table of contents	ix
List of figures	xi
List of tables	xiii
List of abbreviations	xiv
Abstract	1
Chapter 1: Introduction	4
1.1 Zebrafish– A versatile model for tissue and skeletal regeneration studies	5
1.2 The zebrafish caudal fin as a model for skeletal morphogenesis	6
1.3 Epimorphic regeneration is facilitated by the formation of blastema	9
1.4 Cx43 function during skeletal development is conserved across species	14
1.5 Cx43 activity coordinately regulates cell proliferation and joint formation during zebrafish fin regeneration	16
1.6 Research objectives and Hypotheses	17
1.7 Figures	22
1.8 References	33
Chapter 2: Hapln1a is required for Connexin43-dependent growth and patterning in the regenerating fin skeleton	43
2.1 Abstract	44
2.2 Introduction	45
2.3 Materials and Methods	48
2.4 Results	56
2.5 Discussion	62
2.6 Conclusion	65
2.7 Figures	66
2.8 Tables	77
2.9 References	79

Chapter 3: Cx43-dependent skeletal phenotypes are mediated by interactions between the Hapln1a-ECM and Sema3d during fin regeneration	
3.1 Abstract	88
3.2 Introduction	89
3.3 Materials and Methods	92
3.4 Results	102
3.5 Discussion	111
3.6 Figures	116
3.7 Tables	130
3.8 References	131
Chapter 4: Dynamic remodeling of the extra cellular matrix during zebrafish fin regeneration	141
4.1 Abstract	142
4.2 Introduction	142
4.3 Materials and Methods	145
4.4 Results and Discussion	150
4.5 Conclusion	160
4.6 Figures	161
4.7 References	166
Chapter 5: Future directions and Conclusions	176
5.1 Summary	177
5.2 Future directions	179
5.3 Figures	191
5.4 References	194
Curriculum vitae	203

LIST OF FIGURES

- 1.1 The zebrafish fin is a model system for skeletal morphogenesis.
- 1.2 The histological organization of an uninjured and regenerating caudal fin.
- 1.3 The regeneration process of the caudal fin in zebrafish.
- 1.4 Fin length mutants exhibit defects in skeletal morphogenesis.
- 1.5 *cx43* mRNA is detected by *in situ* hybridization.
- 1.6 The *alf^{dy86}* mutant phenotype before and after the rescue.
- 1.7 Model showing Cx43-Sema3d influence on skeletal morphology.
- 1.8 Hapln1a in the Extracellular matrix.
- 1.9 Defining Hapln1a-ECM.
- 2.1 Validation of microarray results by *in situ* hybridization using whole mount *in situ* hybridization on 5 dpa regenerating fins.
- 2.2 Cx43 knock down results in reduced expression levels of *hapln1a*.
- 2.3 *hapln1a* expression pattern at different time points in regenerating fin.
- 2.4 Morpholino mediated knock-down of *hapln1a* recapitulates all *cx43*-dependent phenotypes.
- 2.5 Morpholino mediated knock-down of *hapln1a* in WT regenerating fins results in reduced Hapln1a.
- 2.6 Morpholino mediated knock-down of *hapln1a* in WT regenerating fins results in reduced HA levels.
- 2.7 HA levels are reduced in *sof^{b123}* and in *cx43*-KD regenerating fins.
- 2.8 Hapln1a knock-down does not rescue segment length in *alf^{dy86}*.

- 2.9 The *hapln1a*-KD was effective in *alf^{dy86}*.
- 2.10 Model depicting Cx43-Hapln1a mediated effect on skeletal patterning during fin regeneration.
- 3.1 Whole mount in situ hybridization showing the expression of Hapln1a-ECM components on 5 dpa regenerating fins.
- 3.2 Morpholino mediated knockdown of *has1* and *has2* results in reduced HA.
- 3.3 Reduced HA contributes to Hapln1a knockdown phenotypes.
- 3.4 Morpholino mediated knockdown of *hapln1a* results in reduced Acan protein levels.
- 3.5 Vcan protein levels are unchanged following MO mediated knockdown of *hapln1a*.
- 3.6 Reduced Acan contributes to Hapln1a knockdown phenotypes.
- 3.7 Hapln1a and Sema3d interact genetically to mediate Cx43 phenotypes.
- 3.8 Morpholino mediated knockdown of *hapln1a* results in reduced Sema3d protein levels.
- 3.9 Heat shock induces upregulation of *sema3d* mRNA and Sema3d protein in *Tg(hsp70:sema3d-gfp)*.
- 3.10 Sema3d overexpression rescues *hapln1a* knockdown phenotypes.
- 3.11 Hapln1a and Sema3d function in a common pathway to mediate Cx43 function during fin regeneration.
- 4.1 Cartoon of a longitudinal section illustrating the different compartments in a regenerating fin ray.

- 4.2 Immunostaining and histochemistry for Hapln1a-ECM components during the time course of regeneration.
- 4.3 Immunostaining for TNC, FN and LAM during the time course of regeneration.
- 5.1 Double knockdown of *has2* and *acanb* contribute to Hapln1a phenotypes.
- 5.2 ISH for *rhamm*
- 5.3 ISH for *sox9a* and *sox9b*

LIST OF TABLES

- 2.1 Primers and Morpholinos
- 2.2 Quantitative RT-PCR confirms changes in gene expression
- 3.1 Primer and Morpholino Sequence

LIST OF ABBREVIATIONS

Acan	Aggrecan
<i>alf^{dy86}</i>	<i>another long fin</i>
BLE	Basal layer of epithelium
BMP	Bone morphogenetic protein
β ME	Beta- mercaptoethanol (2- mercaptoethanol)
BSA	Bovine serum albumin
cDNA	Complementary deoxyribonucleic acid
<i>cmd</i>	<i>cartilage matrix deficiency</i>
<i>col</i>	<i>collagen</i>
CRTL1	Cartilage Link Protein 1
Cx	Connexin
DAPI	4', 6-diamidino-2-phenylindole
DIG	Digoxigenin
Dpa	Days post amputation
Dpe	Days post electroporation
ECM	Extracellular matrix
EDTA	Ethylenediaminetetraacetic acid
FGF	Fibroblast growth factor
FN	Fibronectin
GAG	Glycosaminoglycan
GFP	Green fluorescent protein

GJIC	Gap junction intercellular communication
H-3-P	Histone-3-phosphate
HA	Hyaluronic acid
Hapln1a	Hyaluronan and proteoglycan link protein 1a
HAS	Hyaluronic acid synthase
HEPES	4-(2-hydroxyethyl)-1-piperazineethanesulfonic acid
Hpa	Hours post amputation
HRP	Horseradish peroxidase
HS	Heat shock
HYAL	Hyaluronidase
Hyb	Hybridization solution
<i>ihh</i>	<i>indian hedgehog</i>
KD	Knockdown
KDa	Kilo Daltons
LAM	Laminin
LP	Link protein
MABT	Maleic acid buffer with tween 20 solution
MM	Mismatch
MMP	Matrix metallo protease
MO	Morpholino
mRNA	Messenger ribonucleic acid
μg	Microgram

μL	Microliter
μm	Micrometer
μM	Micromolar
NBT/BCIP	Nitro-blue tetrazolium/5-bromo-4-chloro-3'-indolyphosphate
Nrp2a	Neuropilin2a
ODDD	Oculodentaldigital dysplasia
PBS	Phosphate buffered saline
PBST	Phosphate buffered tween 20 saline
PCR	Polymerase chain reaction
PFA	Paraformaldehyde
PG	Proteoglycan
PI	Propidium iodide
PlexA3	PlexinA3
qRT-PCR	Quantitative Real time polymerase chain reaction
RA	Retinoic acid
RHAMM	Receptor for hyaluronan mediated motility
RNA	Ribonucleic acid
rRNA	Ribosomal RNA
SDS	Sodium dodecyl sulphate
<i>sema3d</i>	<i>semaphorin3d</i>
<i>shh</i>	<i>sonic hedgehog</i>

sof^{b123}

SPC

SSC

TNC

tRNA

Vcan

wnt

short fin

Skeletal precursor cell

Saline sodium citrate solution

Tenascin C

Transfer RNA

Versican

wingless

ABSTRACT

Skeletal development is a tightly regulated process and requires proper communication between the cells for efficient exchange of information. Cell–cell communication, facilitating the exchange of small metabolites, ions and second messengers, takes place via aqueous proteinaceous channels called gap junctions. Connexins (Cx) are the subunits of a gap junction channel, and Cx43 is the major Cx expressed in bone cells. Mutations in human and mouse Cx43 result in a severe skeletal disorder called oculodentaldigital dysplasia (ODDD) characterized by craniofacial abnormalities and limb deformities. Mutations in zebrafish *cx43* produces the *short fin (sof^{b123})* phenotype and is characterized by short fins due to reduced segment length of the bony fin rays and reduced cell proliferation. The mechanism by which *CX43*-based mutations cause skeletal defect phenotypes is largely unknown. However, it is apparent that the function of Cx43 in the vertebrate skeleton is conserved. Hence, it is important to understand the role of Cx43 during skeletal development.

The zebrafish caudal fin is an excellent model for studying bone/skeletal morphogenesis during fin regeneration for several reasons. The fin has a simple architecture with few tissue types. The bony fin rays made up of joints and segments are clearly visible, allowing for easy genetic manipulation, and the fin can completely regenerate within 2 weeks after amputation. An important, yet poorly understood, question with respect to mutations in *connexin* genes, in general, is how does gap-junctional intercellular communication (GJIC) impact tangible cellular events like cell division and differentiation? One hypothesis is that Cx43-based GJIC can influence

gene expression patterns. Our lab exploited the availability of the two mutants, *sof*^{b123} and *alf*^{dy86}, in order to identify those genes whose expression depends on Cx43. Previously established results from our lab using the fin mutants demonstrate that Cx43 plays a dual role, regulating both cell proliferation (growth) and joint formation (patterning) during the process of skeletal morphogenesis. Thus, we utilized a novel microarray strategy to identify a set of candidate genes, which are both downregulated in *sof*^{b123} and upregulated in *alf*^{dy86}. Hapln1a (Hyaluronan and Proteoglycan Link Protein 1a) is one among the several genes identified by the microarray analysis.

The focus of this thesis was to elucidate the role and mechanism of Hapln1a in mediating Cx43 function during skeletal development in the regenerating zebrafish fin. Hapln1a belongs to the family of link proteins that play an important role in stabilizing the extracellular matrix (ECM) by linking the aggregates of hyaluronan (HA) and proteoglycans (PGs). In the first part of this study, we have shown that Hapln1a is molecularly and functionally downstream of Cx43, and knockdown of *hapln1a* resulted in reduced segment length, cell proliferation, and reduced HA. In the second part of the study, we have shown that besides destabilization of HA, *hapln1a* knockdown results in reduced aggrecan (Acan) and provides evidence that both HA and Acan are required for skeletal growth and patterning. Additionally, we show that the Hapln1a–ECM stabilizes the secreted growth factor Semaphorin3d (Sema3d) and Hapln1a-dependent ECM provides the required conditions for Sema3d stabilization and function. This study demonstrates the requirement for components of the Hapln1a–ECM for Sema3d signal

transduction. ECM plays a dynamic role during the process of wound healing, embryogenesis, and tissue regeneration, and in the final part of the study, we have shown that a transitional matrix analogous to the one formed during newt skeletal and heart muscle regeneration is synthesized during fin regeneration. We have demonstrated that a provisional matrix rich in hyaluronic acid, tenascin C, and fibronectin is synthesized following amputation. Additionally, we observed that the link protein Hapln1a-dependent ECM, consisting of Hapln1a, HA, and PG aggrecan, is upregulated during fin regeneration. Our findings on zebrafish fin regeneration implicates that changes in the extracellular milieu represent an evolutionarily conserved mechanism that proceeds during tissue regeneration, yet with distinct players depending on the type of tissue that is involved.

Collectively data from this dissertation provide evidence that Cx43 and Hapln1a–ECM function in a common pathway to coordinate skeletal growth and patterning. Moreover, this study provides novel insights into the mechanistic role of the ECM and, in particular, the role of Hapln1a–ECM during vertebrate skeleton regeneration that has not yet been elucidated in any other mammalian systems.

Chapter 1

Introduction

1.1 Zebrafish: A versatile model for tissue and skeletal regeneration studies

Regenerative medicine aims at developing strategies to restore tissues or organs that are damaged or lost. Unlike most animals, some species possess the remarkable capacity to regenerate body parts throughout adult life. A number of human conditions that are a result of injury, aging, and other disorders could be improved if therapies that aid tissue regeneration are made available. There are two broad approaches to the field of regenerative medicine: the first aims for stem cell based models to generate a set of differentiated cells for therapeutic applications and the second exploits the intrinsic regenerative capacity of non-mammalian models to define the molecular events that license tissue regeneration. Although there are a number of animal models such as salamanders and newts with regenerative capacity, zebrafish has emerged as a more powerful vertebrate regenerate model for a number of reasons. Some of the advantages include rapid regeneration time, large number of externally fertilized eggs, recent advances in zebrafish genetics, and the ability to transiently modify gene function during development. Zebrafish possess the remarkable capacity to regenerate their heart muscle, fin, retina, optic nerve, liver, spinal cord, and sensory nerve cells [1]. Understanding the molecular and genetic pathways that function in a coordinated fashion to accomplish regeneration in different model organisms will pave the way for understanding the shared gene networks and the underlying principle to regeneration. This in turn will accelerate the development and generation of therapeutic methods to circumvent the limitations in mammalian regenerative abilities. A number of molecular networks involved in appendage development and regeneration are conserved across

multiple species. For example, key players of the fibroblast growth factor (*fgf*) and wingless (*wnt*) family are well-defined players in human, mouse, chicken, tadpole, and fruit fly limb development and zebrafish caudal fin regeneration. Also, there is growing evidence for the conservation of morphological and molecular events among different organs within a same species. For example, *fgf* signaling [2,3], *hsp60* [3,4], *cx43* [5,6], and *notch* signaling [7] are required for proper regeneration of both heart and the fin tissue of Zebrafish.

1.2 The zebrafish caudal fin as a model for skeletal morphogenesis

The zebrafish caudal fin has several ideal properties for experimental procedures and regeneration studies. First, it is the largest external appendage located at the posterior end of the body, which makes it the most accessible for surgery and imaging. Second, in contrast to the remaining fins, it displays a bi-lobed morphology that is optimal for analysis of the differential growth rate along the medial–lateral axis. Third, the fin has some unique features compared to the amphibian limb. It exhibits a simpler anatomy, lacking certain tissues such as muscles and cartilage. Fourth, the completion of tail regeneration is rapidly and faithfully achieved within 2–4 weeks, depending on the water temperature. Finally, rays can regenerate independently of each other, providing autonomous regenerative units and multiple experimental replicates within the same appendage [8]. These powerful features render the caudal fin an ideal model system to tackle fundamental issues concerning vertebrate organ regeneration.

The zebrafish caudal fin originates predominantly from the ventral side of the larval fin. During adulthood, it remains connected to the vertebral column by bones of ventral origin, with the exception of the dorsal-most rays [9]. Anatomically, this appendage can be defined as a non-muscularized dermal fold that is stabilized by 16–18 main segmented and occasionally bifurcated bony rays spanned by soft interray tissue (Figure 1.1A). The segment length is demarcated by the intersegmental joints that are spaced approximately 240–320 μ m ranging from the distal to proximal terminus of the ray, the formation of which can be mathematically modeled [10]. The bi-lobed shape of the adult fin arises as the result of a higher number of segments in the lateral rays of the lobes compared to the medial rays of the cleft, displaying a difference of approximately four segments between the longest and the shortest ray [11]. As fish can grow during their entire lifespan, fins maintain a capacity of extending their size throughout adulthood. The growth of the fin is achieved by the sequential addition of new ray segments at the tip which, once formed, can become increasingly thicker but cannot elongate [11]. Thus, in contrast to a tetrapod limb with a constant sequence of bones, which is set up during embryogenesis, the number of ray segments increases in proportion to the growth of the animal. Each newly grown ray segment arises as a distal unit, but it acquires a proximal value as the elongation of the tail continues. The robustness of the fin fold depends predominantly on the collagenous bone matrix called lepidotrichia, which is deposited by osteoblasts (also named scleroblasts) underneath the epidermis. The major proximal portion of the ray is supported by calcified bone matrix, while the three to four distal-most segments are thin and remain non-mineralized

(Figure 1.1C, D). The gradient of ray mineralization indicates the smooth transition between the proximal and distal portion of the appendage (Figure 1.1B). The distal-most segment of each ray lacks bone matrix at the tip. However, it is supported by a brush-like bundle of fine spicules named actinotrichia (Figure 1.1C), which are synthesized by non-osteoblasts [12,13]. It is reasonable to assume that mineralized matrix at the base and flexible structures at the tip of the appendage provide optimal architecture for the hydrodynamic function of the fin.

The ray contains two concave bones at each side of the fin fold, called hemirays. The bilateral organization of the ray can be assessed in longitudinal fin sections (Figure 1.2A). In this perspective, the pair of concave bones appears as parallel rods below the multilayered epidermis (Figure 1.2B). The lepidotrichia are tightly covered by flattened osteoblasts that deposit matrix to adjust the diameter of the bone during growth. The space between the hemirays is filled with connective tissue, which, in contrast to typical mammalian dermis, contains densely interconnected fibroblasts (Figure 1.2B). The rays are innervated and vascularized by central arteries [14]. The interrays, which separate adjacent rays, lack skeletal elements and contain veins embedded in a mesenchymal tissue with larger spacing between cells (Figure 1.2C). Taken together, fins are composed of multiple tissues, including connective tissue, lepidotrichia, actinotrichia, blood vessels, nerves, and epidermis, all of which must regenerate coordinately to restore the shape and function of the organ. Direct interactions between adjacent tissues have to be established to synchronize the regrowth and patterning.

1.3 Epimorphic regeneration is facilitated by the formation of blastema

Epimorphic regeneration is a post-traumatic morphogenetic event characterized by aggregation of mesenchymal cells at the wound site to form the blastema [15,16]. Following amputation, regeneration of adult caudal fin is completed in approximately 2 weeks (reviewed in [17]) and involves 3 main phases: (1) wound healing, (2) blastema formation, and (3) regenerative outgrowth (Figure 1.3). Following amputation, within the first day, the wound epidermis thickens and the connective tissue within a distance of approximately 150 μm from the amputation plane undergoes disorganization (Figure 1.2D) [18]. The fibroblasts of the activated mesenchyme round up, express tissue remodeling proteins, such as tenascin C, and start to proliferate [19]. The early regeneration genes are induced to set up the two key structures of the regenerate, namely a specialized wound epithelium and the blastema, with proliferating cells of mesenchymal origin. Specifically, the core of the blastema consists of a loose cluster of mesenchymal cells, while the undifferentiated osteoblasts maintain their original distribution underneath the wound epidermis, recapitulating the pattern of mature bones in the stump (Figure 1.2E–G). Accordingly, the dedifferentiated migrating osteoblasts neither invade the interray tissue nor intermingle with the mesenchymal cells of the rays. In conclusion, the histological architecture of the blastema outgrowth displays a remarkable degree of spatial histological organization that reproduces the pattern of the original structures.

The epithelial–mesenchymal interactions are fundamental to the execution of developmental and regenerative programs [20–22]. Accordingly, the wound epidermis functions not only as a physical barrier to protect the internal fin tissues, but also as an organizer of the underlying blastema. The latter function is attributed particularly to the basal layer of the wound epidermis that consists of a single row of aligned cells forming a niche-like environment for the blastema. The wound epithelium provides architectural cues and secreted factors, such as Sonic hedgehog (Shh), Wnt5b, Fgf24, to control blastema function [23–27]. However, the formation of the specialized wound epithelium is dependent on the signals from the blastema, such as Fgf20a, Sdf1, Igf2b, and retinoic acid (RA) [21, 28–31]. The inhibition of any of these signaling pathways prevents both blastema formation and wound epithelium organization. The reciprocal communication between the wound epithelium and mesenchyme is also one of the prerequisites for blastema formation in the amphibian limb [32], indicating similar principles for appendage regeneration in vertebrates.

After the establishment of the interacting wound epithelium and blastema, cell proliferation takes place very rapidly and the increase of the outgrowth size has to be immediately accompanied by pattern formation. The apical part of the outgrowth is formed by a columnar basal epithelium and the distal-most blastema, which comprises mesenchymal cells with a slow proliferative activity [18]. In situ hybridization analyses demonstrated that several genes, such as *aldh1a2*, *wnt5a*, *fgf3*, demarcate a broader extent of the distal blastema, including rapidly proliferating cells [33–36]. The proximal compartment of the blastema comprises a central cluster of rapidly proliferating

mesenchymal cells and the lateral compact layers of dedifferentiated osteoblasts that are located underneath the cuboidal basal wound epithelium. The cuboidal wound epithelium expresses a signaling protein, Shh, that could be involved in guidance of the underlying osteoblasts through the regeneration process [23,37]. Thus, the wound epithelium and the blastema display a compartmentalization already at the early outgrowth phase. It has been proposed that the apical part of the blastema acts as the upstream organizer of the regenerate through the Wnt signaling pathway, which regulates epidermal patterning, blastemal cell proliferation, and osteoblast maturation indirectly via secondary signals, such as Fgf and bone morphogenetic protein (BMP) [36]. However, the proximal compartment of the blastema has a regenerative task to maintain high cell proliferation and their progressive redifferentiation. Recently, two studies have reported that a balance between the two processes is regulated by the Notch signaling pathway [38,39]. During the outgrowth phase, the blastema becomes vascularized and innervated. Blocking angiogenesis through inhibition of vascular endothelial growth factor receptor does not impair the initial wound epidermis and blastema formation [40]. In the absence of blood supply within the regenerate, the elongation of the outgrowth is terminated at approximately 3 dpa. Although the role of innervation during blastema formation has been extensively investigated in the amphibian limb, little is known about this topic in the context of the fin.

Cell lineage tracing experiments combined with transgenic technologies in zebrafish showed that the regenerated tissues derive from pre-existing cells that retain their developmental identity during their transition in the blastema [41–44]. However,

this lineage commitment displays remarkable plasticity under certain restrictive conditions. The genetic ablation of all osteoblasts using a nitroreductase system did not prevent bone regeneration [45]. This unexpected finding reveals an impressive plasticity of the fin to activate alternative mechanisms in order to generate de novo osteoblasts. Mosaic transgene expression analysis provides no evidence for a contribution by circulating stem cells to the fin regenerate [43,45]. Thus, the new osteoblasts could derive either from putative osteoblast stem cells or through transdifferentiation of mesenchymal blastema cells into bone-forming cells. The latter explanation would involve the reactivation of developmental programs that promote osteoblast formation from the mesenchymal condensations [46]. The recapitulation of developmental processes might be dependent on the activity of the Shh and BMP signaling pathways, which have been implicated in bone regeneration [26,46]. Further studies are needed to understand the mechanisms controlling bone regeneration under normal and specific circumstances.

The factors controlling fin regrowth and morphogenesis can be studied using a genetic approach in zebrafish. Several mutants have been identified that carry abnormally developed fins, some of which also display regeneration defects [26,47]. One of these mutants, called *another long fin* (*alf^{dy86}*), attracted much attention in research due to its extraordinarily elongated fins [48]. The severity of the *alf* mutant phenotype is associated with skeletal defects of the fin, such as irregular and longer segments of the rays and misaligned joints. A lower frequency of elastic ligaments along the ray length was predicted to decrease the flexibility of the fin during swimming,

leading to incidences of bone fractures and bone dislocation [48]. The *alf* mutant locus has recently been identified as a gain-of-function mutation in *kcnk5b*, a gene encoding a two-pore domain potassium channel, which probably causes hyperpolarization of the cell [49]. The authors suggest that a coordinated ion flux may provide some cues for coordination of growth. A concept of molecular bioelectricity has already been implicated in diverse examples of regeneration, development, and oncogenesis [50]. The remaining question is how the bioelectrical signals regulate downstream cellular responses to determine positional information and to induce morphogenetic decisions such as segmental border formation. The opposite phenotype to the *alf* elongated fins is represented by another genetic mutation called *shortfin* (*sof*^{*b123*}) that causes shortened ray segments and shorter fins compared to wild type [51]. *sof* mutants exhibit a decreased expression of *cx43*, a component of gap junctions, as opposed to *alf* mutants with enhanced levels of Cx43 [48,52]. The gap junctions serve as stimuli-regulated intercellular channels for sharing small molecules, such as inorganic ions and metabolites, during development and homeostasis [53–55]. Thus, both opposing fin-size phenotypes of *alf* and *sof* mutants are associated with aberrant membrane channels involved in ion flux. A loss of Cx43 activity leads to short segments, while a gain of Cx43 activity results in longer segments. It becomes evident that the ion flux in a cluster of proliferating cells is essential to orchestrate morphogenetic decisions during development and regeneration.

1.4 Cx43 function during skeletal development is conserved across species

The focus of this dissertation is to study the underlying mechanisms for skeletal morphogenesis, using zebrafish caudal fin regeneration as a tool. We utilize the zebrafish *short fin* mutant (*sof*^{b123}) to address the role of Cx43 during skeletal development. Previous studies from our lab have shown that the mutation in zebrafish *cx43* gene causes the *short fin* (*sof*^{b123}) phenotypes characterized by short bony fin ray segments, short fins, and reduced cell proliferation. The *sof*^{b123} mutant exhibits reduced levels of *cx43* mRNA and Cx43 protein, without a lesion in the coding sequence [51].

In bone tissue, connexins play a direct role in regulating the development and modeling of matrix components. More specifically, the GJ protein, Cx43 is present in several bone cell types including chondrocytes, osteoclasts, and osteocytes [56–58]. The syndrome ODDD, characterized by abnormalities in craniofacial elements, limbs and dentition, has been linked to missense mutations in the *CX43* gene locus in humans [59]. At least 24 separate point mutations have been identified in patients with ODDD [59–61]. The *CX43* knock out (*CX43*^{-/-}) mouse dies perinatally because of cardiac malformations [62,63]. Similarly, targeted gene knock-down of *cx43* results in embryonic heart defects in zebrafish, signifying the essential role of *cx43* during development [51]. The skeletal defects seen in the *CX43*^{-/-} KO mouse model exhibited hypomineralization of craniofacial bones and severely delayed ossification of the appendicular skeleton [57]. Moreover, the ODDD phenotype is similar to a set of craniofacial abnormalities observed in the targeted *CX43* knock-down chick model

[64,65]. In zebrafish, a homozygous mutation in *cx43* causes the *short fin* phenotype, characterized by shorter tail fins due to defects in the fin skeleton (Figure 1.4). The mechanism by which *CX43*-based mutations cause skeletal defect phenotypes is largely unknown. However, it is apparent that the function of Cx43 in the vertebrate skeleton is conserved. Thus, our findings on the role of Cx43 during skeletal morphogenesis are applicable to all vertebrates.

Gap junctions play a critical role in coupling tissue function, and they have long been hypothesized to play a role in the maintenance of homeostasis, morphogenesis, cell differentiation, and growth control in multicellular organisms and during the process of skeletogenesis [66]. Gap junctions are proteinaceous channels formed by the docking of two connexons of neighboring cells and mediate the exchange of low molecular weight metabolites (<1000Da), ions and second messengers between the contacting cells. Each connexon or hemichannel is made up of connexin, a four pass transmembrane domain containing protein. The complex control of cell differentiation and synchronization of events that occur during bone development is mediated by the intercellular diffusion of signaling molecules through gap junctions. This exchange process, termed GJIC [67], occurs through channels made up of connexin proteins.

1.5 Cx43 activity coordinately regulates cell proliferation and joint formation during zebrafish fin regeneration

Skeletal morphogenesis is a complex process involving cell proliferation and differentiation that is coordinated by genetic programs that regulate the mechanisms of

differentiation, function and also their interaction with components of the ECM [68,69]. Newly synthesized bone could be formed either by endochondral ossification (involving a cartilage template) or by intramembranous ossification (without a cartilage template) in which the osteoblasts assemble and mineralize the tissue directly [70,71]. The latter mechanism occurs during zebrafish tail fin regeneration [1,15].

We were interested in revealing molecular mechanisms for role of Cx43 in bone growth. The *sof*^{b123} mutant shows reduced levels of *cx43* mRNA and Cx43 protein without any lesion in the coding sequence [51,72]. However, three additional alleles having missense mutations in the *cx43* gene also resulted in reduced *cx43* mRNA, protein levels, and reduced GJIC [52]. During the process of fin regeneration, the population of actively dividing cells in the blastema shows an upregulation of *cx43* mRNA, and the expression is observed throughout the mesenchyme [72] (Figure 1.5).

Morpholino-mediated knockdown of *cx43* in wild type regenerating fins resulted in reduced fin length, reduced segment length, and reduced cell proliferation, completely recapitulating the phenotypes observed in *sof* alleles [72]. Collectively, these data reveal that reduced levels of *cx43* mRNA or protein or GJIC cause the same set of phenotypes. Thus, any loss of Cx43 function is equivalent to loss of Cx43 activity. Given the fact that loss of Cx43 activity results in reduced cell proliferation and short segments, it is possible to argue that the reduced segment length could be an effect caused by reduced cell proliferation. However, inhibiting cell proliferation via Shh or Fgfr1 signaling pathways resulted in reduced cell proliferation and fin length but did

NOT impinge on the segment length [26,73], suggesting that reducing cell proliferation alone cannot influence segment length. Interestingly, another mutant *alf^{dy86}* exhibits long fins, overlong segments, and stochastic joint failure [47] (Figure 1.6A) that is contrasting to the phenotypes exhibited by the *sof* mutant. We have shown that *alf^{dy86}* has higher levels of *cx43* mRNA, and *cx43* knock-down in *alf^{dy86}* fins rescued the fin and segment length, suggesting that Cx43 over expression is the basis for the *alf^{dy86}* phenotypes [48] (Figure 1.6B). Based on some of the results mentioned earlier, we suggest that in addition to promoting cell proliferation, Cx43 plays an additional role in impacting the segment length by regulating the process of joint formation. Thus, Cx43 functions in more than one way, by positively influencing cell proliferation and also by suppressing joint formation, thereby concomitantly regulating bone growth and skeletal patterning during the process of fin regeneration.

1.6 Research objectives and Hypotheses

An important, yet poorly understood question with respect to mutations in *connexin* genes in general is, how does GJIC impact tangible cellular events like cell division and differentiation? One hypothesis is that Cx43-based GJIC can influence gene expression patterns [58,74]. Our lab exploited the availability of the two mutants, *sof^{b123}* and *alf^{dy86}*, to identify genes whose expression depends on Cx43. Thus, we utilized a novel microarray strategy to identify a set of candidate genes, which are both downregulated in *sof^{b123}* and upregulated in *alf^{dy86}*. To date, there are 15 genes that have been validated to have cx43-dependent functions. Among the 15 genes, the first

gene validated was *sema3d* [75]. So far, we have established that Cx43 coordinates two activities, cell proliferation and joint formation, to precisely regulate segment length. However, we are yet to understand how Cx43 mediates those activities. In other words, it remains unclear how direct cell–cell communication influences cellular functions that in turn effectively regulate morphogenesis. To identify global changes in gene expression occurring downstream of *cx43*, our lab utilized a microarray strategy, focusing on the subset of genes both downregulated in *sof*^{*b123*} and upregulated in *alf*^{*dy86*} to enable the identification of *cx43*-dependent genes. Based on a previous report from our lab, we know that *sema3d*, a secreted signaling molecule is expressed in the skeletal precursor cells and is molecularly and functionally downstream of Cx43, mediating *cx43*-dependent phenotypes (Figure 1.7) [75]. We anticipate that there are other *cx43*-dependent genes that can contribute to the two mechanistic pathways of cell proliferation and joint suppression. Therefore, it is important to identify genes that are expressed downstream of *cx43*, especially genes that are upregulated in *alf*^{*dy86*} and downregulated in *sof*^{*b123*}. The goal of this research was to elucidate the role of *hapln1a* (ECM protein-coding gene identified by the microarray analysis) in mediating Cx43-dependent skeletal phenotypes during fin regeneration.

- 1) In mouse and human, the orthologous protein HAPLN1 has also been referred to as either cartilage link protein (Crtl1) or link protein (LP). The function of Hapln1 is to “link” hyaluronic acid (HA) with proteins termed PGs in the ECM (Figure 1.8). The mouse knockout for *CRTL1* (aka *HAPLN1*) causes dwarfism, craniofacial abnormalities, and perinatal lethality in the mouse [76] and interestingly, cartilage-

specific expression of transgenic Hapln1a rescues skeletal abnormalities in LP knockout mice [77]. Also, single nucleotide polymorphisms identified in the HAPLN1 gene is associated with spinal osteoarthritis in aging females [78]. Together, these studies highlight the importance of this ECM protein during skeletal morphogenesis. Hence, it is interesting to understand the role of Hapln1a during skeletal morphogenesis and to our knowledge this is the first study addressing the role of this ECM protein in a regenerating fin skeleton. We found that knockdown of *hapln1a* recapitulated all of *cx43* knockdown phenotypes, suggesting that *hapln1a* is indeed molecularly and functionally downstream of Cx43. Additionally, we also found that *hapln1a* knockdown destabilizes HA which might be contributing to the observed skeletal phenotypes [79]. This objective is presented as Chapter 2.

2) The ECM can influence the ability of the secreted signaling molecules that act as ligand, to physically interact with their specific cell surface receptors. It is possible that Hapln1a-based ECM, containing HA as the important component, could play a role in signaling by interacting with some of the signaling molecules that are known to be secreted during fin regeneration. For example, the signaling molecule Sema3d is known to mediate Cx43-dependent phenotypes, perhaps via physical binding to Neuropilin and Plexin receptors [75]. We evaluated the genetic and physical interaction between the Hapln1a-dependent ECM and secreted signaling molecule Sema3d. The findings of this study are summarized in Chapter 3. We found that the components of Hapln1a–ECM, namely HA and the PG aggrecan (Acan) are important to mediate Hapln1a functions, namely, cell proliferation (growth) and joint formation

(patterning). And, we provide evidence that Hapln1a–ECM genetically interacts with and stabilizes at least one signaling molecule, Sema3d, during fin regeneration.

3) Skeletal development depends upon appropriate cell proliferation and cell differentiation. The fact that *hapln1a* knockdown causes reduced cell proliferation and reduced segment length provides evidence that at least the HA–Hapln1a based ECM influences these cellular behaviors. However, it is not clear how mutations and defects in ECM proteins cause skeletal disorders. Interestingly, nothing has been published on the role of HA/Hapln1a or other major ECM components during zebrafish fin regeneration. To achieve a better understanding about how the ECM is remodeled during zebrafish fin regeneration, we looked at components of the ECM over time. We focused on the expression pattern of Hapln1a–ECM components (i.e., Hapln1a, HA, Acan, Vcan) (Figure 1.9), as well as the other components of the putative transitional matrix such as FN and TNC [80–83]. In addition, we included laminin (LAM), which is characteristic of differentiated tissues. The findings from this study are summarized in Chapter 4. Our results show that a transitional matrix analogous to the one formed during newt skeletal and heart muscle regeneration is synthesized during fin regeneration. We also demonstrate that a provisional matrix, rich in hyaluronic acid, tenascin C, and fibronectin is synthesized following amputation. Additionally, we observed that the link protein Hapln1a-dependent ECM, consisting of Hapln1a, HA, and PG-Acan, is upregulated during fin regeneration [84]. Our findings on zebrafish fin regeneration implicate that changes in the extracellular milieu represent an

evolutionarily conserved mechanism that proceeds during tissue regeneration, yet with distinct players, depending on the type of tissue that is involved.

1.7 Figures

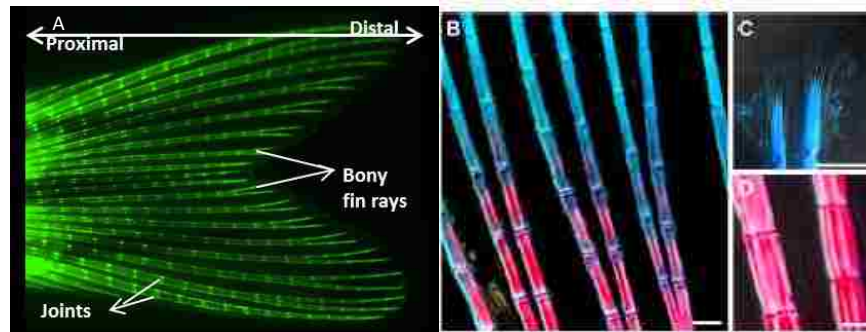


Figure 1.1: The zebrafish fin is a model system for skeletal morphogenesis. (A) The caudal fin is stained with calcein (detects bone matrix). Bony fin rays made of segments separated by joints (Bright green lines) The bi-lobed morphology of the caudal fin fold is stabilized by 16–18 segmented and occasionally bifurcated bony rays (stained structures), named lepidotrichia, that are interconnected by soft interray tissue (unstained regions between the bony rays). The bones are predominantly composed of calcified matrix (magenta), with the exception of the distal parts which remain non-mineralized. (B) A higher magnification of the distal region shows a gradual decrease of the calcification level towards the fin margin. The length of segments is nearly identical in proximal (magenta) and distal (cyan) parts of the rays. (C) The tips of the rays are supported by a brush-like bundle of fine spicules, called actinotrichia, which surround the apical-most segment of the lepidotrichia and expand further distally beyond the end of the bone. (D) The proximal segments of the rays are at least three times broader than the distal calcified segments (compared with B), but their length remains nearly constant. Scale bars: (B)–(D) 100 μm . (B, C, D, adapted from Pfefferli *et al*, 2015)

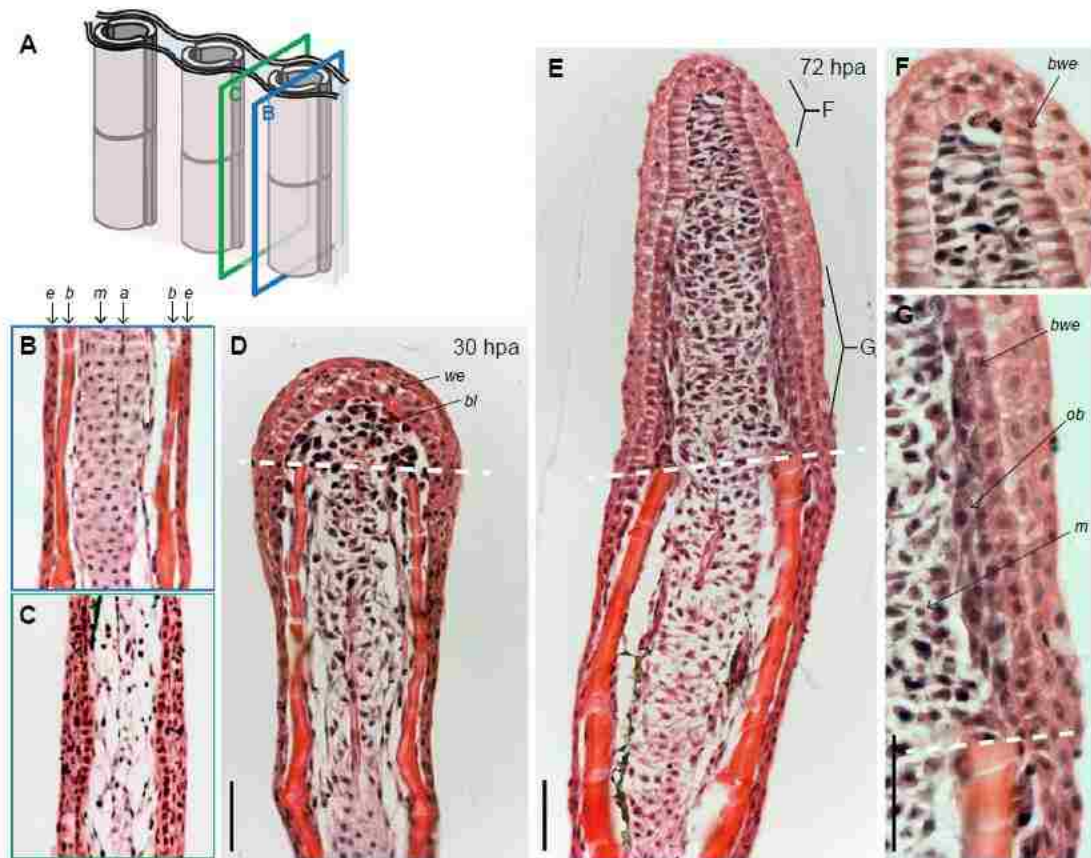


Figure 1.2: The histological organization of an uninjured and regenerating caudal fin. (A) Schematic representation of the fin structure with the planes of sectioning along the interray (green frame) and rays (blue frame). (B)–(I) Longitudinal fin sections stained with hematoxylin and eosin. (B) Each lepidotrichium consists of a pair of concave bones (*b*) that appear as parallel rods underneath the multilayered epidermis (*e*). Bones are tightly covered by flattened osteoblasts that deposit the bone matrix. The mesenchymal tissue (*m*) between the bones is composed of connective tissue containing densely interconnected fibroblasts, nerves, and arteries (*a*). (C) The interray is devoid of skeletal elements and contains loose connective tissue. (D) At 30 hpa, the blastema (*bl*) appears as a cluster of undifferentiated mesenchymal cells covered by a wound epidermis (*we*) above the amputation plane (white dashed line). Blastema formation results from the dedifferentiation of cells located in the stump that progressively lose their specialized morphology, initiate proliferation, and migrate distally toward the

amputation plane. (E) At 72 hpa, the blastemal outgrowth exhibits a spatial organization of the newly formed tissue. (F) Higher magnification of the distal part of the outgrowth (apical signaling zone with slowly cycling cells). Mesenchymal cells become elongated perpendicularly to the growth (proximo-distal) axis. The basal layer of the wound epithelium (*bwe*) contains columnar cells. (G) Higher magnification of the proximal part of the outgrowth (proliferation and redifferentiation zone). Dedifferentiated osteoblasts (*ob*) are tightly interconnected and remain aligned underneath the wound epidermis. The basal layer of the wound epithelium (*bwe*) contains cuboidal cells. The mesenchymal cells are round and loosely distributed. Scale bars: 50 μm . (Adapted from Pfefferli *et al*, 2015).

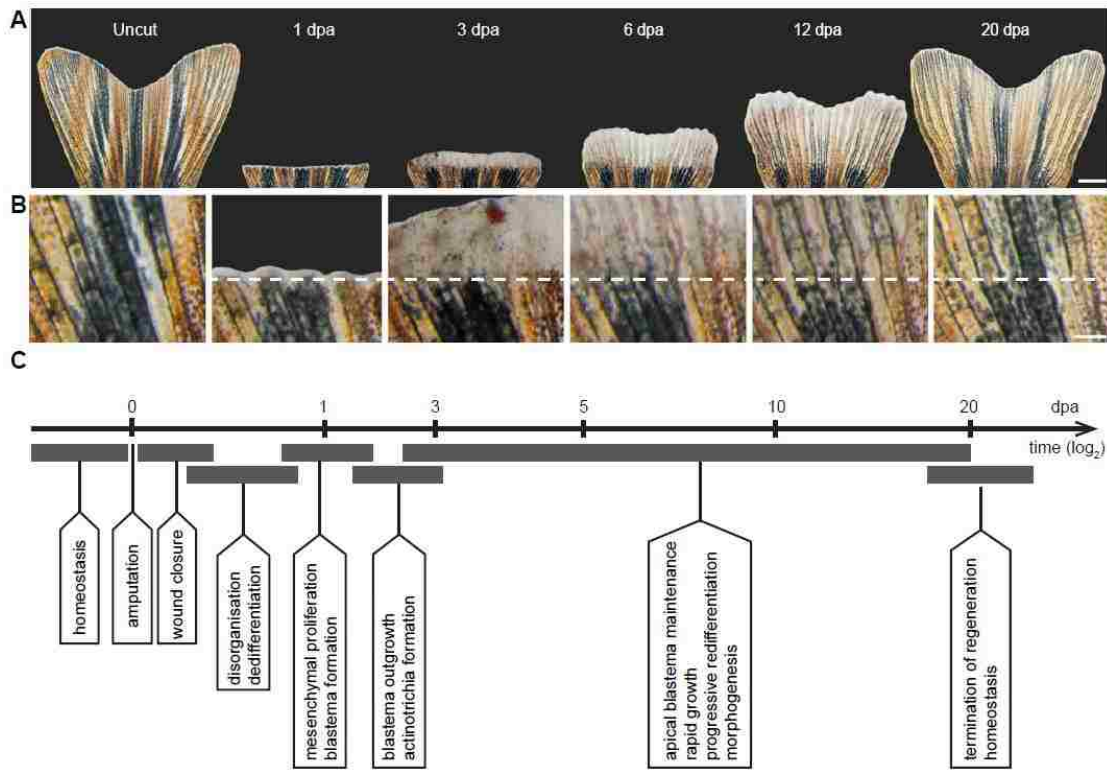


Figure 1.3: The regeneration process of the caudal fin in zebrafish. (A) Time-lapse imaging of the same fin during the regeneration process at 27°C. Uncut, the original fin prior to amputation presents a bi-lobed morphology. At 1 dpa, white tissue above the amputation consists of the wound epidermis and a few blastema cells. At 3 dpa, a white excrescence above the amputation plane contains the blastema, which, despite its uniform appearance, exhibits subdivisions at the cellular and molecular level. At 6 dpa, the outgrowth extends very rapidly; the white tissue is maintained at the fin margin, while the proximal outgrowth starts to display bone structures and pigmentation, which are the macroscopic markers of tissue redifferentiation. At 12 dpa, fin regeneration is at its advanced stage. At 20 dpa, the size of the fin nearly reaches its original size and pattern. The white margin of tissue remains at the tip for homeostatic growth/regeneration. (B) Higher magnifications of the fin surface at the position of amputation (white dashed line) at the respective time points are indicated in the upper

panel (A). (C) The milestones of the fin regeneration process. Scale bars: (A) 1000 μm ;
(B) 200 μm . (Adapted from Pfefferli *et al*, 2015).

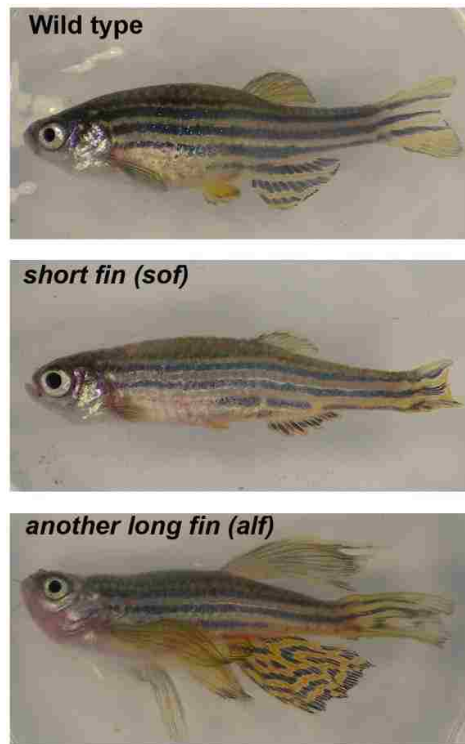


Figure 1.4: Fin length mutants exhibit defects in skeletal morphogenesis. Top: wildtype zebrafish. Middle: *sof b123* mutant. Bottom: *alf dty86* mutant. (Reviewed in Ton and Iovine, 2013).

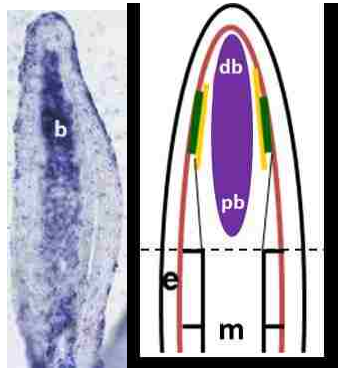


Figure 1.5: *cx43* mRNA is detected by *in situ* hybridization. (A) Cryosection shows the expression of *cx43* in the blastema (b). Picture taken at 20X magnification. (B) Cartoon of a longitudinal cross-section through a single fin ray shows the central mesenchyme (m) and outer epithelium (e). The basal layer of the epithelium is outlined in red. The proximal (pb) and distal (db) blastema (purple) is in the mesenchyme (m) and represents the region of proliferating cells. Skeletal precursor cells (green) are adjacent to dividing cells in the blastema suggesting that Cx43 activity influences joint formation.

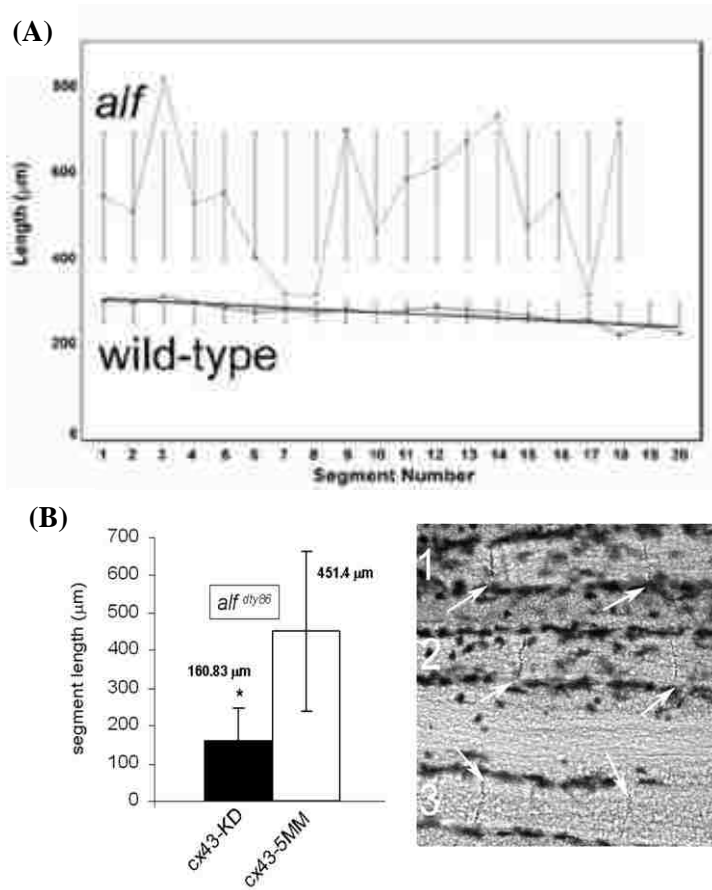


Figure 1.6: The *alf^{dy86}* mutant phenotype before and after the rescue. (A) Before the *cx43* knockdown experiment, the mutant exhibits stochastic joint segments. (B) After the knockdown, segment length is rescued and more joints are formed. Adapted from Sims et al., 2009.

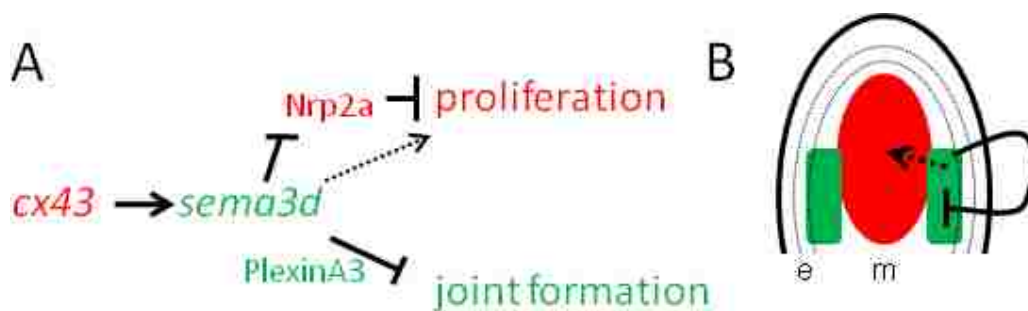


Figure 1.7: Model showing Cx43-Sema3d influence on skeletal morphology. (A) Proposed pathway of Cx43–Sema3d and downstream receptors (text colors are coordinated with the cartoon in B). Cx43 activity influences *sema3d* gene expression, influencing cell proliferation and joint formation independently. Sema3d interacts with Nrp2a to yield a net positive influence on cell proliferation (dotted arrow). Sema3d interacts with PlxnA3 in the skeletal precursor cells to inhibit joint formation. (B) Cartoon illustrating the compartments of gene expression in the Cx43–Sema3d pathway (e, epithelium; m, mesenchyme; basal layer of the epidermis is dotted). The *cx43* mRNA is upregulated in the blastema (red), adjacent to the *sema3d*-positive and *plxna3*-positive skeletal precursor cells (green). Cx43-dependent up-regulation of Sema3d allows Sema3d to signal back to the blastema to provide a net positive signal for growth (dotted arrow), perhaps via Nrp2a. Sema3d signaling via PlxnA3 inhibits joint formation in the skeletal precursor cells, perhaps by influencing osteoblast/joint-forming cell differentiation. (Adapted from Ton and Iovine, 2012).

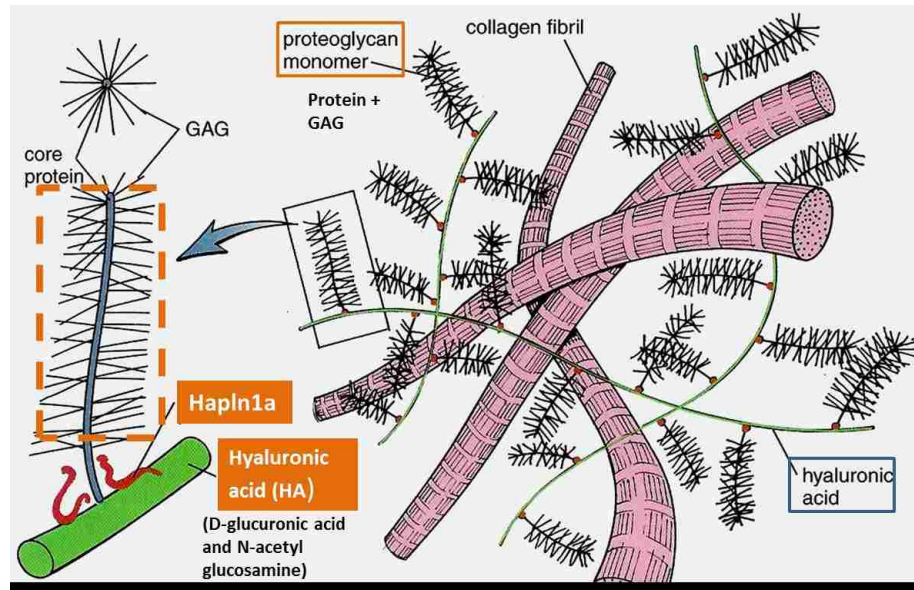


Figure 1.8: Hapln1a in the Extracellular matrix. The link protein Hapln1a (red) stabilizes the interaction between hyaluronic acid (green) and proteoglycan (brush like structure in black). Collagen fibrils in the ECM are represented as tube like structures in pink.

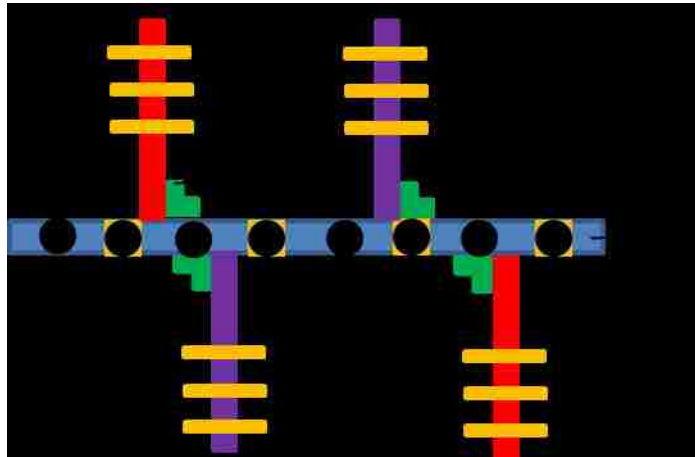


Figure 1.9: Defining Hapln1a-ECM. Hapln1a, HA, Acan and Vcan form Hapln1a-ECM. Bone associated proteoglycans are aggrecan (Acan) and versican (Vcan). Hapln1a, and the associated components stabilized by Hapln1a, namely, HA, Acan and Vcan constitute the Hapln1a-ECM.

1.8 References

1. Poss KD, Keating MT, Nechiporuk A (2003) Tales of regeneration in zebrafish. *Dev Dyn* 226: 202-210.
2. Lepilina A, Coon AN, Kikuchi K, Holdway JE, Roberts RW, et al. (2006) A dynamic epicardial injury response supports progenitor cell activity during zebrafish heart regeneration. *Cell* 127: 607-619.
3. Makino S, Whitehead GG, Lien CL, Kim S, Jhawar P, et al. (2005) Heat-shock protein 60 is required for blastema formation and maintenance during regeneration. *Proc Natl Acad Sci U S A* 102: 14599-14604.
4. Poss KD, Wilson LG, Keating MT (2002) Heart regeneration in zebrafish. *Science* 298: 2188-2190.
5. Iovine MK, Gumpert AM, Falk MM, Mendelson TC (2008) Cx23, a connexin with only four extracellular-loop cysteines, forms functional gap junction channels and hemichannels. *FEBS Lett* 582: 165-170.
6. Yin VP, Lepilina A, Smith A, Poss KD Regulation of zebrafish heart regeneration by miR-133. *Dev Biol* 365: 319-327.
7. Raya A, Koth CM, Buscher D, Kawakami Y, Itoh T, et al. (2003) Activation of Notch signaling pathway precedes heart regeneration in zebrafish. *Proc Natl Acad Sci U S A* 100 Suppl 1: 11889-11895.
8. Nabrit SM (1929) The role of the fin rays in the regeneration in the Tail-Fins of fishes (in *Fundulus* and Goldfish). *The Biological Bulletin* 56: 235-266.

9. Geraudie J, Monnot MJ, Brulfert A, Ferretti P (1995) Caudal fin regeneration in wild type and long-fin mutant zebrafish is affected by retinoic acid. *Int J Dev Biol* 39: 373-381.
10. Rolland-Lagan AG, Paquette M, Tweedle V, Akimenko MA Morphogen-based simulation model of ray growth and joint patterning during fin development and regeneration. *Development* 139: 1188-1197.
11. Goldsmith MI, Iovine MK, O'Reilly-Pol T, Johnson SL (2006) A developmental transition in growth control during zebrafish caudal fin development. *Dev Biol* 296: 450-457.
12. Zhang J, Wagh P, Guay D, Sanchez-Pulido L, Padhi BK, et al. (2010) Loss of fish actinotrichia proteins and the fin-to-limb transition. *Nature* 466: 234-237.
13. Duran I, Mari-Beffa M, Santamaria JA, Becerra J, Santos-Ruiz L (2011) Actinotrichia collagens and their role in fin formation. *Dev Biol* 354: 160-172.
14. Huang CC, Lawson ND, Weinstein BM, Johnson SL (2003) *reg6* is required for branching morphogenesis during blood vessel regeneration in zebrafish caudal fins. *Dev Biol* 264: 263-274.
15. Akimenko MA, Mari-Beffa M, Becerra J, Geraudie J (2003) Old questions, new tools, and some answers to the mystery of fin regeneration. *Dev Dyn* 226: 190-201.
16. Schebesta M, Lien CL, Engel FB, Keating MT (2006) Transcriptional profiling of caudal fin regeneration in zebrafish. *ScientificWorldJournal* 6 Suppl 1: 38-54.
17. Iovine MK (2007) Conserved mechanisms regulate outgrowth in zebrafish fins. *Nat Chem Biol* 3: 613-618.

18. Nechiporuk A, Keating MT (2002) A proliferation gradient between proximal and msxb-expressing distal blastema directs zebrafish fin regeneration. *Development* 129: 2607-2617.
19. Jazwinska A, Badakov R, Keating MT (2007) Activin-betaA signaling is required for zebrafish fin regeneration. *Curr Biol* 17: 1390-1395.
20. Yoshinari N, Kawakami A (2011) Mature and juvenile tissue models of regeneration in small fish species. *Biol Bull* 221: 62-78.
21. Blum N, Begemann G (2013) The roles of endogenous retinoid signaling in organ and appendage regeneration. *Cell Mol Life Sci* 70: 3907-3927.
22. Gemberling M, Bailey TJ, Hyde DR, Poss KD (2013) The zebrafish as a model for complex tissue regeneration. *Trends Genet* 29: 611-620.
23. Laforest L, Brown CW, Poleo G, Geraudie J, Tada M, et al. (1998) Involvement of the sonic hedgehog, patched 1 and bmp2 genes in patterning of the zebrafish dermal fin rays. *Development* 125: 4175-4184.
24. Poss KD, Shen J, Keating MT (2000) Induction of *lef1* during zebrafish fin regeneration. *Dev Dyn* 219: 282-286.
25. Poss KD, Shen J, Nechiporuk A, McMahon G, Thisse B, et al. (2000) Roles for Fgf signaling during zebrafish fin regeneration. *Dev Biol* 222: 347-358.
26. Quint E, Smith A, Avaron F, Laforest L, Miles J, et al. (2002) Bone patterning is altered in the regenerating zebrafish caudal fin after ectopic expression of sonic hedgehog and *bmp2b* or exposure to cyclopamine. *Proc Natl Acad Sci U S A* 99: 8713-8718.

27. Lee Y, Hami D, De Val S, Kagermeier-Schenk B, Wills AA, et al. (2009) Maintenance of blastemal proliferation by functionally diverse epidermis in regenerating zebrafish fins. *Dev Biol* 331: 270-280.
28. Whitehead GG, Makino S, Lien CL, Keating MT (2005) *fgf20* is essential for initiating zebrafish fin regeneration. *Science* 310: 1957-1960.
29. Dufourcq P, Vríz S (2006) The chemokine SDF-1 regulates blastema formation during zebrafish fin regeneration. *Dev Genes Evol* 216: 635-639.
30. Bouzaffour M, Dufourcq P, Lecaudey V, Haas P, Vríz S (2009) Fgf and Sdf-1 pathways interact during zebrafish fin regeneration. *PLoS One* 4: e5824.
31. Chablais F, Jazwinska A (2010) IGF signaling between blastema and wound epidermis is required for fin regeneration. *Development* 137: 871-879.
32. Campbell LJ, Crews CM (2008) Wound epidermis formation and function in urodele amphibian limb regeneration. *Cell Mol Life Sci* 65: 73-79.
33. Stoick-Cooper CL, Weidinger G, Riehle KJ, Hubbert C, Major MB, et al. (2007) Distinct Wnt signaling pathways have opposing roles in appendage regeneration. *Development* 134: 479-489.
34. Mathew LK, Simonich MT, Tanguay RL (2009) AHR-dependent misregulation of Wnt signaling disrupts tissue regeneration. *Biochem Pharmacol* 77: 498-507.
35. Stewart S, Gomez AW, Armstrong BE, Henner A, Stankunas K (2014) Sequential and opposing activities of Wnt and BMP coordinate zebrafish bone regeneration. *Cell Rep* 6: 482-498.

36. Wehner D, Cizelsky W, Vasudevaro MD, Ozhan G, Haase C, et al. (2014) Wnt/beta-catenin signaling defines organizing centers that orchestrate growth and differentiation of the regenerating zebrafish caudal fin. *Cell Rep* 6: 467-481.
37. Smith A, Avaron F, Guay D, Padhi BK, Akimenko MA (2006) Inhibition of BMP signaling during zebrafish fin regeneration disrupts fin growth and scleroblasts differentiation and function. *Dev Biol* 299: 438-454.
38. Grottek B, Wehner D, Weidinger G (2013) Notch signaling coordinates cellular proliferation with differentiation during zebrafish fin regeneration. *Development* 140: 1412-1423.
39. Munch J, Gonzalez-Rajal A, de la Pompa JL Notch regulates blastema proliferation and prevents differentiation during adult zebrafish fin regeneration. *Development* 140: 1402-1411.
40. Bayliss PE, Bellavance KL, Whitehead GG, Abrams JM, Aegerter S, et al. (2006) Chemical modulation of receptor signaling inhibits regenerative angiogenesis in adult zebrafish. *Nat Chem Biol* 2: 265-273.
41. Knopf F, Hammond C, Chekuru A, Kurth T, Hans S, et al. (2011) Bone regenerates via dedifferentiation of osteoblasts in the zebrafish fin. *Dev Cell* 20: 713-724.
42. Sousa S, Afonso N, Bensimon-Brito A, Fonseca M, Simoes M, et al. (2011) Differentiated skeletal cells contribute to blastema formation during zebrafish fin regeneration. *Development* 138: 3897-3905.
43. Tu S, Johnson SL (2011) Fate restriction in the growing and regenerating zebrafish fin. *Dev Cell* 20: 725-732.

44. Stewart S, Stankunas K Limited dedifferentiation provides replacement tissue during zebrafish fin regeneration. *Dev Biol* 365: 339-349.
45. Singh SP, Holdway JE, Poss KD (2012) Regeneration of amputated zebrafish fin rays from de novo osteoblasts. *Dev Cell* 22: 879-886.
46. Grandel H, Schulte-Merker S (1998) The development of the paired fins in the zebrafish (*Danio rerio*). *Mech Dev* 79: 99-120.
47. van Eeden FJ, Granato, M., Schach, U., Brand, M., Furutani-Seiki, M., Haffter, P., Hammerschmidt, M., Heisenberg, C. P., Jiang, Y. J., Kane, D. A., Kelsh, R. N., Mullins, M. C., Odenthal, J., Warga, R. M., Nusslein-Volhard, C. (1996) Genetic analysis of fin formation in the zebrafish, *Danio rerio*. *Development* 123: 255-262.
48. Sims K, Jr., Eble DM, Iovine MK (2009) Connexin43 regulates joint location in zebrafish fins. *Dev Biol* 327: 410-418.
49. Perathoner S, Daane JM, Henrion U, Seebohm G, Higdon CW, et al. (2014) Bioelectric signaling regulates size in zebrafish fins. *PLoS Genet* 10: e1004080.
50. Levin M (2014) Molecular bioelectricity: how endogenous voltage potentials control cell behavior and instruct pattern regulation in vivo. *Mol Biol Cell* 25: 3835-3850.
51. Iovine MK, Higgins EP, Hinds A, Coblitz B, Johnson SL (2005) Mutations in connexin43 (GJA1) perturb bone growth in zebrafish fins. *Dev Biol* 278: 208-219.
52. Hoptak-Solga AD, Klein KA, DeRosa AM, White TW, Iovine MK (2007) Zebrafish short fin mutations in connexin43 lead to aberrant gap junctional intercellular communication. *FEBS Lett* 581: 3297-3302.

53. Goodenough DA, Goliger JA, Paul DL (1996) Connexins, connexons, and intercellular communication. *Annu Rev Biochem* 65: 475-502.
54. Kumar NM, Gilula NB (1996) The gap junction communication channel. *Cell* 84: 381-388.
55. Ton QV, Iovine MK (2013) Identification of an *evx1*-dependent joint-formation pathway during FIN regeneration. *PLoS One* 8: e81240.
56. Chaible LM, Sanches DS, Cogliati B, Mennequier G, Dagli ML Delayed osteoblastic differentiation and bone development in Cx43 knockout mice. *Toxicol Pathol* 39: 1046-1055.
57. Lecanda F, Warlow PM, Sheikh S, Furlan F, Steinberg TH, et al. (2000) Connexin43 deficiency causes delayed ossification, craniofacial abnormalities, and osteoblast dysfunction. *J Cell Biol* 151: 931-944.
58. Stains JP, Civitelli R (2005) Cell-cell interactions in regulating osteogenesis and osteoblast function. *Birth Defects Res C Embryo Today* 75: 72-80.
59. Paznekas WA, Boyadjiev SA, Shapiro RE, Daniels O, Wollnik B, et al. (2003) Connexin 43 (GJA1) mutations cause the pleiotropic phenotype of oculodentodigital dysplasia. *Am J Hum Genet* 72: 408-418.
60. Kjaer KW, Hansen L, Eiberg H, Leicht P, Opitz JM, et al. (2004) Novel Connexin 43 (GJA1) mutation causes oculo-dento-digital dysplasia with curly hair. *Am J Med Genet A* 127A: 152-157.

61. Richardson R, Donnai D, Meire F, Dixon MJ (2004) Expression of Gja1 correlates with the phenotype observed in oculodentodigital syndrome/type III syndactyly. *J Med Genet* 41: 60-67.
62. Reaume AG, de Sousa PA, Kulkarni S, Langille BL, Zhu D, et al. (1995) Cardiac malformation in neonatal mice lacking connexin43. *Science* 267: 1831-1834.
63. Ya J, Erdtsieck-Ernste EB, de Boer PA, van Kempen MJ, Jongsma H, et al. (1998) Heart defects in connexin43-deficient mice. *Circ Res* 82: 360-366.
64. Becker DL, McGonnell I, Makarenkova HP, Patel K, Tickle C, et al. (1999) Roles for alpha 1 connexin in morphogenesis of chick embryos revealed using a novel antisense approach. *Dev Genet* 24: 33-42.
65. Law LY, Lin JS, Becker DL, Green CR (2002) Knockdown of connexin43-mediated regulation of the zone of polarizing activity in the developing chick limb leads to digit truncation. *Dev Growth Differ* 44: 537-547.
66. Oyamada M, Oyamada Y, Takamatsu T (2005) Regulation of connexin expression. *Biochim Biophys Acta* 1719: 6-23.
67. Civitelli R (2008) Cell-cell communication in the osteoblast/osteocyte lineage. *Arch Biochem Biophys* 473: 188-192.
68. Karsenty G (1999) The genetic transformation of bone biology. *Genes Dev* 13: 3037-3051.
69. Erlebacher A, Filvaroff EH, Gitelman SE, Derynck R (1995) Toward a molecular understanding of skeletal development. *Cell* 80: 371-378.

70. Stains JP, Civitelli R (2005) Gap junctions in skeletal development and function. *Biochim Biophys Acta* 1719: 69-81.
71. Stains JP, Civitelli R (2005) Gap junctions regulate extracellular signal-regulated kinase signaling to affect gene transcription. *Mol Biol Cell* 16: 64-72.
72. Hoptak-Solga AD, Nielsen S, Jain I, Thummel R, Hyde DR, et al. (2008) Connexin43 (GJA1) is required in the population of dividing cells during fin regeneration. *Dev Biol* 317: 541-548.
73. Lee Y, Grill S, Sanchez A, Murphy-Ryan M, Poss KD (2005) Fgf signaling instructs position-dependent growth rate during zebrafish fin regeneration. *Development* 132: 5173-5183.
74. Stains JP, Lecanda F, Screen J, Towler DA, Civitelli R (2003) Gap junctional communication modulates gene transcription by altering the recruitment of Sp1 and Sp3 to connexin-response elements in osteoblast promoters. *J Biol Chem* 278: 24377-24387.
75. Ton QV, Iovine M (2012) Semaphorin3d mediates Cx43-dependent phenotypes during fin regeneration. *Dev Biol* 366: 195-203.
76. Watanabe H, Yamada Y (1999) Mice lacking link protein develop dwarfism and craniofacial abnormalities. *Nat Genet* 21: 225-229.
77. Czipri M, Otto JM, Cs-Szabo G, Kamath RV, Vermes C, et al. (2003) Genetic rescue of chondrodysplasia and the perinatal lethal effect of cartilage link protein deficiency. *J Biol Chem* 278: 39214-39223.
78. Urano T, Narusawa K, Shiraki M, Sasaki N, Hosoi T, et al. (2011) Single-nucleotide polymorphism in the hyaluronan and proteoglycan link protein 1 (HAPLN1) gene is

associated with spinal osteophyte formation and disc degeneration in Japanese women. *Eur Spine J* 20: 572-577.

79. Govindan J, Iovine MK (2014) Hapln1a is required for connexin43-dependent growth and patterning in the regenerating fin skeleton. *PLoS One* 9: e88574.

80. Mailman ML, Dresden MH (1976) Collagen metabolism in the regenerating forelimb of *Notophthalmus viridescens*: synthesis, accumulation, and maturation. *Dev Biol* 50: 378-394.

81. Gulati AK, Zalewski AA, Reddi AH (1983) An immunofluorescent study of the distribution of fibronectin and laminin during limb regeneration in the adult newt. *Dev Biol* 96: 355-365.

82. Mercer SE, Odelberg SJ, Simon HG (2013) A dynamic spatiotemporal extracellular matrix facilitates epicardial-mediated vertebrate heart regeneration. *Dev Biol* 382: 457-469.

83. Calve S, Odelberg SJ, Simon HG (2010) A transitional extracellular matrix instructs cell behavior during muscle regeneration. *Dev Biol* 344: 259-271.

84. Govindan J, Iovine MK (2015) Dynamic remodeling of the extra cellular matrix during zebrafish fin regeneration. *Gene Expr Patterns*.

Chapter 2

Hapln1a is required for Connexin43-Dependent Growth and Patterning in the Regenerating Fin Skeleton

PLoS ONE 9(2): e88574. [doi:10.1371/journal.pone.0088574](https://doi.org/10.1371/journal.pone.0088574)

2.1 Abstract

Cell–cell communication, facilitating the exchange of small metabolites, ions and second messengers, takes place via aqueous proteinaceous channels called gap junctions. Connexins (Cx) are the subunits of a gap junction channel. Mutations in zebrafish *cx43* produces the *short fin (sof^{b123})* phenotype and is characterized by short fins due to reduced segment length of the bony fin rays and reduced cell proliferation. Previously established results from our lab demonstrate that Cx43 plays a dual role regulating both cell proliferation (growth) and joint formation (patterning) during the process of skeletal morphogenesis. In this study, we show that Hapln1a (Hyaluronan and Proteoglycan Link Protein 1a) functions downstream of *cx43*. Hapln1a belongs to the family of link proteins that play an important role in stabilizing the ECM by linking the aggregates of hyaluronan and proteoglycans. We validated that *hapln1a* is expressed downstream of *cx43* by in situ hybridization and quantitative RT-PCR methods. Moreover, in situ hybridization at different time points revealed that *hapln1a* expression peaks at 3 days post amputation. Expression of *hapln1a* is located in the medial mesenchyme and in the lateral skeletal precursor cells. Furthermore, morpholino mediated knockdown of *hapln1a* resulted in reduced fin regenerate length, reduced bony segment length and reduced cell proliferation, recapitulating all the phenotypes of *cx43* knockdown. Moreover, Hyaluronic Acid (HA) levels are dramatically reduced in *hapln1a* knockdown fins, attesting the importance of Hapln1a in stabilizing the ECM. Attempts to place *hapln1a* in our previously defined *cx43–sema3d* pathway suggest that *hapln1a* functions in a parallel genetic pathway. Collectively, our data suggest that

Cx43 mediates independent Sema3d and Hapln1a pathways in order to coordinate skeletal growth and patterning.

2.2 Introduction

Gap junctions play a critical role in coupling tissue function and they have long been hypothesized to play a role in the maintenance of homeostasis, morphogenesis, cell differentiation, growth control and the process of skeletogenesis in multicellular organisms [1]. Gap junctions are proteinaceous channels formed by the docking of two connexons between neighboring cells, and they mediate the exchange of low molecular weight metabolites (<1000 Da), ions and second messengers between the contacting cells [2]. Each connexon or hemichannel is made up of six connexins, each protein containing a four pass transmembrane domain. The syndrome Oculodentodigital dysplasia (ODDD), characterized by abnormalities in craniofacial elements, limbs and dentition, has been linked to missense mutations in the *GJA1* gene locus in humans [3]. At least 24 separate point mutations in *GJA1*, which codes for Connexin43 (Cx43), have been identified in patients with ODDD [3]–[5]. The *CX43* knock out (*CX43*^{-/-}) mouse dies perinatally because of cardiac malformations [6], [7]. Similarly, targeted gene knockdown of *cx43* results in embryonic heart defects in zebrafish, signifying the essential role of *cx43* during development [8]. The skeletal defects seen in the *CX43*^{-/-} KO mouse model exhibited hypomineralization of craniofacial bones and severely delayed ossification of the appendicular skeleton [9]. Moreover, the ODDD phenotype is similar to a set of craniofacial abnormalities observed in the

targeted *CX43* knockdown chick model [10], [11]. In zebrafish, a homozygous mutation in *cx43* causes the *short fin* phenotype, characterized by shorter tail fins due to defects in the fin skeleton. The mechanism by which *CX43* based mutations cause skeletal defect phenotypes is largely unknown. However, it is apparent that the function of Cx43 in the vertebrate skeleton is conserved.

We utilize the zebrafish *short fin* mutant (*sof*^{*b123*}) to address the role of Cx43 during skeletal development. Our lab has found that the mutation in zebrafish *cx43* gene causes the *short fin* (*sof*^{*b123*}) phenotypes characterized by short bony fin ray segments, short fins, and reduced cell proliferation. The *sof*^{*b123*} mutant exhibits reduced levels of *cx43* mRNA and Cx43 protein, without a lesion in the coding sequence [8]. Moreover, three additional alleles that cause missense mutations also resulted in reduced gap junctional intercellular communication (GJIC), short segments, and reduced cell proliferation [12]. Furthermore, morpholino mediated knockdown of Cx43 in wild type zebrafish completely recapitulate all the phenotypes produced by *sof* alleles [13]. In contrast to *sof*^{*b123*}, the *another long fin* (*alf*^{*dy86*}) mutant exhibits fin overgrowth and overlong segments due to stochastic joint failure [14]. These phenotypes are opposite to those of *sof*, and we have shown that *alf*^{*dy86*} exhibits increased levels of *cx43* mRNA [15]. Indeed, *cx43* knockdown in *alf*^{*dy86*} rescues the segment length phenotype, suggesting that Cx43 over expression contributes to the *alf*^{*dy86*} phenotypes (note that the mutation causing *alf*^{*dy86*} phenotypes is not located in the *cx43* gene [15]). We interpret the *cx43*-dependent loss of joints in *alf*^{*dy86*} and the premature joint formation (i.e. short segment) phenotype in *sof* to indicate that Cx43

suppresses joint formation. At the same time, Cx43 is positively associated with cell proliferation. Thus, Cx43 functions in more than one way, both positively influencing cell proliferation and negatively influencing joint formation, thereby concomitantly regulating bone growth and skeletal patterning during the process of fin regeneration.

An important, yet poorly understood question with respect to mutations in *connexin* genes in general is, how does GJIC impact tangible cellular events like cell division and differentiation? One hypothesis is that Cx43 based GJIC can influence gene expression patterns [16], [17]. Our lab exploited the availability of the two mutants, *sof*^{b123} and *alf*^{dy86}, in order to identify genes whose expression depends on Cx43. Thus, we utilized a novel microarray strategy to identify a set of candidate genes, which are both downregulated in *sof*^{b123} and upregulated in *alf*^{dy86}. The first gene validated from this microarray is *semaphorin3d* (*sema3d*) [18]. Here, we provide molecular and functional validation of another gene identified from the microarray analysis, *hapln1a* (*hyaluronan and proteoglycan link protein 1a*). In mouse and human, the orthologous protein Hapln1 has also been referred to as either cartilage link protein (Crtl1) or link protein (LP). The function of Hapln1 is to “link” hyaluronic acid (HA) with proteins termed proteoglycans (PG) in the extracellular matrix (ECM). Remarkably, the mouse knockout for *CRTL1* (aka *HAPLNI*) causes dwarfism, craniofacial abnormalities, and perinatal lethality in the mouse [19].

The ECM is a complex mixture of proteins and carbohydrates that forms a dense network surrounding cells. Little is known about the functional role of the ECM during

zebrafish fin regeneration. Pharmacological treatments that alter the localization of PGs and collagen, as well as the expression levels of matrix metalloproteases, have been found to restrict outgrowth during fin regeneration [20], [21]. Even less is known about the particular role of the Hapln1a-based ECM, including HA, in the regenerating fin. HA is a large molecular weight carbohydrate polymer with a molecular mass up to 10^6 – 10^7 Da [22], [23]. The structure of the ECM is stabilized by Haplns by virtue of forming stable associations between HA and PGs [24]–[26]. Unsulfated glycosaminoglycans (such as HA) are prominent in the blastemas of late stage regenerating cichlid fins, although their function has not been elucidated [27]. Apart from contributing to the physicochemical properties, ECM turnover and remodeling are critical events during tissue injury and repair. HA is also known to regulate cell migration, proliferation, and differentiation through activation of HA-specific cell surface receptors [28]–[30]. This is the first study to evaluate the effects of destabilizing the Hapln1a-based ECM during zebrafish fin regeneration. We find that reduced Hapln1a causes skeletal growth and patterning defects during fin regeneration, perhaps via destabilization of HA. Furthermore, we find that *hapln1a* functions downstream of *cx43*, providing novel insights into how skeletal morphogenesis could be influenced by Cx43.

2.3 Materials and Methods

Statement on the ethical treatment of animals

This study was carried out in strict accordance with the recommendations in the Guide for the Care and Use of Laboratory Animals of the National Institutes of Health.

The protocols used for this manuscript were approved by Lehigh's Institutional Animal Care and Use Committee (IACUC) (protocol identification #128, approved 11/14/2012). Lehigh University's Animal Welfare Assurance Number is A-3877-01. All experiments were performed to minimize pain and discomfort.

Animal procedures

The following zebrafish (*Danio rerio*) strains were used in this study: wild-type C32, *sof*^{b123} [31] and *alf*^{dy86} [14]. Fish were maintained at a constant temperature of 25°C with 14 light: 10 dark photoperiod [32]. Fish were anaesthetized in 0.1% tricaine and caudal-fin amputations were performed at the 50% level using razor blades. Fin regeneration was then allowed to proceed until the desired time period and the regenerated fins were harvested from anaesthetized fish. Fins were fixed overnight in 4% paraformaldehyde (PFA) in PBS and dehydrated in 100% methanol at -20°C. Knockdown and whole mount in situ hybridization experiments were performed in triplicate with 5 fins per trial. For histochemistry on sectioned tissue, a minimum of 10 sections were evaluated from each of 3 different fins. For quantitative analyses, student's t-tests were completed to determine statistical significance (p<0.05).

In situ hybridization on whole mount and cryosectioned fins

RNA probes were generated from PCR amplified linear DNA in which the reverse primer contained the T7 RNA polymerase binding site. The primers used in this study for ISH are summarized in Table 2.1. Digoxigenin (DIG) labeled RNA probes

were synthesized using DIG labeling mix (Roche) and in situ hybridization on regenerated whole fins was carried out as described [18]. Briefly, for the whole mount method, fins stored in methanol were sequentially rehydrated with methanol/PBST and then treated with 5 µg/ml proteinase K for 45 min and re-fixed in 4% PFA in PBS for 20 min followed by extensive washes with PBST and finally the pre-hybridization process was carried out with HYB (50% formamide, 5X SSC, 10 mM citric acid, 0.1% Tween20, heparin and tRNA) at 65°C for 0.5–1 h. Hybridization with DIG labeled probes suspended in HYB was carried out overnight at 65°C followed by sequential washes with HYB/PBST and finally with PBST. Anti-DIG Fab (Roche) fragments were used at 1:5000 dilution, followed by extensive PBST washes and short washes in staining buffer. Subsequently fins were transferred to a staining solution containing NBT and BCIP and allowed to develop under dark conditions until purple color was observed. The reaction was stopped by washing in PBST and fixing overnight with 4% PFA. Finally the fins were mounted on a glass slide and analyzed using a Nikon Eclipse 80i microscope. Pictures were taken using a digital Nikon camera.

For in situ on sections, fins were fixed overnight with 4% PFA in PBS after harvest. After a brief methanol wash, fins were dehydrated in 100% methanol and stored at –20°C until use. Before sectioning, fins were sequentially rehydrated in a methanol-PBS series of washes and then were embedded in 1.5% agarose/5% sucrose dissolved in PBS and equilibrated overnight in 30% sucrose. Fins were mounted in OCT and cryosectioned (15 µm sections) using a Reichertâ Jung 2800 Frigocut cryostat. Sections were collected on Superfrost Plus slides (Fisher) and allowed to air dry overnight at

room temperature. Sections can be stored at -20°C for up to a year. Before use, the slides were brought to room temperature for at least an hour. Using a marking pen (ImmEdge Pen H-4000; PAP pen, VWR Laboratories), sections were circled. An appropriate amount of probe was pre-hybridized with a mixture of 1X salt solution (NaCl, Tris HCl, Tris Base, $\text{Na}_2\text{HPO}_4 \cdot 7\text{H}_2\text{O}$, NaH_2PO_4 , and 0.5 M EDTA) containing 50% deionized formamide (Sigma), 10% dextran sulfate, 1 mg/mL tRNA, and 1X Denhart's (Fisher) at 70°C for 5 mins. Hybridization with DIG-labeled antisense probes was carried out at 65°C overnight. The following day, slides were taken through a series of washes in a solution of 1X SSC, 50% formamide and 0.1% Tween-20 at 65°C . Slides were brought to room temperature and washed extensively in MABT (100 mM Maleic acid, 150 mM NaCl, and 0.1% Tween-20) and incubated in a blocking solution (MABT, Goat serum and 10% milk) for at least 2 hours. Anti-DIG Fab fragments (pre-absorbed against zebrafish fin tissue) were used at 1:5000 dilution and incubated overnight at 4°C . On day 3, slides were washed 4X in MABT (30 min each) followed by 2X short washes (5–10 min) with staining buffer (100 mM Tris, 9.5, 50 mM MgCl_2 , 100 mM NaCl, and 0.1% Tween20). Slides were then transferred to 10% polyvinyl alcohol (PVA; MW: 86,000) staining solution with NBT/BCIP stock solution (Roche) and allowed to develop overnight at 37°C . When a purple color started to appear on the sections, the reaction was stopped by washing the slides with PBST for at least 3 h and then stored in PBST at 4°C until imaging. Sections were mounted in 100% glycerol and examined on a Nikon Eclipse 80i microscope.

Morpholino mediated gene knockdown in regenerating fins

All morpholinos (MOs) used in this study were fluorescein tagged, obtained from Gene Tools, LLC and used at a 1 mM concentration for injection. The sequences for MOs used in this study can be found in Table 2.1. Injection and electroporation were carried out as described previously [18]. Briefly, 3 dpa fish were anesthetized and approximately 50 nl of MO (targeting or mismatch [MM] control) was injected into either the dorsal or the ventral half of the tail fin. The un-injected half of the fin served as the internal control. Following injection, the entire fin was electroporated using a CUY21 Square Wave electroporator (Protech International Inc). MO-positive fish were selected 24 hpe (hours post electroporation) by examination under a fluorescence microscope. For H3P staining and qRT-PCR analysis, the fins were harvested 1 dpe, and for the analysis of regenerate length and segment length, the fins were harvested 4 dpe. For each MO (i.e., targeting or mismatch) 5–6 fish were injected on one half of the fin with the un-injected side serving as an internal control. Reproducibility was confirmed by testing the MO in three independent experiments. Statistical significance was determined using the student's *t*-test ($P < 0.05$).

Immunochemistry and detection of HA

The following primary antibodies were used: Rabbit anti-histone-3-phosphate (anti-H3P, Millipore, 1:200); Mouse anti-Hapln1a antibody (MD Bioproducts, 1:500). The following secondary antibodies were used: anti-mouse Alexa 488 or 546 (1:200); anti-rabbit Alex 546 (1:200). For H3P staining, whole fins were harvested 1 dpe, after MO mediated knockdown and the experiment was carried out as described [18]. HA

was detected by biotinylated-HABP (US Biological, 1:300) followed by fluorescently labeled streptavidin-Alexa-546 conjugate, (Invitrogen, 1:200). For detection of Hapln1a or HA after MO injection (targeting or MM control), the fins were harvested 1 dpe, fixed in 4% PFA overnight and then stored in Methanol. Cryosectioning was done as described [18] and the sections were allowed to dry overnight. The sections were then rehydrated in PBS, twice for 10 min followed by two washes with Immunostaining block (2% BSA, 0.1% Tween in PBS). Then, sections were blocked for another 1 h at room temperature with the immunostaining block and then incubated in primary antibody or biotin-HABP overnight at 4°C. The sections were washed with block (3x, 15 min each), incubated at room temperature for 1 hr with secondary antibody or streptavidin-Alexa-546 (pre-absorbed for 1 hr. at room temperature with fixed zebrafish fins to reduce background staining), washed (3x, 15 min each), incubated with HOECHST stain for 10 min at room temperature, followed by a quick wash with distilled water. They were blotted dry and then mounted for imaging. To test for specificity of HABP, WT fin sections were treated with bovine hyaluronidase (Sigma-H3506, final concentration 200 U/ml) in 10 mM phosphate buffer containing 100 mM NaCl (pH 6.0) for 2 hours at 37°C [33], [34]. Untreated sections were incubated in buffer without enzyme. Following treatment the sections were washed two times in Immunostaining block before staining for HABP as described above.

Lysate preparation and Immunoblotting

For WT and *sof*^{b123}, 5 dpa regenerating fins were harvested from 10–15 fish. For MO injected fins, the injections were performed at 3 dpa fish (20–25 fish) and harvested the next day. Regenerating fins were harvested into 300–500 µl of RIPA lysis buffer, supplemented with protease inhibitor (Thermo scientific, Halt™ Protease and Phosphatase Inhibitor Cocktail) and homogenized using a tissue homogenizer (Bio-Gen, PRO 200) at high speed (5X) for 5 seconds with 10 second cooling intervals. Homogenized samples were centrifuged at 200 g for 10 min at 4°C and supernatant was used for further analysis. The protein samples were concentrated using a lyophilizer (Edwards-Freeze dryer super modulyo) and the pellet was resuspended in a minimal volume of PBS containing (Thermo scientific, Halt™ Protease and Phosphatase Inhibitor Cocktail, 100X) and the protein levels estimated by Bradford's assay.

To release Hapln1a from HA for detection by immunoblotting, equal concentrations of Hapln1a MO and MM lysates were treated with 100 U/ml of bovine hyaluronidase (Sigma) for 2 hours at 37°C as described [35]. Immunoblotting was performed as described [13] using mouse anti-Hapln1a (MD Bioproducts, 1:500) and anti- α -tubulin (Sigma, 1:3000) in combination with peroxidase-conjugated goat anti-mouse IgG (1:10,000). Signal detection was performed using ECL Prime western blotting detection reagent (Amersham™ - GE Healthcare).

Measurements

The regenerate length, segment length, and the number of dividing cells were estimated/calculated as described [18]. For each experiment, at least 5 fish were

evaluated in triplicate and a student's *t*-test was performed to evaluate statistical significance. Image Pro software was used to measure the regenerate length from the plane of amputation to the tip of the fin and segment length between two joints under bright field. Cell number was calculated by counting the number of histone-3-phosphate (H3P) positive cells from the distal-most 250 μm^2 of the 3rd fin ray.

Quantitative real-time PCR

For qRT-PCR analysis, TRIZOL RNA extraction was made from the 5 dpa regenerating fins of wild-type, *sof*^{*b123*}, and *alf*^{*dy86*} and 1 dpe for MO injected fins (targeting or MM). A minimum of 10 fins was used for total RNA extraction. For each sample, 1 μg of total RNA were reverse transcribed with Super Script III reverse transcriptase (Invitrogen) using oligo-dT primers. Primers for qPCR analysis of *hapln1a*, *sema3d* and *actin* were designed using Primer express software (Table 2.1). Three independent RNA samples were used for the experimental comparison and qPCR for each gene was done in duplicates. The samples were analyzed using Rotor-Gene 6000 series software (Corbette Research) and the average cycle number (C_T) was determined for each amplicon. Delta C_T (ΔC_T) values represent normalized expression levels of the test with respect to *actin*, the internal control. The relative level of gene expression, which is the fold difference, was determined using the delta delta C_T ($\Delta\Delta C_T$) method (i.e., $2^{-\Delta\Delta C_T}$).

2.4 Results

hapln1a* is expressed downstream of *cx43

Recently, we described a microarray strategy to identify genes that function downstream of Cx43. We identified ~50 genes that were both downregulated in *sof*^{b123} and upregulated in *alf*^{dy86} [18]. One of the candidate genes identified was *hapln1a*. To validate that *hapln1a* is expressed downstream of *cx43*, we compared the expression levels of *hapln1a* in WT, *sof*^{b123}, and *alf*^{dy86} regenerating fins by whole mount in situ hybridization (Figure 2.1). As expected, *hapln1a* mRNA expression appeared to be downregulated in *sof*^{b123}. We noticed some variability among *alf*^{dy86} regenerating fins, where some fins exhibited upregulation and some appeared more similar to WT regenerating fins (two representative images are shown in Figure 2.1). Therefore, we performed quantitative RT-PCR (qPCR) to evaluate the level of *hapln1a* expression in *sof*^{b123} and *alf*^{dy86} regenerating fins compared with WT (Table 2.2). As expected, *hapln1a* is downregulated in *sof*^{b123}. However, we did not observe an upregulation of *hapln1a* in *alf*^{dy86}, suggesting that among a population of *alf*^{dy86} regenerating fins, there is little difference in the expression level of *hapln1a* between WT and *alf*^{dy86}. To determine the tissue-specific expression of *hapln1a*, we performed in situ hybridization on cryosections. The longitudinal section of a regenerating fin ray reveals several outer epidermal layers, including the basal layer of epidermis, which is adjacent to the mesenchyme. The mesenchyme is located medially. Within the mesenchymal compartment, a blastema is established at the distal or growing end, of each ray. Blastemas are comprised largely of dividing cells that contribute to new tissue growth (reviewed in [36], [37]). The *hapln1a* mRNA is

expressed throughout the mesenchyme with slightly higher expression in the blastema, and to a lesser extent in the skeletal precursor cells (Figure 2.1).

In order to provide a secondary test to demonstrate *cx43*-dependence of *hapln1a*, we examined its expression in fins treated for *cx43* knockdown [13]. Indeed, the expression of *hapln1a* is reduced in WT fins treated for *cx43* knockdown compared to *cx43* mismatch-treated fins by both in situ hybridization (Figure 2.2) and by qPCR (Table 2.2). In contrast, *cx43* expression is not reduced in WT fins treated for *hapln1a* knockdown (Table 2.2), indicating that *cx43* expression does not depend on *hapln1a*. In summary, we find that *hapln1a* is reduced both in *sof*^{b123} and in *cx43* knockdown fins, providing independent confirmation that *hapln1a* is expressed in a *cx43*-dependent manner. Together, these data support the conclusion that *hapln1a* is molecularly downstream of *cx43*.

To evaluate when during fin growth *hapln1a* may be required in WT regenerating fins, we examined the expression pattern of *hapln1a* in non-regenerating fins, and at 2 dpa, 3 dpa, 5 dpa and 8 dpa (Figure 2.3). In non-regenerating fins *hapln1a* expression was not detectable. By 2 dpa, the expression of *hapln1a* was slightly up-regulated, and by 3 dpa *hapln1a* was expressed strongly within each fin ray. At 5 dpa, there was a clear decrease in expression, and its expression was decreased even more by 8 dpa. Thus, *hapln1a* expression is expressed at 2 dpa and is maximally expressed at 3 dpa. The maximum expression at 3 dpa corresponds with the time point at which maximum rate of regeneration has been observed [38].

Hapln1a is functionally downstream of Cx43

In order to determine if *hapln1a* is functionally downstream of *cx43*, we completed morpholino-mediated gene knockdown of *hapln1a* in WT regenerating fins [13], [15]. Two targeting morpholinos (MOs) were generated, an ATG blocker (ATG MO) that inhibits protein translation and a splice blocker (Splice MO) that was designed to inhibit the splicing of intron 1. As a control, we used a mismatch MO (MM MO), which includes five mismatches to the target sequence for the ATG-blocking MO (Table 2.1). All MOs are conjugated to fluorescein, permitting validation of cellular uptake. Following microinjection and electroporation, MO-positive fish were selected for fluorescein-positive cells at 24 hours post electroporation (hpe). Positive fins were either harvested for analysis of cell proliferation or permitted to regenerate for 4 additional days for evaluation of segment length and regenerate length. The effect of *hapln1a* knockdown on cell proliferation was evaluated by counting the number of mitotic cells detected by H3P immunostaining. Regenerate length was measured as the distance between the amputation plane and the distal end of the fin. Segment length was measured as the distance between the first two joints in the regenerate. Interestingly, we found that *hapln1a* knockdown with both the ATG MO and Splice MO exhibited the same phenotypes as *cx43* knockdown. Thus, knockdown fins exhibited reduced fin length (Figure 2.4A), reduced segment length (Figure 2.4B), and reduced cell proliferation (Figure 2.4C). The specificity of these knockdowns is demonstrated by the use of two independent gene-targeting MOs and also by the mismatch control.

Collectively, these data reveal that *cx43* and *hapln1a* act in a common pathway to promote cell proliferation and to inhibit joint formation.

Hapln1a knockdown destabilizes HA

To evaluate the effect of *hapln1a* knockdown on HA in WT regenerating fins, we completed a MO-mediated *hapln1a* knockdown (i.e. using the ATG MO) and evaluated both Hapln1a staining and HA staining on the treated fins. The success of *hapln1a* MO-mediated protein knockdown was further confirmed by immunostaining. Thus, comparison of the MM MO treated fins with the ATG MO treated fins revealed that Hapln1a protein is reduced following *hapln1a* knockdown (Figure 2.5A-B). Moreover, reduced Hapln1a protein levels in ATG MO treated fins were confirmed through immunoblotting (Figure 2.5C). Hapln1a protein is glycosylated and typically detected as several bands above its predicted molecular weight of 38 kD [35]. All bands are reduced following Hapln1a knockdown. Since Hapln1a is crucial for the stabilization of the HA-PG network in the ECM, we also evaluated the level of HA in *hapln1a* knockdown fins. We utilized biotinylated HA-binding protein (HABP-biotin) in combination with streptavidin-Alexa546 to detect HA. First, we demonstrate that HABP is specific for the detection of HA by treating fin sections with the HA-degrading enzyme hyaluronidase. Endogenous levels of HA may be observed in WT 5 dpa fins (untreated). In contrast, treatment of fin sections with hyaluronidase greatly reduced the staining by HABP (Figure 2.6A-B), suggesting that HA is required for detection. Importantly, we also observed a clear reduction in the amount of detectable

HA following *hapln1a* knockdown (Figure 2.6C-D). These findings strongly support the hypothesis that HA is destabilized in the absence of sufficient Hapln1a.

To further demonstrate that *hapln1a* functions in a *cx43*-dependent manner, we next evaluated HA levels in both *sof*^{b123} regenerating fins and in fins treated for *cx43*-knockdown [13]. Since *hapln1a* levels depend upon Cx43 activity, we predicted that reduced Cx43 would similarly lead to reduced levels of HA. Indeed, this is what we found. In *sof*^{b123} regenerating fins compared with WT regenerating fins, we observed reduced levels of HA (Figure 2.7A-B). Similarly, in WT fins treated for MO mediated *cx43* knockdown, HA levels are reduced compared with the MM control-treated fins (Figure 2.7C-D). Together with our previous findings, these data strongly support the conclusion that *hapln1a* functions in a common pathway with *cx43*, and that this pathway mediates cell proliferation and joint formation at least in part through influencing the Hapln1a-based ECM.

Hapln1a functions in a cx43-dependent and sema3d-independent genetic pathway

In our recent study, we found that Cx43 and Sema3d function in a common molecular pathway to promote cell proliferation and joint formation [18]. We next wished to determine how *hapln1a* contributes to this previously defined pathway. Our prior findings suggest that Sema3d utilizes the Nrp2a receptor to mediate cell proliferation and the PlxnA3 receptor to mediate joint formation. Indeed, in addition to Cx43 knockdown, both Sema3d- and PlxnA3 knockdown rescues joint formation in *alf*^{dy86}. Therefore, we first tested if *hapln1a* knockdown functioned similarly.

Interestingly, segment length was not rescued in *alf^{dy86}* fins by *hapln1a* knockdown (Figure 2.8). Failure of *hapln1a* knockdown to rescue segment length in *alf^{dy86}* was not due to a failure of the knockdown, since both Hapln1a and HA was similarly reduced (i.e. evaluated by immunostaining for Hapln1a protein or for HA levels as completed above, see Figure 2.9). The finding that *hapln1a* knockdown does not rescue joint formation in *alf^{dy86}* is consistent with our finding that *hapln1a* is not up-regulated in *alf^{dy86}*. Moreover, this suggests that *hapln1a* functions independently of *sema3d-plxna3*-dependent joint formation. We next evaluated changes in *hapln1a* and *sema3d* gene expression following reciprocal knockdown experiments. Thus, in *sema3d* knockdown fins *hapln1a* is not affected (Table 2.2), suggesting that *hapln1a* is not downstream of *sema3d*. Similarly, in *hapln1a* knockdown fins *sema3d* expression is not affected (Table 2.2), suggesting that *sema3d* is not downstream of *hapln1a*. Collectively, our findings provide evidence that *hapln1a* and *sema3d* both function downstream of *cx43*, but independently of each other. Therefore, these data suggest that at least two pathways contribute to *cx43*-dependent cell proliferation and *cx43*-dependent joint formation (Figure 2.8A). Future studies will be completed to determine if the *Sema3d* and *Hapln1a* gene products instead functionally interact in a common pathway.

2.5 Discussion

This is the first report to provide a functional analysis of *hapln1a* in zebrafish. Our finding that *Hapln1a* functions downstream of *Cx43* is supported by multiple

independent lines of evidence. The *hapln1a* gene exhibited reduced expression levels in *sof*^{b123} and *cx43* knockdown fins compared to WT regenerating fins by in situ hybridization. Additionally, qPCR analysis confirmed that *hapln1a* expression is dependent upon the level of *cx43* expression. Knockdown of Hapln1a using two independent MOs recapitulated all of the Cx43-dependent phenotypes, namely reduced regenerate length, reduced segment length, and reduced cell proliferation. Thus, *hapln1a* functions downstream of *cx43*. Moreover, we found that HA levels were strongly reduced in Hapln1a knockdown fins, suggesting that the loss of Hapln1a protein influences the stability of HA. The finding that HA levels are similarly reduced in *sof*^{b123} and in *cx43* knockdown fins provides additional evidence that *cx43* and *hapln1a* function in a common pathway. Attempts to include *hapln1a* in the established *cx43-sema3d* pathway suggest that *hapln1a* may function independently of *sema3d* (Figure 2.10A). Therefore, Cx43 promotes cell proliferation and suppresses joint formation via the coordination of (at least) two downstream pathways. We find it interesting that Hapln1a is located in the ECM that physically connects the medial *cx43*-positive compartment of dividing cells [8] and the lateral *sema3d*-positive compartment of skeletal precursor cells [18]. The functional significance of this observation is unclear.

Hapln1a belongs to the hyaluronectin superfamily, which includes four members in mammals (HAPLN1-4) and five in zebrafish, where the *hapln1* gene appears to have duplicated into *hapln1a* and *hapln1b*. These genes share high degrees of sequence homology, especially in the amino acid sequence coding for the link

module [25], [39]. Hapln1 was first identified in cartilage, however it can also be found in non-cartilaginous tissue like sclera [40], aorta [41], brain [42], dermis of the embryonic skin [43], and in chicken embryonic mesonephros [44]. During zebrafish embryogenesis, expression of *hapln1a* has been observed in multiple tissues, including somites, floor plate, hypochord, and rhombomeres [45]. During jaw and skull formation, *hapln1a* expression co-localized with the PG aggrecan in the pharyngeal arches and with the PG dermacan in the pectoral fins [45]. Functional studies were not performed as part of these studies. However, reduced Hapln1 function is correlated with skeletal defects in other animals, including human. For example, single-nucleotide polymorphisms identified in the *HAPLN1* gene have recently been associated with spinal osteoarthritis in aging female populations [46]. Moreover, targeted gene knockout of *CRTL1* (aka *HAPLN1*) in the mouse reveals that Crtl1/Hapln1 is indispensable during skeletal development. For example, the *CRTL1*^{-/-} mouse showed defects in cartilage and bone development with short limbs and craniofacial abnormalities, suggesting a prominent function for Crtl1 during chondrocyte differentiation [19]. In addition to these skeletal defects, *CRTL1*^{-/-} mice die perinatally and exhibit a spectrum of myocardial defects. These defects have been attributed to the reduction in the PG versican [47], which may promote cell proliferation [48]–[50]. Interestingly, cartilage-specific expression of transgenic Crtl1/Hapln1a inhibits perinatal lethality and rescues skeletal abnormalities in *CRTL1*^{-/-} mice [51], reinforcing the importance of the HA-PG network during heart development and skeletogenesis. These studies provide evidence that the “link” function of Hapln1 is critical for stability

of components of the ECM and for regulation of cell differentiation and cell proliferation. Our findings on the function of Hapln1a in the regenerating fin are consistent with the role of Hapln1 in the developing mouse skeleton. Future studies will be focused on defining how Hapln1a mediates skeletal growth and patterning.

We propose that Cx43 activity in the blastema activates gene expression of *hapln1a* in the medial mesenchyme (Figure 2.10B). Secretion of Hapln1a in the ECM establishes the HA-PG network, stabilizes HA, and contributes to the regulation of cell proliferation and joint formation via unknown mechanisms. The Hapln1a-dependent ECM might be involved in providing the necessary microenvironment for the surrounding cells. Alternatively, Hapln1a may be required to maintain a stable population of HA, which in turn mediates signaling pathways through interaction with HA-specific cell surface receptors. Indeed, it is known that HA has diverse functions in skeletal biology including bone remodeling [22], bone resorption [52], and osteogenesis [53], [54]. Further, there is growing evidence that the ECM can influence interactions between locally secreted growth factors and their receptors [55]–[59]. Continued studies are required to determine if Hapln1a plays direct or indirect roles in influencing cellular behaviors required during fin skeletal morphogenesis.

2.6 Conclusions

The identification of the Cx43-dependent Hapln1a pathway is novel and reveals tangible roles for the ECM during bone growth and skeletal patterning. We find that reduced Hapln1a levels are correlated with reduced HA levels, which may provide

insights into the underlying mechanism of Hapln1a function. Combined with known skeletal defects associated with the loss of Hapln1 in the mouse, and with skeletal diseases associated with Hapln1 polymorphisms in human, these findings demonstrate that the role of Hapln1a is conserved in zebrafish. Therefore, continued studies designed to elucidate the mechanism of Hapln1a-dependent cell proliferation and joint formation will provide new and relevant insights into skeletal development in all vertebrates.

2.7 Figures

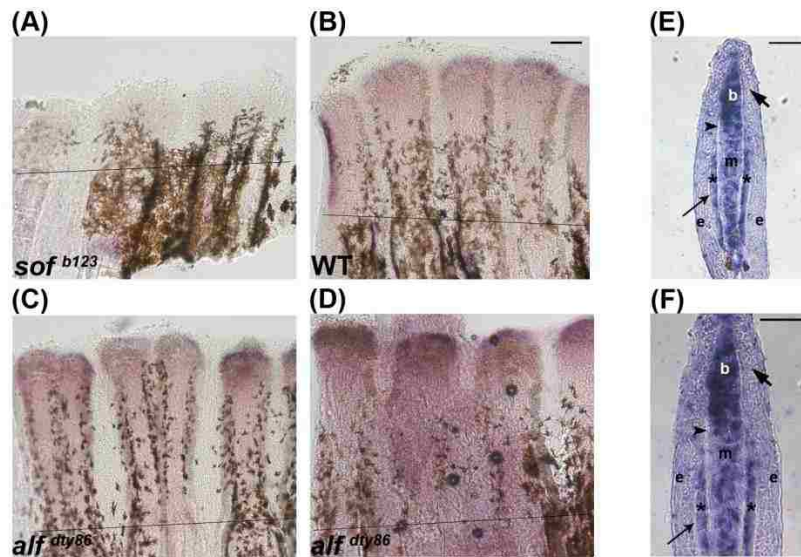


Figure 2.1: Validation of microarray results by in situ hybridization using whole mount in situ hybridization on 5 dpa regenerating fins. (A) *hapln1a* expression is reduced in *sof*^{b123} compared with WT (B). (C,D) *alf*^{dty86} expression is variable. (E,F) In situ hybridization on a WT 5 dpa cryosection reveals compartment specific expression of *hapln1a*, mainly in the blastema (b), in the mesenchyme (m), and skeletal precursor cells (*). The thick arrow identifies the basal layer of the epidermis, which underlies the epidermis (e). The thin arrow identifies lepidotrichia and the arrowhead identifies the actinotrichia. The amputation plane is indicated in panels A-D. Scale bar in E and F is 50 μ m.

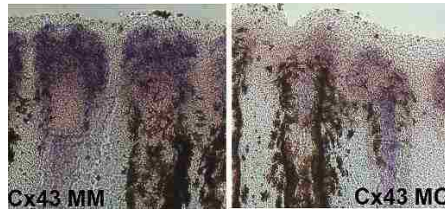


Figure 2.2: Cx43 knock down results in reduced expression levels of *hapln1a*. Whole mount in situ hybridization shows reduced expression of *hapln1a* in WT fins treated for *cx43* knock-down (Cx43KD) fins compared to WT fins treated for *cx43* mismatch control (Cx43MM) control fins.

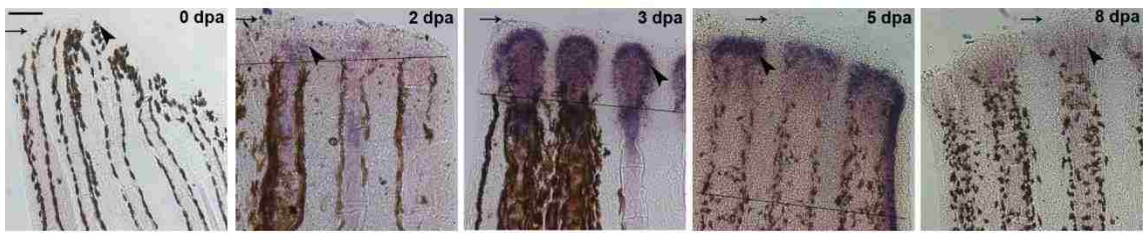


Figure 2.3: *hapln1a* expression pattern at different time points in regenerating fin.

Whole mount in situ hybridization for *hapln1a* on regenerating fins at different time points. The *hapln1a* gene is not expressed during normal fin growth (uncut). Expression of *hapln1a* initiates around 2 dpa and is maximally expressed at 3 dpa, followed by gradual reduction at 5 dpa and 8 dpa. Arrow identifies the distal end of the fin; the arrowhead identifies region of staining (or where staining would be observed in uncut fins). The amputation plane is indicated for 2 dpa, 3 dpa, and 5 dpa, and is out of the field of view for the 8 dpa image. Scale bar is 50 μ m.

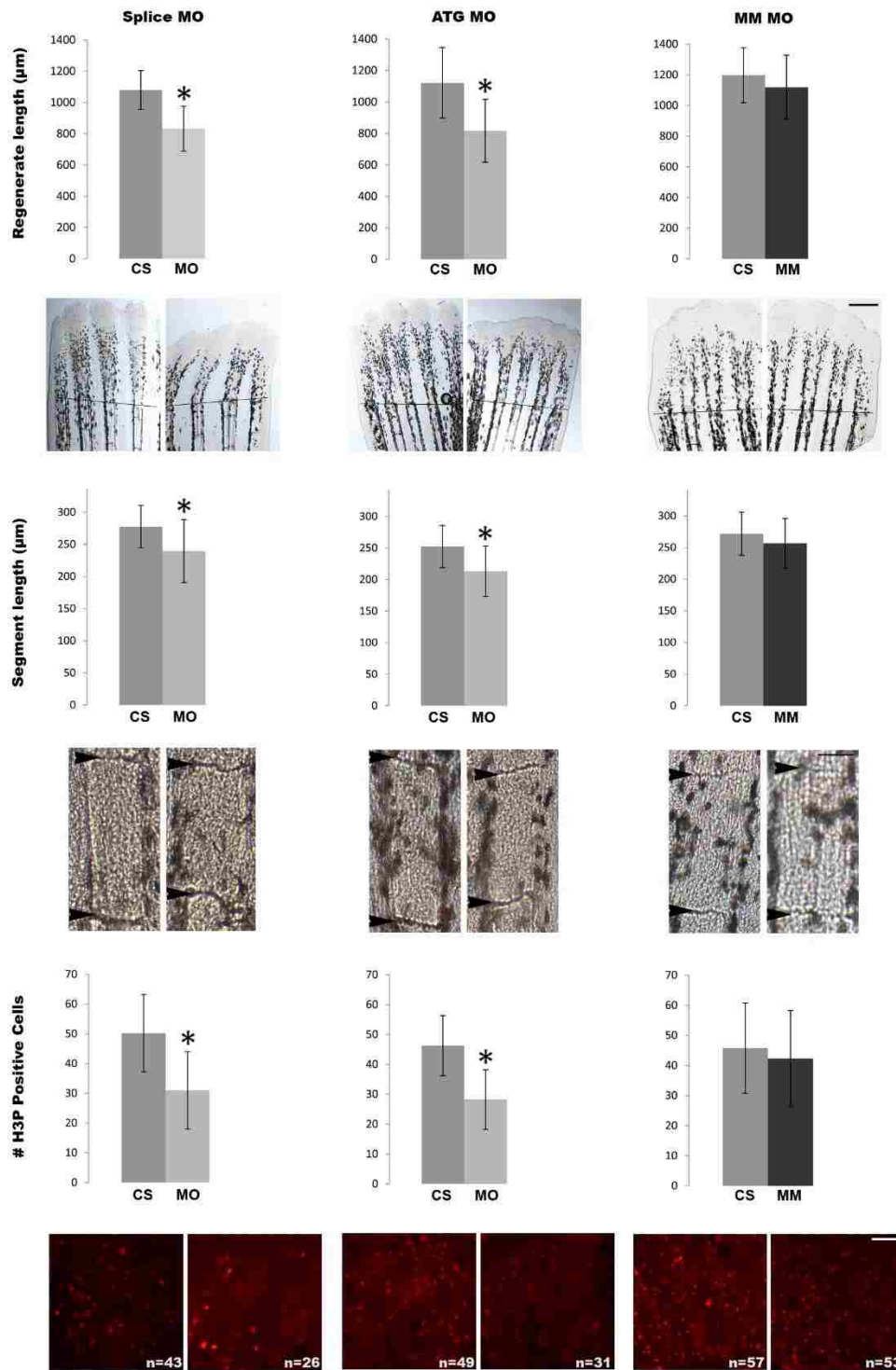


Figure 2.4: Morpholino mediated knock-down of *hapln1a* recapitulates all *cx43*-dependent phenotypes. (Top row) Total regenerate length was measured in MO and MM treated fins. *Hapln1a* knock-down resulted in reduced fin length (*). The dotted

line represents the amputation plane. (Middle row) Segment length was measured in MO and MM treated fins. Hapln1a knock-down resulted in reduction of segment length (*). Arrowheads identify joints. (Bottom row) Total number of H3P positive cells (red) was counted. Images of representative whole fins stained for H3P are shown for each condition. Knock-down of Hapln1a resulted in reduced cell proliferation (*) compared to the mismatch control. MO represents targeting morpholino; ATG MO targets translation initiation; Splice MO targets splicing event; MM represents control morpholino with 5 mismatches to target sequence; CS represents uninjected/untreated side. All experiments were completed in triplicate with a minimum of five fins treated with MO per trial. Statistical significance was determined by student's *t*-test where $p < 0.05$. By student's *t*-test, there is no statistical difference between MM and CS. Error bars represent the standard deviation. Scale bar is 50 μm .

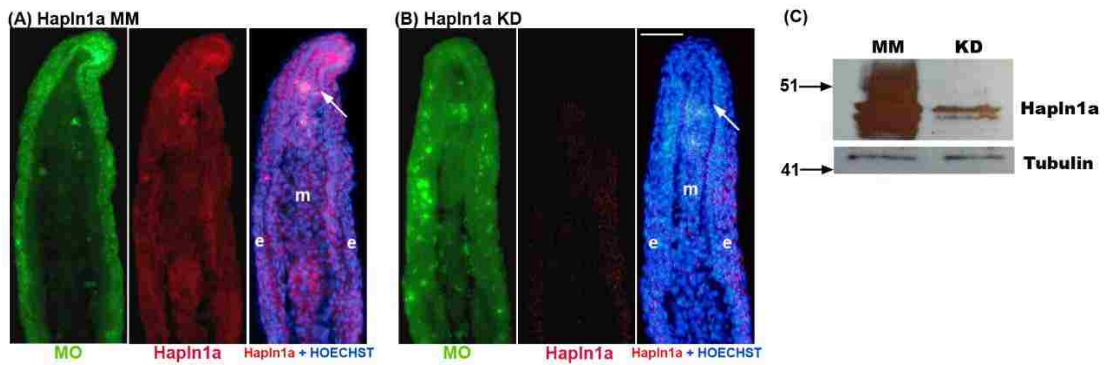


Figure 2.5: Morpholino mediated knock-down of *hapln1a* in WT regenerating fins results in reduced Hapln1a. Immunostaining for Hapln1a and HOECHST staining for DNA (blue). The green reveals the location of the targeting and control MOs, which are fluorescein tagged. (A) Longitudinal section of a fin ray treated with Hapln1a control morpholino (MM). (B) Longitudinal section of a fin ray knocked down for Hapln1a with a targeting morpholino (KD). Compared to the control MM fins, Hapln1a knock-down (KD) fins exhibit reduced staining for Hapln1a. (C) Immunoblots confirming reduced levels of Hapln1a protein following Hapln1a knockdown. Hapln1a-MO treated fins (KD) were compared to control morpholino (MM). Tubulin was used as a loading control. Arrow identifies the basal layer of the epidermis; m, mesenchyme; e, epithelium. Scale bar is 50 μ m.

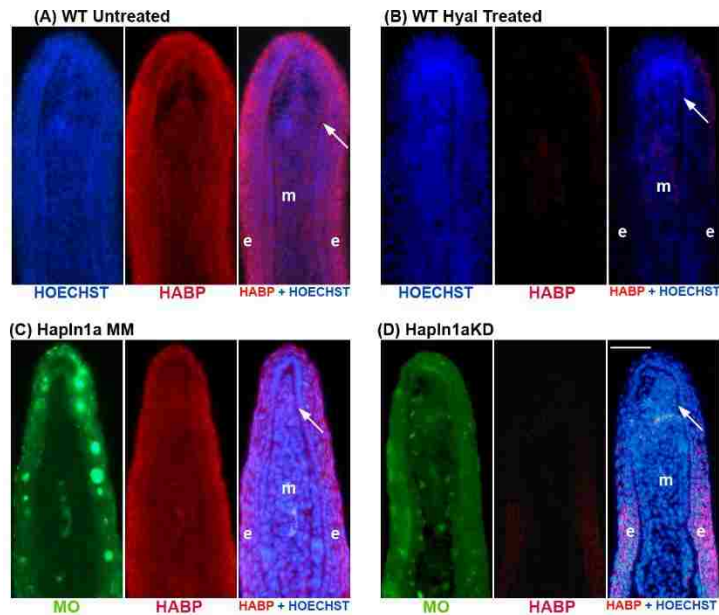


Figure 2.6: Morpholino mediated knock-down of *hapln1a* in WT regenerating fins results in reduced HA levels. HA is detected by biotin-HABP with streptavidin-Alexa-546. HOECHST detects DNA (blue). The green reveals the location of the targeting and control MOs, which are fluorescein tagged. (A, B) Fin sections from 5 dpa WT regenerating fins were either untreated or treated with hyaluronidase. The reduced signal in the hyaluronidase-treated sections demonstrates that HABP detects HA. (C) Longitudinal section of a fin ray treated with Hapln1a control morpholino (MM). (D) Longitudinal section of a fin ray knocked down for Hapln1a with a targeting morpholino (KD). Compared to the control MM fins, Hapln1a knock-down (KD) fins exhibit reduced staining for HA. Arrow identifies the basal layer of the epidermis; m, mesenchyme; e, epithelium. Scale bar is 50 μ m.

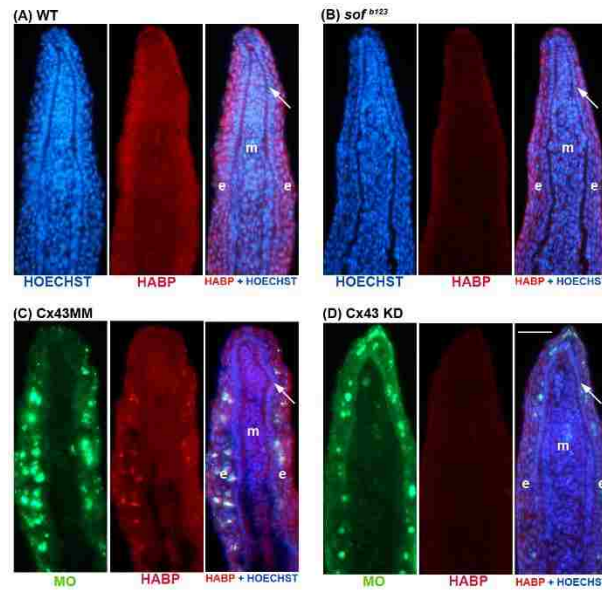


Figure 2.7: HA levels are reduced in *sof*^{b123} and in *cx43*-KD regenerating fins. Immunostaining for HA (Red) and HOECHST staining for DNA (blue). In the panels treated for *cx43*-MO or MM, the green reveals the location of the MOs, which are fluorescein tagged. HA levels were detected as described in [Figure 2.5](#). (A,C) HA levels in WT 5 dpa regenerating fins and in WT fins treated for *cx43*-MM. (B,D) HA levels are reduced in *sof*^{b123} regenerating fins and in WT fins treated for *cx43*-MO. Arrow identifies the basal layer of the epidermis; m, mesenchyme; e, epithelium. Scale bar is 50 μ m.

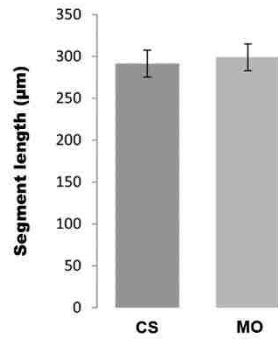


Figure 2.8: Hapln1a knock-down does not rescue segment length in *alf^{dy86}*. Compared to the uninjected control side (CS) the Hapln1a morpholino treated side (MO) does not show significant difference in the segment length. Statistical significance was determined by Student's *t*-test where $p < 0.05$. Error bars represent the standard deviation.

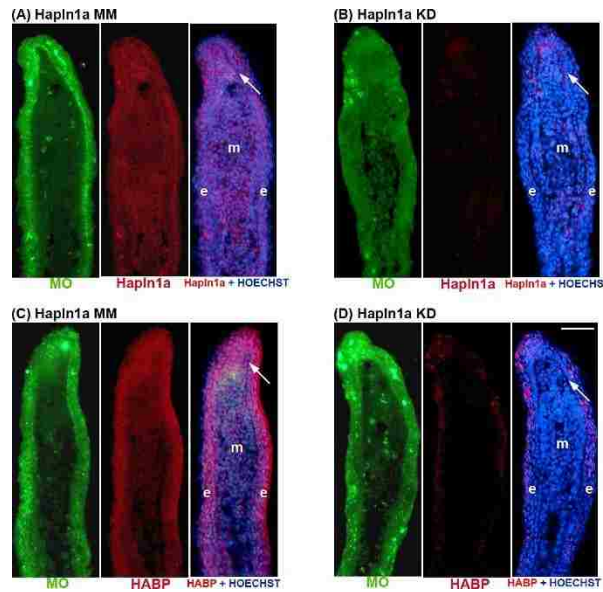


Figure 2.9: The *hapln1a*-KD was effective in *alf^{dy86}*. Immunostaining for Hapln1a or HA (Red) and HOECHST staining for DNA (blue). The green reveals the location of the targeting and control MOs, which are fluorescein tagged (A) Longitudinal section of an *alf^{dy86}* fin ray treated with Hapln1a control morpholino (MM). (B) Longitudinal section of an *alf^{dy86}* fin ray knocked down for Hapln1a with a targeting morpholino (KD). Compared to the control MM fins, Hapln1a knock-down (KD) fins exhibit reduced staining for Hapln1a. HA was detected by biotinylated-HABP followed by streptavidin-Alexa 546 conjugate. (C) Longitudinal section of an *alf^{dy86}* fin ray treated with Hapln1a control morpholino (MM). (D) Longitudinal section of an *alf^{dy86}* fin ray knocked down for Hapln1a with a targeting morpholino (KD). Compared to the control MM fins, Hapln1a knock-down (KD) fins exhibit reduced staining for HA. Arrow identifies the basal layer of the epidermis; m, mesenchyme; e, epithelium. Scale bar is 50 μ m.

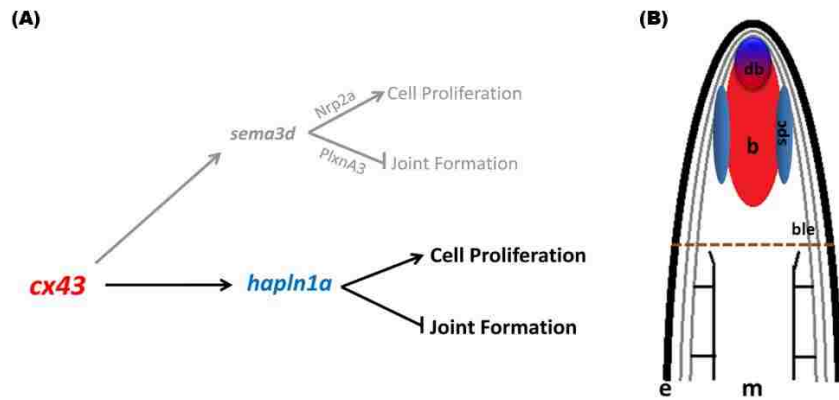


Figure 2.10: Model depicting Cx43-Hapln1a mediated effect on skeletal patterning during fin regeneration. (A) Proposed pathway for Hapln1a mediated effects of Cx43. Hapln1a functions in *cx43*-dependent, but *sema3d*-independent pathway, positively influencing cell proliferation and inhibiting joint formation. (B) Cartoon illustrating the compartments of gene in the regenerating fin: The *cx43* mRNA is expressed throughout the mesenchyme (red) accompanied by *cx43*-dependent *hapln1a* upregulation in the same compartment (red), but primarily in the distal blastema (blue-red) and to a lesser extent in the proximal skeletal precursor cells (blue). e, epithelium; m, mesenchyme; b, blastema; db, distal blastema; spc, skeletal precursor cells; ble, basal layer of epidermis.

2.8 Tables

Gene	Primers for ISH	Primers for qRT-PCR	Morpholinos
<i>hapln1a</i>	F = GGTCTCCGCTTG- GCAGCG RT7 = TAATACGA- CTCACTATAGGGCCCA- TCCCTGCCCTAAGACC	F = AACGACTATGGCACATACCGG R = AAGGTTGTACCGCCCCAAA	Splice MO = ATCAAAAGTGAT- TCTTACCTTGTC ATG MO = GCCAC- AGAAAACAGAGCAATCATCT 5MM MO = GCCAGACAAAAGAGACCAATGATCT
<i>sema3d</i>	F = CGAAGTGTAGTACCATTACG RT7 = TAATACGACTCACTATA- GGGTATGAGGATCATATGTCC	F = TGGATGAGGAGAGAAGCCGAT R = GCAGGCCAGCTCAACTTTTT	MO = TGTCCGGCTCCCTGCAGTCTTCAT 5MM = TGTCCCGCTGCCCTCCACTCTTCAT
<i>actin</i>		F = TTTTGTGGAGATGATGCC R = CCAACCATCACTCCCTGATGT	

The T7 RNA polymerase binding site is in bold in the reverse primers. F = Forward primer; RT7 = Reverse primer; MO = targeting morpholino; ATG MO = targets translation initiation; Splice MO = targets splicing event; 5MM = control morpholino with 5 mismatch pairs to target sequence. All primers and MOs are shown in the 5'-3' orientation.

doi:10.1371/journal.pone.0088574.t001

Table 2.1 Primers and Morpholinos

Samples compared	Gene	$\Delta C_T(\text{Mut/} \text{MO})$ Gene-Actin ^a	$\Delta C_T(\text{WT/MM})$ Gene-Actin ^a	$\Delta \Delta C_T = \Delta C_T(\text{Mut/} \text{MO}) - (\text{WT/MM})$ ^b	Fold difference relative to WT/MM ^c
<i>sof</i> ^{bt23} with WT	<i>hapln1a</i>	6.51±0.13	4.99±0.10	1.52±0.13	0.35 (0.32–0.38)
<i>alj</i> ^{dy86} with WT	<i>hapln1a</i>	4.97±0.25	4.99±0.10	−0.02±0.25	1.01 (0.85–1.20)
<i>cx43</i> KD with MM	<i>hapln1a</i>	6.57±0.23	5.67±0.08	0.90±0.23	0.53 (0.46–0.63)
<i>sema3d</i> KD with MM	<i>hapln1a</i>	4.89±0.20	5.13±0.19	−0.24±0.20	1.18 (1.03–1.36)
<i>hapln1a</i> KD with MM	<i>cx43</i>	2.78±0.10	2.84±0.19	−0.06±0.10	1.04 (0.97–1.12)
<i>hapln1a</i> KD with MM	<i>sema3d</i>	6.69±0.15	6.90±0.15	−0.21±0.15	1.15 (1.04–1.28)

a. The ΔC_T value is determined by subtracting the average Actin C_T value from the average Gene C_T value. The standard deviation of the difference is calculated from the standard deviations of the gene and actin values using the Comparative Method.

b. The calculation of $\Delta \Delta C_T$ involves subtraction by the ΔC_T calibrator value. This is subtraction of an arbitrary constant, so the standard deviation of $\Delta \Delta C_T$ is the same as the standard deviation of the ΔC_T value.

c. The range given for gene relative to WT/MM is determined by evaluating the expression: $2^{\Delta \Delta C_T}$ with $\Delta \Delta C_T + s$ and $\Delta \Delta C_T - s$, where s = the standard deviation of the $\Delta \Delta C_T$ value.

doi:10.1371/journal.pone.0088574.t002

Table 2.2 Quantitative RT-PCR confirms changes in gene expression

2.9 References

1. Oyamada M, Oyamada Y, Takamatsu T (2005) Regulation of connexin expression. *Biochim Biophys Acta* 1719: 6–23.
2. Goodenough DA, Goliger JA, Paul DL (1996) Connexins, connexons, and intercellular communication. *Annu Rev Biochem* 65: 475–502.
3. Paznekas WA, Boyadjiev SA, Shapiro RE, Daniels O, Wollnik B, et al. (2003) Connexin 43 (GJA1) mutations cause the pleiotropic phenotype of oculodentodigital dysplasia. *Am J Hum Genet* 72: 408–418.
4. Kjaer KW, Hansen L, Eiberg H, Leicht P, Opitz JM, et al. (2004) Novel Connexin 43 (GJA1) mutation causes oculo-dento-digital dysplasia with curly hair. *Am J Med Genet A* 127A: 152–157.
5. Richardson R, Donnai D, Meire F, Dixon MJ (2004) Expression of Gja1 correlates with the phenotype observed in oculodentodigital syndrome/type III syndactyly. *J Med Genet* 41: 60–67.
6. Reaume AG, de Sousa PA, Kulkarni S, Langille BL, Zhu D, et al. (1995) Cardiac malformation in neonatal mice lacking connexin43. *Science* 267: 1831– 1834.
7. Ya J, Erdtsieck-Ernste EB, de Boer PA, van Kempen MJ, Jongsma H, et al. (1998) Heart defects in connexin43-deficient mice. *Circ Res* 82: 360–366.
8. Iovine MK, Higgins EP, Hindes A, Coblitz B, Johnson SL (2005) Mutations in connexin43 (GJA1) perturb bone growth in zebrafish fins. *Dev Biol* 278: 208– 219.

9. Lecanda F, Warlow PM, Sheikh S, Furlan F, Steinberg TH, et al. (2000) Connexin43 deficiency causes delayed ossification, craniofacial abnormalities, and osteoblast dysfunction. *J Cell Biol* 151: 931–944.
10. Becker DL, McGonnell I, Makarenkova HP, Patel K, Tickle C, et al. (1999) Roles for alpha 1 connexin in morphogenesis of chick embryos revealed using a novel antisense approach. *Dev Genet* 24: 33–42.
11. Law LY, Lin JS, Becker DL, Green CR (2002) Knockdown of connexin43-mediated regulation of the zone of polarizing activity in the developing chick limb leads to digit truncation. *Dev Growth Differ* 44: 537–547.
12. Hoptak-Solga AD, Klein KA, DeRosa AM, White TW, Iovine MK (2007) Zebrafish short fin mutations in connexin43 lead to aberrant gap junctional intercellular communication. *FEBS Lett* 581: 3297–3302.
13. Hoptak-Solga AD, Nielsen S, Jain I, Thummel R, Hyde DR, et al. (2008) Connexin43 (GJA1) is required in the population of dividing cells during fin regeneration. *Dev Biol* 317: 541–548.
14. van Eeden FJ, Granato M., Schach U., Brand M., Furutani-Seiki M., Haffter P., Hammerschmidt M., Heisenberg, C P., Jiang, Y J., Kane, D A., Kelsh, R N., Mullins, M C., Odenthal J., Warga, R M., Nusslein-Volhard C. (1996) Genetic analysis of fin formation in the zebrafish, *Danio rerio*. *Development* 123: 255– 262.
15. Sims K, Jr., Eble DM, Iovine MK (2009) Connexin43 regulates joint location in zebrafish fins. *Dev Biol* 327: 410–418.

16. Stains JP, Civitelli R (2005) Cell-cell interactions in regulating osteogenesis and osteoblast function. *Birth Defects Res C Embryo Today* 75: 72–80.
17. Stains JP, Lecanda F, Screen J, Towler DA, Civitelli R (2003) Gap junctional communication modulates gene transcription by altering the recruitment of Sp1 and Sp3 to connexin-response elements in osteoblast promoters. *J Biol Chem* 278: 24377–24387.
18. Ton QV, Iovine M (2012) Semaphorin3d mediates Cx43-dependent phenotypes during fin regeneration. *Dev Biol* 366: 195–203.
19. Watanabe H, Yamada Y (1999) Mice lacking link protein develop dwarfism and craniofacial abnormalities. *Nat Genet* 21: 225–229.
20. Andreasen EA, Mathew LK, Lohr CV, Hasson R, Tanguay RL (2007) Aryl hydrocarbon receptor activation impairs extracellular matrix remodeling during zebra fish fin regeneration. *Toxicol Sci* 95: 215–226.
21. Bai SX, Wang YL, Qin L, Xiao ZJ, Herva R, et al. (2005) Dynamic expression of matrix metalloproteinases (MMP-2, -9 and -14) and the tissue inhibitors of MMPs (TIMP-1, -2 and -3) at the implantation site during tubal pregnancy. *Reproduction* 129: 103–113.
22. Bastow ER, Byers S, Golub SB, Clarkin CE, Pitsillides AA, et al. (2008) Hyaluronan synthesis and degradation in cartilage and bone. *Cell Mol Life Sci* 65: 395–413.

23. Contreras EG, Gaete M, Sanchez N, Carrasco H, Larrain J (2009) Early requirement of Hyaluronan for tail regeneration in *Xenopus* tadpoles. *Development* 136: 2987–2996.
24. Knudson CB, Knudson W (1993) Hyaluronan-binding proteins in development, tissue homeostasis, and disease. *FASEB J* 7: 1233–1241.
25. Neame PJ, Barry FP (1993) The link proteins. *Experientia* 49: 393–402.
26. Sherman L, Sleeman J, Herrlich P, Ponta H (1994) Hyaluronate receptors: key players in growth, differentiation, migration and tumor progression. *Curr Opin Cell Biol* 6: 726–733.
27. Santamaria JA, Becerra J (1991) Tail fin regeneration in teleosts: cell-extracellular matrix interaction in blastemal differentiation. *J Anat* 176: 9–21.
28. Ghatak S, Misra S, Toole BP (2005) Hyaluronan constitutively regulates ErbB2 phosphorylation and signaling complex formation in carcinoma cells. *J Biol Chem* 280: 8875–8883.
29. Jiang D, Liang J, Noble PW (2007) Hyaluronan in tissue injury and repair. *Annu Rev Cell Dev Biol* 23: 435–461.
30. Misra S, Toole BP, Ghatak S (2006) Hyaluronan constitutively regulates activation of multiple receptor tyrosine kinases in epithelial and carcinoma cells. *J Biol Chem* 281: 34936–34941.
31. Iovine MK, Johnson SL (2000) Genetic analysis of isometric growth control mechanisms in the zebrafish caudal fin. *Genetics* 155: 1321–1329.

32. Westerfield M (1993) *The Zebrafish Book: A guide for the laboratory use of zebrafish (Brachydanio rerio)*. University of Oregon Press, Eugene, OR.
33. Li Y, Toole BP, Dealy CN, Kosher RA (2007) Hyaluronan in limb morphogenesis. *Dev Biol* 305: 411–420.
34. Matsumoto K, Li Y, Jakuba C, Sugiyama Y, Sayo T, et al. (2009) Conditional inactivation of Has2 reveals a crucial role for hyaluronan in skeletal growth, patterning, chondrocyte maturation and joint formation in the developing limb. *Development* 136: 2825–2835.
35. Sun GW, Kobayashi H, Suzuki M, Kanayama N, Terao T (2002) Production of cartilage link protein by human granulosa-lutein cells. *J Endocrinol* 175: 505– 515.
36. Akimenko MA, Mari-Beffa M, Becerra J, Geraudie J (2003) Old questions, new tools, and some answers to the mystery of fin regeneration. *Dev Dyn* 226: 190– 201.
37. Poss KD, Keating MT, Nechiporuk A (2003) Tales of regeneration in zebrafish. *Dev Dyn* 226: 202–210.
38. Lee Y, Grill S, Sanchez A, Murphy-Ryan M, Poss KD (2005) Fgf signaling instructs position-dependent growth rate during zebrafish fin regeneration. *Development* 132: 5173–5183.
39. Kohda D, Morton CJ, Parkar AA, Hatanaka H, Inagaki FM, et al. (1996) Solution structure of the link module: a hyaluronan-binding domain involved in extracellular matrix stability and cell migration. *Cell* 86: 767–775.

40. Lohmander LS, De Luca S, Nilsson B, Hascall VC, Caputo CB, et al. (1980) Oligosaccharides on proteoglycans from the swarm rat chondrosarcoma. *J Biol Chem* 255: 6084–6091.
41. Gardell S, Baker J, Caterson B, Heinegard D, Roden L (1980) Link protein and a hyaluronic acid-binding region as components of aorta proteoglycan. *Biochem Biophys Res Commun* 95: 1823–1831.
42. Ripellino JA, Margolis RU, Margolis RK (1989) Immunoelectron microscopic localization of hyaluronic acid-binding region and link protein epitopes in brain. *J Cell Biol* 108: 1899–1907.
43. Binette F, Cravens J, Kahoussi B, Haudenschild DR, Goetinck PF (1994) Link protein is ubiquitously expressed in non-cartilaginous tissues where it enhances and stabilizes the interaction of proteoglycans with hyaluronic acid. *J Biol Chem* 269: 19116–19122.
44. Stirpe NS, Dickerson KT, Goetinck PF (1990) The chicken embryonic mesonephros synthesizes link protein, an extracellular matrix molecule usually found in cartilage. *Dev Biol* 137: 419–424.
45. Kang JS, Kawakami Y, Bekku Y, Ninomiya Y, Izpisua Belmonte JC, et al. (2008) Molecular cloning and developmental expression of a hyaluronan and proteoglycan link protein gene, *crtl1/hapln1*, in zebrafish. *Zoolog Sci* 25: 912–918.
46. Urano T, Narusawa K, Shiraki M, Sasaki N, Hosoi T, et al. (2011) Singlenucleotide polymorphism in the hyaluronan and proteoglycan link protein 1 (HAPLN1) gene is

associated with spinal osteophyte formation and disc degeneration in Japanese women. *Eur Spine J* 20: 572–577.

47. Wirrig EE, Snarr BS, Chintalapudi MR, O'Neal J L, Phelps AL, et al. (2007) Cartilage link protein 1 (Crtl1), an extracellular matrix component playing an important role in heart development. *Dev Biol* 310: 291–303.

48. Evanko SP, Johnson PY, Braun KR, Underhill CB, Dudhia J, et al. (2001) Platelet-derived growth factor stimulates the formation of versican-hyaluronan aggregates and pericellular matrix expansion in arterial smooth muscle cells. *Arch Biochem Biophys* 394: 29–38.

49. Sheng W, Wang G, Wang Y, Liang J, Wen J, et al. (2005) The roles of versican V1 and V2 isoforms in cell proliferation and apoptosis. *Mol Biol Cell* 16: 1330–1340.

50. Wight TN (2002) Versican: a versatile extracellular matrix proteoglycan in cell biology. *Curr Opin Cell Biol* 14: 617–623.

51. Czipri M, Otto JM, Cs-Szabo G, Kamath RV, Vermes C, et al. (2003) Genetic rescue of chondrodysplasia and the perinatal lethal effect of cartilage link protein deficiency. *J Biol Chem* 278: 39214–39223.

52. Prince CW (2004) Roles of hyaluronan in bone resorption. *BMC Musculoskelet Disord* 5: 12.

53. Huang L, Cheng YY, Koo PL, Lee KM, Qin L, et al. (2003) The effect of hyaluronan on osteoblast proliferation and differentiation in rat calvarial-derived cell cultures. *J Biomed Mater Res A* 66: 880–884.
54. Nagahata M, Tsuchiya T, Ishiguro T, Matsuda N, Nakatsuchi Y, et al. (2004) A novel function of N-cadherin and Connexin43: marked enhancement of alkaline phosphatase activity in rat calvarial osteoblast exposed to sulfated hyaluronan. *Biochem Biophys Res Commun* 315: 603–611.
55. Slevin M, Krupinski J, Kumar S, Gaffney J (1998) Angiogenic oligosaccharides of hyaluronan induce protein tyrosine kinase activity in endothelial cells and activate a cytoplasmic signal transduction pathway resulting in proliferation. *Lab Invest* 78: 987–1003.
56. Slevin M, West D, Kumar P, Rooney P, Kumar S (2004) Hyaluronan, angiogenesis and malignant disease. *Int J Cancer* 109: 793–794; author reply 795–796.
57. Taylor KR, Trowbridge JM, Rudisill JA, Termeer CC, Simon JC, et al. (2004) Hyaluronan fragments stimulate endothelial recognition of injury through TLR4. *J Biol Chem* 279: 17079–17084.
58. West DC, Kumar S (1989) Hyaluronan and angiogenesis. *Ciba Found Symp* 143: 187–201; discussion 201–187, 281–185.
59. West DC, Kumar S (1989) The effect of hyaluronate and its oligosaccharides on endothelial cell proliferation and monolayer integrity. *Exp Cell Res* 183: 179–196.

Chapter 3

Cx43-dependent skeletal phenotypes are mediated by interactions between the Hapln1a-ECM and Sema3d during fin regeneration

PLoS ONE, Submitted on July 22nd PONE-D-15-32259

3.1 Abstract

Skeletal development is a tightly regulated process and requires proper communication between the cells for efficient exchange of information. Analysis of fin length mutants has revealed that the gap junction protein Connexin43 (Cx43) coordinates cell proliferation (growth) and joint formation (patterning) during zebrafish caudal fin regeneration. Previous studies have shown that the extra cellular matrix (ECM) protein Hyaluronan and Proteoglycan Link Protein1a (Hapln1a) is molecularly and functionally downstream of Cx43, and that *hapln1a* knockdown leads to destabilization of the glycosaminoglycan hyaluronan. Here we find that the proteoglycan aggrecan is similarly destabilized when Hapln1a is reduced. Notably, we demonstrate that both hyaluronan and aggrecan are required for skeletal growth and patterning. Moreover, we provide evidence that the Hapln1a-ECM stabilizes the secreted growth factor Semaphorin3d (Sema3d), which has been independently shown to mediate Cx43 dependent skeletal phenotypes during skeletal regeneration. Double knockdown of *hapln1a* and *sema3d* reveal synergistic interactions. Further, *hapln1a* knockdown phenotypes were rescued by Sema3d overexpression. Therefore, Hapln1a maintains the composition of specific components of the ECM, which appears to be required for the stabilization of at least one growth factor, Sema3d. We propose that the Hapln1a dependent ECM provides the required conditions for Sema3d stabilization and function. Interactions between the ECM and signaling molecules are complex and our study demonstrates the requirement for components of the Hapln1a-ECM for Sema3d signal transduction.

3.2 Introduction

Vertebrate skeletal morphogenesis is a highly coordinated and tightly regulated process that contributes to the formation of bones of the correct size and shape. The underlying mechanisms that control the regulation of skeletal development are largely unknown. However, it is clear that proper communication and exchange of information between different cells of the skeletal tissue is crucial for proper bone formation. Gap junction mediated intercellular communication is one such mechanism that is known to contribute to skeletal development [1,2,3]. Intercellular communication through gap junctions involves the direct exchange of ions, second messengers and small metabolites between the cells and allows for coordinated cellular activity. It is hypothesized that gap junctional intercellular communication (GJIC) facilitates a range of functions including growth, differentiation, morphogenesis, skeletogenesis and developmental signaling [4,5]. Gap junctions are composed of oligomeric integral membrane protein subunits called connexons. Connexons from adjacent cells join to form the continuous gap junction channel that connects their cytoplasmic milieu allowing for direct exchange of low molecular weight (<1000 Da) metabolites [6]. Each connexon in turn is made up of trans-membrane protein subunits called connexins. Among the 21 different connexins known to be expressed in humans [7], *CONNEXIN43 (CX43)* is the major connexin expressed in bone cells [8]. Autosomal dominant missense mutations in human and mouse *CX43* results in the syndrome Oculodentodigital dysplasia (ODDD), characterized by craniofacial and limb abnormalities [1,2]. The *CX43*^{-/-} knockout mouse model exhibits severely delayed appendicular skeletal ossification and hypo-

mineralization of craniofacial bones [9]. A similar set of phenotypes was observed in the targeted *CX43* knockdown chick model [10,11]. Recessive homozygous mutations in zebrafish *cx43* results in the *short fin (sof^{b123})* phenotype characterized by short fins, reduced cell proliferation and short bony fin ray segments [3]. Together, these studies reveal that Cx43-dependent GJIC exhibits conserved skeletal functions across vertebrates. The mechanisms by which *CX43* dependent mutations result in the observed skeletal phenotypes remain largely unknown.

To study the role of Cx43 during skeletal morphogenesis, we utilize the fin length mutant *sof^{b123}* that expresses reduced levels of *cx43* mRNA and Cx43 protein without a lesion in the coding sequence. Three additional alleles of *sof* are caused by missense mutations in the *cx43* coding sequence, which exhibit defects in GJIC using heterologous assays [12]. Based on the *sof* phenotypes of reduced cell proliferation and short segments (i.e. premature joint formation), we suggest that Cx43 regulates skeletal morphogenesis by coordinating growth (i.e., promoting cell proliferation) and patterning (i.e., inhibiting joint formation) [13,14].

To understand how Cx43-based GJIC influences tangible cellular events like proliferation and differentiation, we completed a microarray analysis to identify candidate genes that may function downstream of *cx43* [15]. Two genes identified by the microarray and subsequently validated include *semaphorin3d (sema3d)*, a secreted signaling molecule, and *hyaluronan and proteoglycan link protein 1a (hapln1a)*, an extracellular matrix (ECM) protein [15,16]. Through previous studies, we have shown that Hapln1a and Sema3d are molecularly and functionally downstream of Cx43,

mediating Cx43-dependent cell proliferation and joint formation. We have also shown that *sema3d* and *hapln1a* are transcriptionally independent of each other, since knockdown of one does not affect the expression of the other [16]. However, the possibility remains that the *sema3d* and *hapln1a* gene products functionally interact.

The major function of Hapln1 is to “link” and stabilize the interaction between the glycosaminoglycan (GAG) hyaluronic acid (HA) and proteoglycans (PGs) in the ECM. In humans and mouse, the orthologous protein Hapln1 has also been referred to as link protein (LP) or cartilage link protein (CRTL1). The mouse knockout for *CRTL1* (aka *HAPLNI*) results in perinatal lethality, dwarfism, delayed ossification, short limbs, defects in cartilage and bone development and craniofacial abnormalities [17] showing that CRTL1 is critical for proper skeletal development. In a recent study, we found that *hapln1a* knockdown in regenerating zebrafish fins causes reduced levels of HA in vivo, suggesting that the ECM becomes partially destabilized when Hapln1a is reduced [16]. However, since Hapln1a is involved in stabilizing the interaction between HA and PGs, it is possible that, in addition to HA, the PG levels could also be affected upon *hapln1a* knockdown. ECM remodeling is well known to be essential for proper skeletal development and regeneration [18,19,20,21]. Mounting evidence suggests that in addition to providing structural stability the ECM also has roles in sequestering growth factors, presenting growth factors to their receptors, and sensing and transducing mechanical signals [22,23]. Therefore, it is of interest to define how reduced Hapln1a causes Cx43-dependent skeletal phenotypes.

This report builds upon our prior studies showing that *hapln1a* knockdown results in reduced regenerate length, reduced segment length, reduced cell proliferation and destabilization of HA [16]. Here, we explore the possibility of whether reduced HA is sufficient to cause the observed skeletal phenotypes. As a part of these studies, we also found that aggrecan (Acan) levels are reduced following *hapln1a* knockdown and that reduced Acan also contributes to the *hapln1a* knockdown phenotypes. Finally, we provide evidence that, while *hapln1a* and *sema3d* gene transcription are independently regulated downstream of *cx43* [16], the Hapln1a and Sema3d protein products appear to interact functionally. These findings provide important new insights into the role of Hapln1a during skeletal morphogenesis and, into the requirement for the ECM during Sema3d-based signal transduction.

3.3 Materials and Method

Statement on the ethical treatment of animals

This study was carried out in strict accordance with the recommendations in the Guide for the Care and Use of Laboratory Animals of the National Institutes of Health. The protocols used for this manuscript were approved by Lehigh's Institutional Animal Care and Use Committee (IACUC) (protocol identification #128, approved 11/16/2014). Lehigh University's Animal Welfare Assurance Number is A-3877-01. All experiments were performed to minimize pain and discomfort.

Housing and husbandry

Zebrafish are housed in a re-circulating system built by Aquatic Habitats (now Pentair). Both 3 L tanks (up to 12 fish/tank) and 10 L tanks (up to 30 fish/tank) are used. The fish room has a 14:10 light:dark cycle and room temperature (RT) varies from 27-29°C [24]. Water quality is automatically monitored and dosed to maintain conductivity (400-600 μ s) and pH (6.95-7.30). Nitrogen levels are maintained by a bio filter. A 10% water change occurs daily. Recirculating water is filtered sequentially through pad filters, bag filters, and a carbon canister before circulating over UV lights for sterilization. Fish are fed three times daily, once with brine shrimp (hatched from INVE artemia cysts) and twice with flake food (Aquatox AX5) supplemented with 7.5% micropellets (Hikari), 7.5% Golden Pearl (300-500 micron, Brine Shrimp direct), and 5% Cyclo-Peeze (Argent).

Experimental procedures and animals

Wild-type C32 zebrafish (*Danio rerio*) and *Tg(hsp70:sema3dgifp)* (generously provided by Mary C. Halloran) were used in this study. Fish were anaesthetized in 0.1% tricaine and caudal-fin amputations were performed at 50% level. Fin regeneration was allowed to proceed until the desired time period (3- 7 days post amputation [dpa]) depending on the type of experiment. The regenerated fins were harvested at the required time point after anaesthetizing the fish. Whole mount in situ hybridization, immunofluorescence and histochemical staining were performed on regenerating fins. Descriptions of each of these methods follow.

In situ hybridization on whole mount fins

Fins were fixed overnight in 4% paraformaldehyde (PFA) in PBS and dehydrated in 100% methanol and stored at -20°C until use, for in situ hybridization (ISH). RNA probes were generated from PCR amplified linear DNA in which the reverse primer contained the T7 RNA polymerase binding site. The primers used in this study for ISH are summarized in Table 3.1. Digoxigenin (DIG) labeled RNA probes were synthesized using DIG labeling mix (Roche) and in situ hybridization on regenerated whole fins was carried out following standard protocols [15,16]. For each gene under study, a minimum of 4-5 fins were used per trial and 3 independent trials were performed.

Morpholino mediated gene knockdown in regenerating fins

All MOs used in this study were fluorescein tagged, obtained from Gene Tools, LLC and used at a final concentration of 1mM for injection, unless otherwise described. The sequences for MOs used in this study can be found in Table 3.1. Injection and electroporation were carried out as described previously [16,25]. Briefly, 3 dpa fish were anesthetized and approximately 50nl of MO (targeting morpholino [MO] or mismatch control morpholino [MM]) or standard control MO 5' CCTCTTACCTCAGTTACAATTTATA 3' was injected into either the dorsal or the ventral half of the tail fin. The un-injected half of the fin served as the internal control. Following injection, the entire fin was electroporated using a CUY21 Square Wave electroporator (Protech International Inc). MO-positive fish were selected 24 hpe (hours post electroporation) by examination under a fluorescence microscope. The knockdown fins were evaluated for regenerate length, segment length, histone-3-phosphate (H3P)

analysis, alizarin red staining, immuno-fluorescence and histochemical experiments. The procedure for each analysis is described separately. For each MO (i.e., targeting or mismatch) 6-8 fish were used. Reproducibility was confirmed by testing the MO in three independent experiments. Statistical significance was determined using the student's *t*-test ($P < 0.05$).

Rescue of hapln1a knockdown phenotypes with sema3d overexpression

We used three groups of fish for these experiments. Groups 1 and 2 were positive for the transgene, Tg(*hsp70:sema3dgfp*), while Group 3 fish were negative for the transgene. Knockdown of *hapln1a* was performed on 3 dpa fins as described above. Four hours after *hapln1a* knockdown, heat shock was performed for one hour at 37°C (Groups 1 and 3). Alternatively, Group 2 fish were positive for the transgene but were not exposed to heat shock. Induction of transgene expression in Group 1 animals was confirmed after 24 hours of heat shock by screening for GFP-positive fins. For regenerate and segment length analyses the fins were harvested 4 dpe (days post electroporation) and data analysis was performed as described below. For each experiment a minimum of 6-8 fins were used per trial and 3 independent trials were performed. Statistical significance was determined using the student's *t*-test ($P < 0.05$).

Fin regenerate length, segment length and H3P analysis

For each type of analysis, minimum of 6-8 fins were used per trial and 3 independent trials were performed. Statistical significance was determined using the student's *t*-test ($P < 0.05$). Images were collected on a Nikon SMZ1500 dissecting

microscope using a Nikon DXM1200 digital camera unless otherwise stated. Measurements were performed using Image Pro software.

Fin regenerate length analysis was performed as described [15]. Briefly, fins were harvested at 4 dpe, fixed and stored in methanol until use at -20°C. The measurements were taken from the longest fin ray (i.e. the third ray from either the dorsal or ventral end) that was previously established as a standard [26]. Fin regenerate length was measured using Image Pro Software from the amputation plane (clearly visible in bright field) to the tip of the fin. To evaluate the phenotypic effect of MO based knockdown experiments on fin regenerate length, the targeting MO or control MM injected side of each fin is compared to its un-injected side by the percent similarity method as described [27]. Briefly, the percent similarity for each fin is calculated as $([\text{length of the injected side in } \mu\text{m} / \text{length of the un-injected side in } \mu\text{m}] \times 100)$. Values close to 100% indicate that the injected MO has no effect on the phenotype whereas a value less than 100% indicate that the MO has an effect on the observed phenotype. The mean of percent similarity for the MO treated experimental group and the corresponding MM treated control group were estimated and compared. Percent similarity of greater than 100 % reflects the fact that the experimental side can be measurably larger than the control un-injected side. Statistical significance was determined using the student's *t*-test ($P < 0.05$).

Segment length analysis was performed on calcein stained fins. Calcein staining was performed on live fish as described [28]. Briefly, fish were permitted to swim in 0.2 % calcein for 10 min, followed by 10 min in fresh water. Fish were anesthetized as

described above and fins were imaged at 4X. For segment length, the distance between the first two newly formed joints following amputation was measured in the third fin ray from either the dorsal or ventral end [26]. Segment length was measured using Image Pro Software. To evaluate the phenotypic effect of MO based knockdown experiments on segment length, the percent similarity method was used as described above.

For H3P analysis, the fins were harvested 1 dpe, fixed overnight in 4% paraformaldehyde (PFA) in PBS and dehydrated in 100% methanol and stored at -20°C until use. Cell proliferation analysis was performed by counting number of mitotic cells by H3P immuno-staining as described [15]. H3P positive cells were counted from within the distal most 250 μm of each fin above the third fin ray from either the dorsal or ventral end [26]. To evaluate the phenotypic effect of MO based knockdown experiments on cell proliferation, the percent similarity method was used as described above. For cell proliferation, the percent similarity for each fin is calculated as ($[\# \text{ H3P positive cells per } 250 \mu\text{m}^2 \text{ of injected side} / \# \text{ H3P positive cells per } 250 \mu\text{m}^2 \text{ of un-injected side}] \times 100$).

Alizarin red staining

For alizarin red staining, the fins were harvested 4 dpe, fixed overnight in 4% paraformaldehyde (PFA) in PBS and dehydrated in 100% methanol and stored at -20°C until use. Fins were rehydrated through a decreasing methanol series as described for ISH. Following that fins were bleached for 30 minutes in 0.8% KOH, 0.6% H_2O_2 (should be prepared and used within one week). Subsequently, fins were washed twice

with water and then washed for 1hr in a saturated Alizarin Red solution containing 1% KOH [29] followed by 30 minutes wash in water and mounted in glycerol for imaging. The extent of mineralization was calculated as the ratio of the zone of mineralization (extent of detectable alizarin red staining length) to the total regenerate length. To evaluate the phenotypic effect of MO based knockdown experiments on alizarin red staining, the % similarity method was used as described above. The % similarity for each fin is calculated as ([ratio of {regenerate length : alizarin red staining length} of the injected side / ratio of {regenerate length : alizarin red staining length} of un-injected side] X 100). The mean of % similarity for the MO treated experimental group and the corresponding MM treated control group were estimated and compared, and the statistical significance between the groups was determined using two tailed unpaired student's *t*-test (P<0.05). For each experiment minimum of 6-8 fins were used per trial and 3 independent trials were performed.

Cryosectioning for immunofluorescence and histochemistry

Fixed and embedded fins were mounted in OCT and cryosectioned (15 μ m sections) using a Reichertâ Jung 2800 Frigocut cryostat. Sections were collected on Superfrost Plus slides (Fisher) and allowed to air dry O/N at RT. Sections can be stored at -20°C for up to a year. The slides were stored at -20°C for at least one day before starting the experiment. For all experiments using cryosections, the slides were brought to RT for one hour. Sections were circled using a marking pen (ImmEdge Pen H-4000; PAP pen, VWR Laboratories). To confirm reproducibility, minimum of 3-5 different

fins were used for each experiment and approximately 8-12 sections per fin were analyzed.

Vcan Immunofluorescence

For detection of Vcan, fins were fixed for 10 min with 2% PFA at RT followed by three 10 min washes with 1X PBS, and then embedded in 1.5% agarose/5% sucrose in PBS and equilibrated in 30% sucrose in PBS and sectioned as described above. For Vcan immuno-staining, the sections were rehydrated twice for 10 min in PBS followed by two washes with block (2% BSA, 0.1% TritonX 100 in PBS). Then, sections were blocked for another one hour at RT and then incubated in primary antibody, Rabbit anti-versican (H-56) (Santa Cruz Biotechnology-SC-25831) O/N at 4°C. Following incubation with primary antibodies, sections were washed three times in block (15 min each), incubated at RT for one hour with respective secondary antibody goat anti-rabbit Alexa-663 (Invitrogen, 1:200) and washed again three times in block (15 min each). Sections were next incubated with propidium iodide (final concentration 0.01mg/ml in block) for 30 min at RT to stain nuclei, followed by a quick wash with distilled water.

Acan Immunofluorescence

For detection of Acan, fins were fixed for 10 min with 2% PFA at RT followed by three 10 min washes with 1X PBS, and then embedded in 1.5% agarose/5% sucrose in PBS and equilibrated in 30% sucrose in PBS and sectioned as described above. Acan immuno-staining was performed as described earlier [30]. Briefly, the sections were rehydrated twice for 10 min in PBS at RT, followed by antigen unmasking by digestion

with chondroitinase. First, the slides were incubated with the chondroitinase treatment buffer (50mM Tris, 60mM sodium acetate, 0.02% BSA, pH 8.0) at 37°C for 5 min, followed by deglycosylation using chondroitinase ABC enzyme (Sigma-C2905, final concentration 0.05U in the treatment buffer) for 2 h at 37°C. Following that, slides were washed with block for 10 min at RT. Then, sections were blocked for another one hour at RT, incubated with Mouse anti-aggrecan (BC-3) (Thermo Scientific-MA3-16888) primary antibody O/N at 4°C. Following incubation with primary antibodies, sections were washed three times in block (15 min each), incubated at RT for one hour with secondary antibody goat anti-mouse Alexa-663 (Invitrogen, 1:200) or goat anti-mouse Alexa-568 (Invitrogen, 1:200) and washed again three times in block (15 min each). Sections were next incubated with propidium iodide (final concentration 0.01mg/ml in block) or To-Pro-3-iodide (Life Technologies, 1:1000) for 30 min at RT, followed by a quick wash with distilled water.

Sema3d Immunofluorescence

For detection of Sema3d, fins were fixed for 30 min with 2% PFA at RT followed by three 10 min washes with 1X PBS, and then embedded in 1.5% agarose/5% sucrose in PBS and equilibrated in 30% sucrose in PBS and sectioned as described above. For Sema3d immuno-staining, the sections were rehydrated twice for 10 min in PBS followed by antigen retrieval. Slides were transferred to coplin jars containing 10 mM sodium citrate (pH=6) and incubated at 99.5 °C water bath for 10 minutes. The slides were allowed to cool down to room temperature and again washed in 1X PBS (2X, five minutes each). Following that slides were washed twice with block (2% BSA,

0.1% TritonX 100 in PBS). Then, sections were blocked for another one hour at RT and then incubated in primary antibody, Rabbit anti-Sema3d (Sigma-SAB1402064, 1:500) or Mouse anti-EGFP (Clonetech, 1:1000) O/N at 4°C. Following incubation with primary antibodies, sections were washed three times in block (15 min each), incubated at RT for one hour with secondary antibody goat anti-rabbit Alexa-663 (Invitrogen, 1:200) or goat anti-mouse Alexa 488 and washed again three times in block (15 min each). Sections were next incubated with propidium iodide (final concentration 0.01mg/ml in block) or DAPI (1:1000) for 30 min at RT, followed by a quick wash with distilled water.

Histo-chemical analysis of HA

For detection of HA, fins were fixed overnight (O/N) with 4% PFA in PBS. After a brief methanol wash, fins were dehydrated in 100% methanol and stored at –20°C until use. Before sectioning, fins were sequentially rehydrated in a methanol-PBS series of washes and then were embedded in 1.5% agarose / 5% sucrose in PBS and equilibrated in 30% sucrose in PBS and then sectioned as described above. HA was detected as described [16]. Briefly the sections were rehydrated twice for 10 min in PBS followed by two washes with block. Then, sections were blocked for another one hour at RT, incubated with biotinylated hyaluronic acid binding protein (bHABP-Calbiochem-385911, 1:100) O/N at 4°C. The sections were washed three times in block (15 min each), incubated at RT for one hour with streptavidin-Alexa-546 conjugate, (Invitrogen, 1:200) and washed again three times in block (15 min each). Sections were next incubated with propidium iodide (final concentration 0.01mg/ml in block) or To-

Pro-3-iodide (Life Technologies, 1:1000) for 30 min at RT, followed by a quick wash with distilled water. Then the slides were blotted dry and mounted for imaging as described above.

Confocal microscopy

The slides were blotted dry and mounted with vectashield for imaging. Confocal microscopy was used to image the sections using a 40×/1.3 numerical aperture objective on an inverted microscope (Axiovert 200 M; Carl Zeiss, Jena, Germany) equipped with an LSM510 META scan head (Carl Zeiss). Argon ion and HeNe lasers were used to generate the 488 and 543/633 lines used for excitation, and pinholes were typically set to 1–1.5 Airy units. Images were exported as TIFF files and printed using Photoshop.

3.4 Results

Components of Hapln1a-ECM are expressed in the regenerating fin

In a recent study, we showed that *hapln1a* knockdown results in Cx43 dependent skeletal phenotypes: reduced fin regenerate length, reduced segment length and reduced cell proliferation [16]. Since Hapln1a links HA with PGs we were interested in the expression of genes responsible for synthesis of HA and in the expression of PGs. HA is synthesized by hyaluronic acid synthases (Has) and Acan and Vcan are the two major bone associated PGs involved in matrix organization [31]. We performed whole mount in situ hybridization on WT 5 days post amputation (dpa) regenerating fins to determine which of the HA synthesizing enzymes (*has1*, *has2* and *has3*) and which of the skeletal PGs (i.e, *acana*, *acانب*, *vcana* and *vcانب*) are expressed. Of the three different HA

synthesizing enzymes, *has1* and *has2* are expressed in the regenerating fin. Of the duplicate copies of *acan* and *vcan*, only *acانب* and *vcanب* are expressed in regenerating fins (Figure 3.1).

Reduced HA levels only partially contribute to the Hapln1a mediated phenotypes

Because *hapln1a* knockdown results in reduced HA [16], we hypothesized that manipulating the HA levels by targeting the HA synthesizing enzymes should recapitulate the *hapln1a* knockdown phenotypes. Since it is likely that homozygous mutations in genes required for the Hapln1a-ECM will be essential, or will cause serious global skeletal defects, we rely on morpholino (MO) based knockdown for evaluation of gene function in the regenerating fin. As controls, we use either paired 5 mismatch (MM) non-targeting control MOs or the standard control MO. Further, we also confirm that the target is reduced following knockdown. We find that this is a suitable method to establish specificity for target genes. In order to manipulate the HA levels, we completed MO mediated knockdown of the HA-synthesizing enzymes *has1* and *has2* in WT regenerating fins, and we used MM treated fish as control. All MOs used in this study are fluorescein tagged, permitting the confirmation of cellular uptake. Following MO microinjection and electroporation at 3 dpa, MO positive fish were screened 24 hours post electroporation (hpe) by detection of fluorescein positive cells. To evaluate the effect of the knockdown of the HA synthesizing enzymes (*has1* and *has2*) on HA levels, MO or MM positive fins were harvested 24 hpe and processed for immunohistochemical analysis for HA using biotinylated HA binding protein. During regeneration, HA is predominantly upregulated in epidermis and in the proximal

mesenchyme of the regenerate, and in the mesenchyme of the stump tissue [16,30]. Histochemical analysis for HA on *has1* and *has2* knockdown fins revealed reduced levels of HA compared to the MM treated fins, indicating that HA synthesis has been successfully down regulated upon knockdown of these synthesizing enzymes (Figure 3.2).

We next evaluated the effect of the *has1* and *has2* knockdowns on Cx43-Hapln1a dependent phenotypes and compared to the MM treated fish. Either the target MO or the control MM is injected into fin rays in one half of the fin, and the other half is un-injected. Next, the injected side was compared with the respective un-injected side and the percent similarity was determined. This method reduces the effect of fin to fin variation. High similarity between the injected and un-injected side (i.e. close to 100%) indicates little or no effect of the MO treatment, whereas values with low similarity (i.e. less than 100%) indicates that the MO had an effect on treatment side. Fin length was measured at 4 dpe as the distance from the amputation plane to the distal end of the regenerate (Figure 3.3A). We observed that knockdown of *has1* had no effect on regenerate length, whereas *has2* knockdown resulted in significant reduction in regenerate length (~14% reduced) compared to the MM control (Figure 3.3B). The segment length was measured at 4 dpe by calcein staining as the distance between the first two joints distal to the amputation plane (Figure 3.3C). Similar to regenerate length, *has1* knockdown had no effect on segment length; whereas *has2* knockdown resulted in significant reduction in segment length phenotype (~12% reduced) (Figure 3.3D). The effect of the knockdown of these enzymes on cell proliferation was evaluated by

counting the number of mitotic cells following immuno-fluorescence for H3P at 1 dpe (Figure 3.3E). For cell proliferation we found that *has1* knockdown resulted in ~ 20% reduction, whereas *has2* knockdown had a stronger effect (~ 32% reduced); both resulted in significant reduction in cell proliferation compared to the control MM treated fins (Figure 3.3F). Overall, compared to *has1* knockdown, *has2* knockdown showed a stronger effect and showed a significant effect on all of the *hapln1a* phenotypes. Since *has1* and *has2* knockdown both lead to reduced HA levels, it is unclear why *has2* knockdown has a much stronger effect than *has1* knockdown. However, it has been shown that *HAS2* knockout is lethal in mice, while *HAS1* or *HAS3* knockout mice appear healthy [32,33]. Further, *HAS2* knockout cannot be compensated by expression of Has1 or Has3 [34]. These studies support the idea that HA synthesized by Has2 may be distinct from HA synthesized by Has1 and Has3.

To determine if reduced HA is sufficient to mediate Hapln1a effects, we compared the reduction in regenerate length, segment length and cell proliferation of *has2* knockdown (~14%, ~12% and ~32% respectively) with *hapln1a* knockdown (~26%, ~23% and ~40% respectively). The effect of *hapln1a* knockdown levels are represented as a dotted line in Figures 3D, E and F. Interestingly, we find that *hapln1a* knockdown alone resulted in a much stronger effect than the knockdown of *has2*. Therefore, in addition to HA there could be other Hapln1a-ECM components contributing to Hapln1a-Cx43 dependent skeletal phenotypes that account for the stronger *hapln1a* knockdown phenotype.

Acan, but not Vcan, contributes to the observed hapln1a knockdown skeletal phenotypes

Acan and Vcan are the major PGs associated with bones [31]. In addition to HA, we hypothesized that the Hapln1a associated PGs may also contribute to Hapln1a mediated skeletal phenotypes. We first determined if either Acan or Vcan protein levels are reduced in *hapln1a* knockdown fins using immuno-histochemistry. In prior studies we found that Acan is initially upregulated in mesenchyme during regeneration (around 3-4 dpa), and later expressed more prominently in the lepidotrichia (around 5 dpa). In contrast, Vcan is primarily expressed in the epidermis and less so in the mesenchyme at both time points [30]. Upon *hapln1a* knockdown, we observed that Acan protein levels are down regulated in *hapln1a* MO treated fins compared to the control MM treated fins (Figure 3.4). In contrast, Vcan protein levels appeared unchanged, (Figure 3.5) suggesting that Vcan is not involved in mediating Hapln1a phenotypes. Next, we determined whether Acan contributes to Hapln1a-Cx43 dependent skeletal phenotypes. We used a MO targeting the *acanb* mRNA to knockdown Acan. The effect of *acanb* knockdown on Acan protein levels was confirmed by immuno-staining analysis for Acan, showing that *acanb* knockdown caused significant reduction of Acan protein levels (Figure 3.6A). We next evaluated the effect of *acanb* knockdown on Hapln1a mediated phenotypes. Knockdown of *acanb* resulted in significant reduction of regenerate length (~13% reduced), segment length (~20% reduced) and cell proliferation (~16% reduced) (Figure 3.6B). Since Acan is important for bone mineralization, we examined bone calcification at 4 dpe using alizarin red, which stains

mature bone matrix. The extent of mineralization was determined by calculating the ratio of the total regenerate length to the zone of mineralization (i.e., the length of detectable alizarin red staining). Either the target MO or the control MM injected side was compared with the respective un-injected side and the percent similarity was determined. In contrast to the control MM treated fins, *acanb* MO treated fins showed a much shorter zone of bone calcification (~20% reduced) (Figure 3.6C, D), suggesting that Acan might play a role in regulating bone matrix maturation and joint formation.

Similar to *has2* knockdown, the effect of *acanb* knockdown was not as strong as observed for the *hapln1a* knockdown (see dotted lines in Figures 3.6B). Interestingly, the additive effects of reduced HA and reduced Acan are similar to the total effects of reduced Hapln1a. Moreover, we observed that *has2* knockdown (reduced HA) had a stronger effect on cell proliferation (~32% reduction) compared to *acanb* knockdown (~16% reduction), suggesting that HA might play a more significant role in regulating cell proliferation. On the other hand, *acanb* knockdown had a stronger effect on segment length (~20% reduction) compared to *has2* knockdown (~13% reduction), suggesting Acan might play a more significant role in regulating joint formation. Together, these results suggest that both HA and Acan are crucial for proper skeletal regeneration and contribute to the Hapln1a-Cx43 dependent phenotypes.

Hapln1a and Sema3d gene products interact to mediate Cx43 dependent skeletal phenotypes

Data from our recent study suggested that *hapln1a* and *sema3d* are transcriptionally independent of each other, meaning that the expression of either does

not depend upon the other [16]. However, these findings do not exclude the possibility that the two proteins work together. Several studies demonstrate that GAGs and the ECM function together to regulate signal transduction pathways. For example, GAGs in the ECM play a role during physiological and pathological remodeling processes, such as regeneration, bone development, cancer metastasis and osteoarthritis [35,36,37]. Moreover, GAGs have been implicated in regulating signaling pathways of molecules such as FGFs, BMPs, Wnts, Hhs and IGFs (reviewed in [38]). *Sema3d* is a signaling molecule that is known to mediate Cx43 dependent skeletal phenotypes [15] and *Hapln1a* is an ECM protein known to mediate Cx43 dependent skeletal phenotypes [16]. Therefore, we wished to test the hypothesis that the protein products function together. To test this hypothesis, we looked for evidence of genetic interaction by performing double knockdowns of *sema3d* and *hapln1a* and testing for synergistic effects. We first identified sub-threshold concentrations for both the *sema3d* and *hapln1a* MOs, where neither single knockdown resulted in a skeletal phenotype. We found that 0.5mM concentration of the *hapln1a* MO and 0.25mM concentration of the *sema3d* MO did not result in skeletal phenotypes (data not shown). Next, we performed double knockdowns of both *hapln1a* and *sema3d* using these sub-threshold concentrations (0.5mM *Hapln1a* MO + 0.25mM *Sema3d* MO) and compared with the double MM control at the same concentrations. Either the double MO or the double control MM injected side was compared with the respective un-injected side and the percent similarity was determined as described earlier. Interestingly, we observed that the double knockdown resulted in reduced regenerate length (~11% reduced), reduced segment length (~12% reduced)

and reduced cell proliferation (~34% reduced) (Figure 3.7), revealing that *hapln1a* and *sema3d* gene products act synergistically and indeed function in a common molecular pathway.

Hapln1a-ECM stabilizes Sema3d

Based on the genetic interaction data, we hypothesized that Hapln1a-ECM is playing a role in mediating Sema3d dependent signal transduction. It is well known that the ECM can contribute to stabilizing growth factors and thereby influencing growth factor dependent signaling [39]. Hence, it is possible that when Hapln1a protein levels are reduced by *hapln1a* knockdown, the disruption of Hapln1a-ECM affects either the stabilization of Sema3d or affects the presentation of Sema3d to its receptors. To determine whether Sema3d stability depends on Hapln1a, we examined the Sema3d protein levels following *hapln1a* knockdown and compared to control MM treated fins by immuno-staining analysis. We observed that Sema3d protein is reduced following *hapln1a* knockdown (Figure 3.8), suggesting that Hapln1a is required for the stability of Sema3d.

To distinguish the possibility of whether Hapln1a is required for stabilization, or required for both stabilization and presentation of Sema3d to its receptors, we asked if Sema3d overexpression could rescue *hapln1a* knockdown phenotypes. We utilized the transgenic line, *Tg(hsp70:sema3d_{gfp})* that overexpresses Sema3d-GFP under the control of a heat shock promoter [40]. If Hapln1a is required primarily for the presentation of Sema3d to its receptors, then *hapln1a* knockdown phenotypes will likely not be rescued by overexpression of Sema3d. On the other hand, if Hapln1a dependent

ECM is required mainly for Sema3d stabilization, then we expect that *hapln1a* knockdown phenotypes would be rescued by Sema3d overexpression. We first confirmed overexpression of *sema3d* mRNA and Sema3d-GFP protein in regenerating fins by whole mount ISH for *sema3d* and immuno-staining for Sema3d and GFP on heat shocked versus non-heat shocked *Tg(hsp70sema3d**gfp)* fins. We observed that both *sema3d* mRNA and Sema3d-GFP protein expression was increased in heat shocked fins compared with fins not treated with heat shock (Figure 3.9).

The rescue experiment involved 3 different groups of animals (Figure 3.10A). Group 1 animals (experimental group) were positive for the transgene. This group was treated for *hapln1a* knockdown and Sema3d-GFP was induced 4 hours after knockdown by a 1 hour heat shock at 37°C. Group 2 animals (control 1) were also positive for transgene. This group was also treated for *hapln1a* knockdown, but did not receive the heat shock (and therefore do not overexpress Sema3d). Group 3 animals (control 2) were transgene negative siblings. This group was treated for *hapln1a* knockdown and received 1 hour of heat shock at 37°C. At 24 hours post *hapln1a* knockdown, all animals were screened for GFP expression. Only Group 1 animals showed positive GFP expression in the fin, since they all carried the transgene and were heat shocked for the overexpression of Sema3d (Figure 3.10B). Only GFP positive fish were selected from Group 1 for further analysis. All three groups were treated for knockdown at 3 dpa. Four hours post knockdown, Groups 1 and 3 were treated for a 1 hour heat shock at 37°C. Fins were harvested from all groups at 4 dpe and regenerate and segment length analyses were completed using the percent similarity method. Therefore, within each group, the

injected side was compared with the respective un-injected side and the percent similarity was determined. We found that Group 1 had a high percent similarity (i.e., close to 100%) between the injected vs un-injected side showing that *hapln1a* knockdown phenotypes were fully rescued by overexpression of *Sema3d* (Figure 3.10C). We showed that rescue depended on both the heat shock to induce *Sema3d* overexpression and on the presence of the transgene since neither animals from Group 2 nor animals from Group 3 exhibited rescue of skeletal phenotypes. Thus, for both control groups regenerate length was reduced by ~20% and for segment length, Group 2 showed ~23% reduction and Group 3 showed ~20% reduction (Figure 3.10C). Therefore, *Sema3d* overexpression rescues *hapln1a* knockdown phenotypes. These experiments highlight the importance of the *Hapln1a*-ECM for stabilization *Sema3d*, and for *Sema3d*-based signal transduction.

3.5 Discussion

Previously we have shown that *hapln1a* knockdown results in significant reduction in HA levels during fin regeneration [16]. Here we tested whether HA is sufficient to cause the observed *Hapln1a* dependent skeletal phenotypes. We found that in addition to HA, *Acan* also contributes to the phenotypes. The effects of HA and *Acan* seem to be additive, where HA has a stronger impact on cell proliferation while *Acan* has a stronger impact on joint formation. Further, we demonstrate the dependence of *Sema3d* on the presence of the *Hapln1a*-ECM. We show that *Hapln1a* and *Sema3d* genetically interact and we find that *sema3d* overexpression can rescue *hapln1a* knockdown phenotypes. Based on this current study we propose a new model for the

Cx43 pathway (Figure 3.11). Even though transcriptionally *hapln1a* and *sema3d* have been shown to be independent of each other [16], the current study demonstrates that the Hapln1a-ECM plays a role in stabilizing Sema3d protein. Therefore, it is likely that Sema3d signal transduction requires the Hapln1a-ECM. Our findings indicate that the Sema3d and Hapln1a gene products work together to mediate Cx43 phenotypes during skeletal growth and patterning in the regenerating fin.

Independent studies in different model systems provide evidence that components of the Hapln1a-ECM (link protein/Hapln, HA, PGs Acan and Vcan) are interdependent and critical during skeletal morphogenesis. HA plays a central role in organizing the matrix where it serves as a central backbone binding to the PGs Acan/Vcan via the link protein. Moreover, in addition to reduced HA, *Has2* deficiency also resulted in reduced Acan content [41]. Conditional knockout of *HAPLNI* (also called *CRTL1*) in the mouse reveals that the function of link protein is indispensable during skeletal development for stabilizing the HA-PG aggregate [17]. The *HAPLNI* knock out mouse dies perinatally due to myocardial defects. These defects are attributed to reduced Vcan levels leading to decreased cell proliferation [42,43]. Vcan itself is also known to play a role during joint morphogenesis and patterning of muscles and nerves in mouse embryonic limb morphogenesis [44]. Acan deficient mice and chicks are characterized by dwarf limbs, craniofacial abnormalities, and perinatal lethality [45,46,47]. We find that loss of Hapln1a protein is associated with reduced cell proliferation, reduced bony segment length, reduced HA levels [16], and reduced Acan levels (this study). Therefore, requirements for the Hapln1a-ECM are conserved in the

skeleton. Future studies will reveal how particular components of the Hapln1a-ECM contribute to specific cellular functions.

HA is ubiquitously present throughout the body and in all the bones and cartilages of the skeleton. Depending on its molecular size, HA fulfills various structural and metabolic functions (Reviewed in [48,49]), [41,50]). The three HA synthases Has1, Has2 and Has3 reside on the plasma membrane and extrude HA directly into the extracellular space [51,52,53,54,55]. All three are integral membrane proteins with six putative transmembrane domains [55], and all contain conserved amino acid residues that have both GlcNAc and GlcA transferase activity [56]. The Has enzymes each synthesize HA of similar composition but may differ in the rate of synthesis, chain length and the ease with which HA is released from the cell surface [57]. Has2 in particular is believed to play a major role during development of the skeleton. For example, while chondrocytes express all three Has genes, Has2 exhibits the highest expression levels in all cartilages [32,58,59]. Moreover, knockout of the *HAS2* gene in mice results in embryonic lethality whereas knockout mice of *HAS1* and *HAS3* are viable and appear normal [34]. Conditional *HAS2* gene knockout in mice is sufficient to cause shortened axial and appendicular skeleton and defects in patterning of digits [41,60]. Strikingly, overexpression of Has2 in the developing chick limb bud mesoderm also perturbs limb morphogenesis, leading to shortened bones with abnormal morphology and positioning [50], suggesting the need for regulated HA synthesis during skeletal development and patterning. Collectively, these findings highlight the significance of HA produced by Has2, and may explain our findings that knockdown of

has2 results in a stronger effect on Hapln1a dependent skeletal phenotypes compared to *has1* knockdown (i.e. even though knockdown of either gene reduces the amount of HA).

During fin regeneration, reduced HA exhibited a stronger effect on cell proliferation than on patterning. Previously, we found that HA is expressed in a conserved pattern during fin regeneration [30]. HA is strongly upregulated in the distal stump and proximal blastema (i.e., just above and below the amputation plane) compared to the distal end of the regenerate, where it may maintain the proliferative state of the mesenchymal cells by limiting contact inhibition between cells that leads to tissue differentiation [61,62,63,64,65]. In contrast, knockdown of *acanb* exhibited a stronger effect on segment length than on cell proliferation, and also caused reduced bone mineralization of the fin rays. Changes in the bone matrix may influence differentiation of bone-forming cells and/or joint-forming cells, resulting in short bony segments.

The ECM is no longer considered to be an inert substance surrounding cells, but rather, can contribute to the regulation of multiple signaling pathways [66]. For example, the ECM can serve as a reservoir for secreted growth factors. Local release of ECM-bound growth factors could influence temporal regulation of signal transduction pathways, and/or the half-life of secreted growth factors. Moreover, the concentration of signaling molecules at a particular location may contribute to the establishment of morphogen gradients that play critical roles during patterning and developmental processes [67,68]. Our findings reveal that the Hapln1a-ECM is crucial for the stability

of the secreted growth factor, Sema3d. Further work is required to understand how Sema3d interacts with components of the Hapln1a-ECM, and how these interactions may regulate Sema3d-receptor based signal transduction.

3.6 Figures

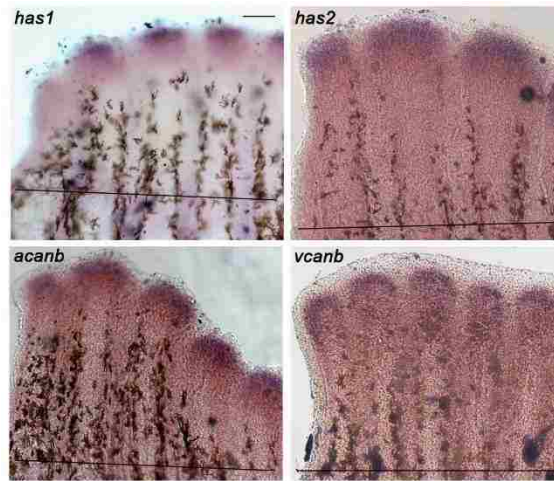


Figure 3.1: Whole mount in situ hybridization showing the expression of Hapln1a-ECM components on 5 dpa regenerating fins. Components of the Hapln1a-ECM namely, *has1*, *has2*, *acanb* and *vcnb* are expressed during fin regeneration. The amputation plane is indicated by a black line in all the panels. Scale bar represents 100 μ m.

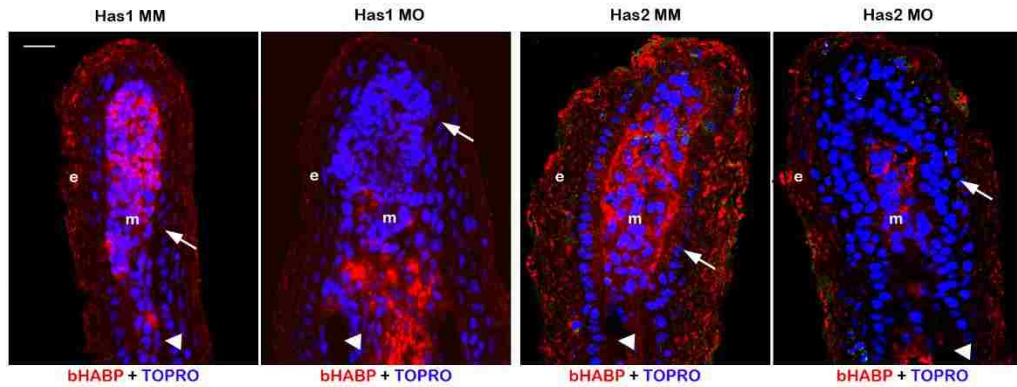


Figure 3.2: Morpholino mediated knockdown of *has1* and *has2* results in reduced HA. Longitudinal section of fin rays treated with *has1* control morpholino (Has1 MM), *has1* target morpholino (Has1 MO), *has2* control morpholino (Has2 MM) and *has2* target morpholino (Has2 MO). HA is detected by histochemical staining using biotinylated HABP and Streptavidin-Alexa 546. TO-PRO is used as the counterstain and detects DNA (blue). Compared to Has1 MM and Has2 MM treated fins, Has1 MO and Has2 MO treated fins exhibit reduced staining for HA. Arrow identifies the basal layer of epithelium; arrow head identifies the bone; m, mesenchyme; e, epithelium. Scale bar represents 20 μm .

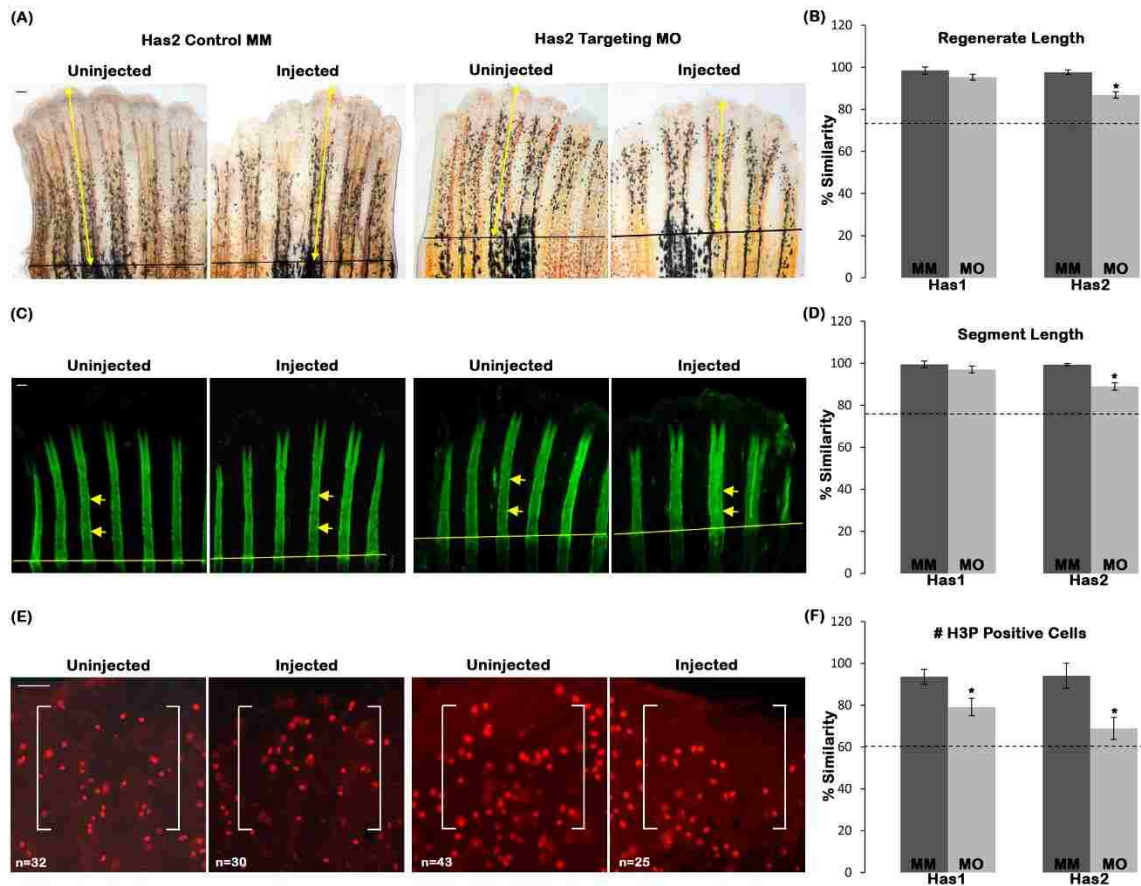


Figure 3.3: Reduced HA contributes to Hapln1a knockdown phenotypes. Prior to knockdown and electroporation, all fins were amputated at 50% level and allowed to regenerate for 3 days (amputation plane indicated by horizontal lines). Fin rays treated with targeting MO or standard control MM were measured and compared to their uninjected sides. The ratio of injected (MO or control MM) and un-injected side multiplied by 100 is the percent similarity. Percent similarity greater than 100% reflects the fact that the experimental side can be measurably larger than the control injected side. (A) Representative images showing regenerate length for Has2 MM and Has2 MO treated fins. Total regenerate length was evaluated by measuring the distance between the amputation plane (black line) to the distal end of the fin using the 3rd fin ray (marked by yellow arrows). (B) Bar graph shows that regenerate length is significantly reduced upon *has2* knockdown but not in *has1* knockdown. The black dotted line indicates the extent of *hapln1a* knockdown effect compared to *has1* and *has2* knockdowns. (C)

Representative calcein stained fins showing segment length for Has2 MM and Has2 MO treated fins. Segment length was evaluated by measuring the distance between first two joints in the regenerate (marked by yellow arrows). (D) Bar graph shows that segment length is significantly reduced upon *has2* knockdown but not in *has1* knockdown. The black dotted line indicates the extent of *hapln1a* knockdown effect compared to *has1* and *has2* knockdowns. (E) Representative H3P stained fins showing H3P positive cells for Has2 MM and Has2 MO treated fins. H3P positive cells were counted within a defined area (marked by white brackets). (F) Bar graph shows that cell proliferation is significantly reduced upon *has1* and *has2* knockdown, with *has2* having a greater effect than *has1*. The black dotted line indicates the extent of *hapln1a* knockdown effect, compared to *has1* and *has2* knockdowns. Students t-test was performed ($p < 0.05$) to determine significance, and the error bars indicate standard error of the mean. Scale bar is 50 μm in all panels.

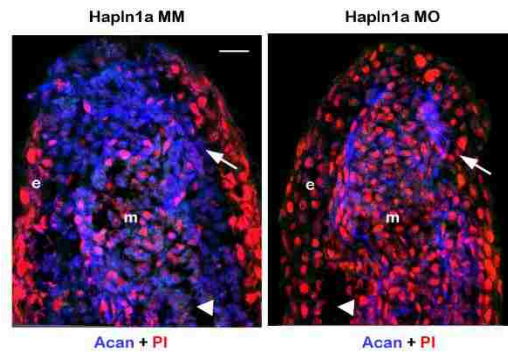


Figure 3.4: Morpholino mediated knockdown of *hapln1a* results in reduced Acan protein levels. Longitudinal section of fin rays treated with *hapln1a* control morpholino (Hapln1a MM) and *hapln1a* targeting morpholino (Hapln1a MO). Immuno-staining for Acan (blue) and counterstained for nuclei with Propidium Iodide (PI, red). Compared to the control Hapln1a MM treated fins, Hapln1a MO treated fins show reduced staining for Acan. Arrow identifies the basal layer of epithelium; arrow head identifies the bone; m, mesenchyme; e, epithelium. Scale bar represents 20 μm .

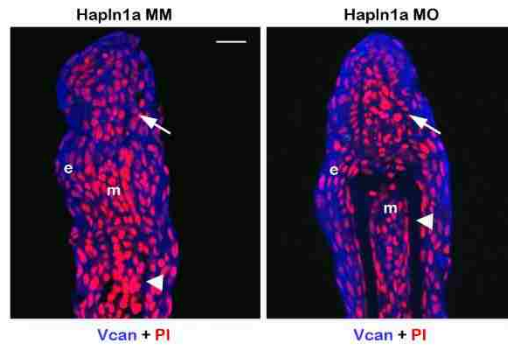


Figure 3.5: Vcan protein levels are unchanged following MO mediated knockdown of *hapln1a*. Longitudinal section of fin rays treated with *hapln1a* control morpholino (Hapln1a MM) and *hapln1a* targeting morpholino (Hapln1a MO). Immuno-staining for Vcan (blue) and counterstained for nuclei with Propidium Iodide (PI, red). Hapln1a MM treated fins and Hapln1a MO treated fins show similar levels of staining for Vcan. Arrow identifies the basal layer of epithelium; arrow head identifies the bone; m, mesenchyme; e, epithelium. Scale bar represents 20 μ m.

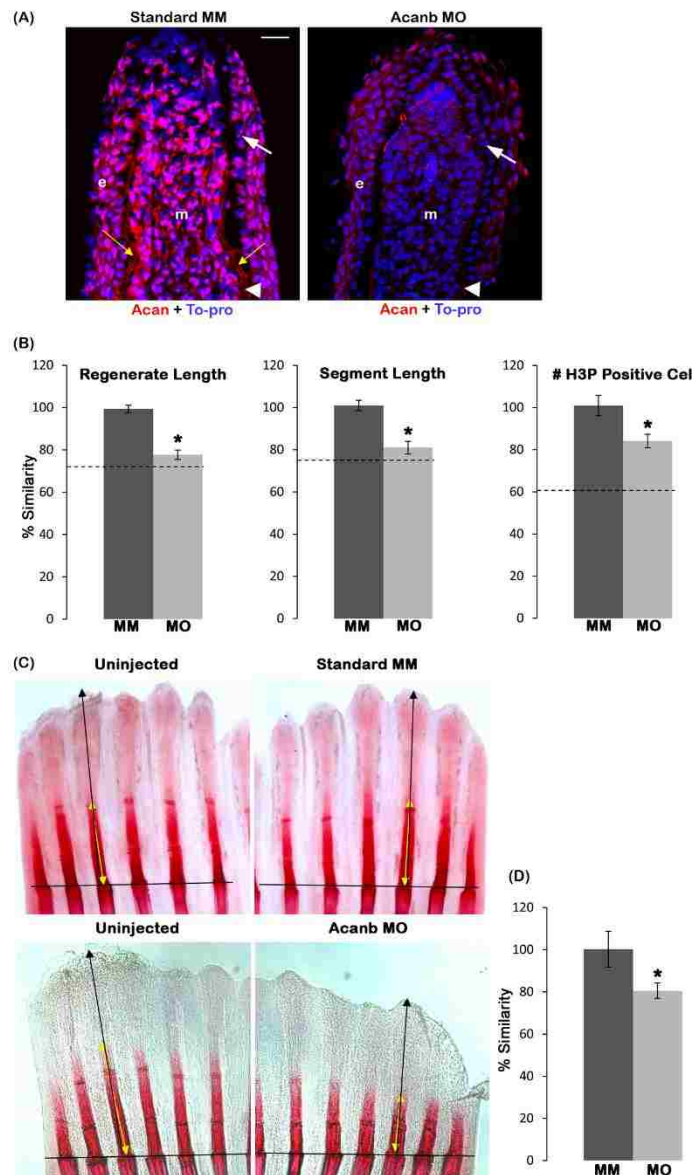


Figure 3.6: Reduced Acan contributes to Hapln1a knockdown phenotypes. Prior to knockdown and electroporation, all fins were amputated at 50% level and allowed to regenerate for 3 days. Fin rays treated with targeting MO or standard control MM were measured and compared to their un-injected sides. The ratio of injected (MO or control MO) and un-injected side multiplied by 100 is the percent similarity. Percent similarity greater than 100% reflects the fact that the experimental side can be measurably larger than the control un-injected side. (A) Longitudinal section of fin rays treated with

standard control morpholino (Standard MM) and *acanb* target morpholino (Acanb MO). Immuno-staining for Acan (red) and counterstained for nuclei with To-pro (blue). Compared to the standard MM treated fins, Acanb MO treated fins show reduced staining for Acan. White arrow identifies the basal layer of epithelium; yellow arrow identifies Acan staining in the lepidotrichia, arrow head identifies the bone; m, mesenchyme; e, epithelium. Scale bar represents 20 μm . (B) Bar graph shows that regenerate length, segment length and cell proliferation is significantly reduced upon *acanb* knockdown. The mean of percent similarity for the MO treated experimental group and the corresponding MM treated control group were estimated and compared. Statistical significance was determined using the student's *t*-test ($P < 0.05$) and the error bars represent standard error of mean. The black dotted line indicates the extent of *hapln1a* knockdown effect compared to *acanb* knockdown. (C) Representative alizarin red stained fins showing extent of bone calcification. The black line indicates the amputation plane. (D) The extent of mineralization was calculated as the ratio of the zone of mineralization (extent of detectable alizarin red staining length) to the total regenerate length. The mean of percent similarity for the MO treated experimental group and the corresponding MM treated control group were estimated and compared, and the statistical significance between the groups was determined using two tailed unpaired student's *t*-test ($P < 0.05$) and the error bars indicate the standard error of mean.

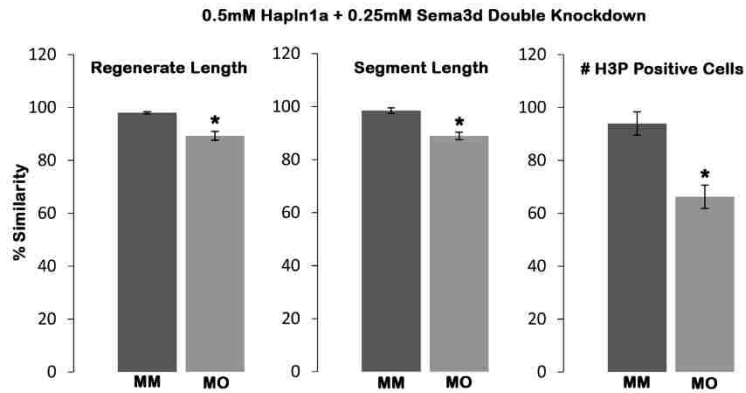


Figure 3.7: Hapln1a and Sema3d interact genetically to mediate Cx43 phenotypes.

Prior to knockdown and electroporation, all fins were amputated at 50% level and allowed to regenerate for 3 days. Fin rays treated with combined targeting MO or combined control MM were measured and compared to their un-injected sides. The ratio of injected (MO or control MO) and un-injected side multiplied by 100 is the percent similarity. Percent similarity greater than 100% reflects the fact that the experimental side can be measurably larger than the control un-injected side. Independent *hapln1a* knockdown at 0.5mM concentration and *sema3d* knockdown at 0.25mM concentration did not produce significant effects on Cx43 dependent phenotypes (not shown). Bar graphs reveal that double knockdown at MO concentrations of 0.5mM Hapln1a and 0.25mM of Sema3d recapitulated the Cx43 knockdown phenotypes (reduced regenerate length, segment length and cell proliferation), suggesting that Hapln1a and Sema3d interact genetically to promote Cx43 function. Students t-test was performed ($p < 0.05$) to determine significance, and the error bars indicate standard error of the mean.

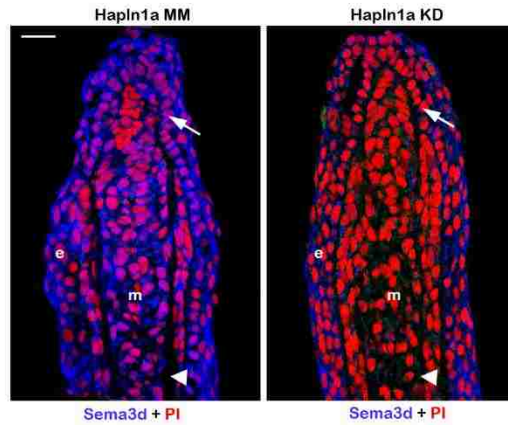


Figure 3.8: Morpholino mediated knockdown of *hapln1a* results in reduced Sema3d protein levels. Longitudinal section of fin rays treated with *hapln1a* control morpholino (Hapln1a MM) and *hapln1a* targeting morpholino (Hapln1a MO). Immunostaining for Sema3d (blue) and counterstained for nuclei with Propidium Iodide (PI, red). Compared to the control MM treated fins, Hapln1a MO treated fins show reduced staining for Sema3d. Arrow identifies the basal layer of epithelium; arrow head identifies the bone; m, mesenchyme; e, epithelium. Scale bar represents 20 μm .

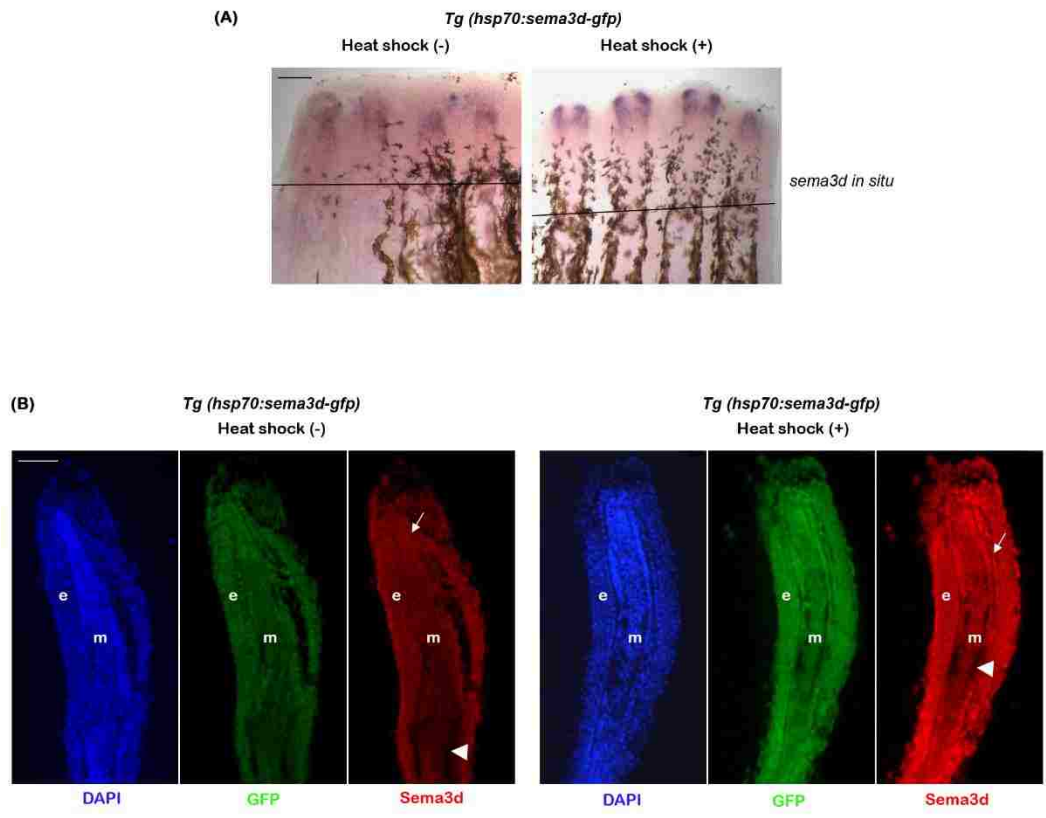


Figure 3.9: Heat shock induces upregulation of *sema3d* mRNA and Sema3d protein in *Tg(hsp70:sema3d-gfp)*. (A) Whole mount in situ hybridization shows increased expression of *sema3d* mRNA in heat shock treated fins compared to the untreated fins. Black line indicates amputation plane. (B) Immuno-staining analysis of longitudinal fin sections reveal increased expression of GFP (green) and Sema3d (Red) in heat shock treated fins compared to the untreated fins. DAPI (blue) is used as the counter stain and stains the nuclei. Arrows indicate basal layer of epithelium and arrow head marks the bone. e, epidermis; m, mesenchyme. Scale bar represents 100 μ m in both panels.

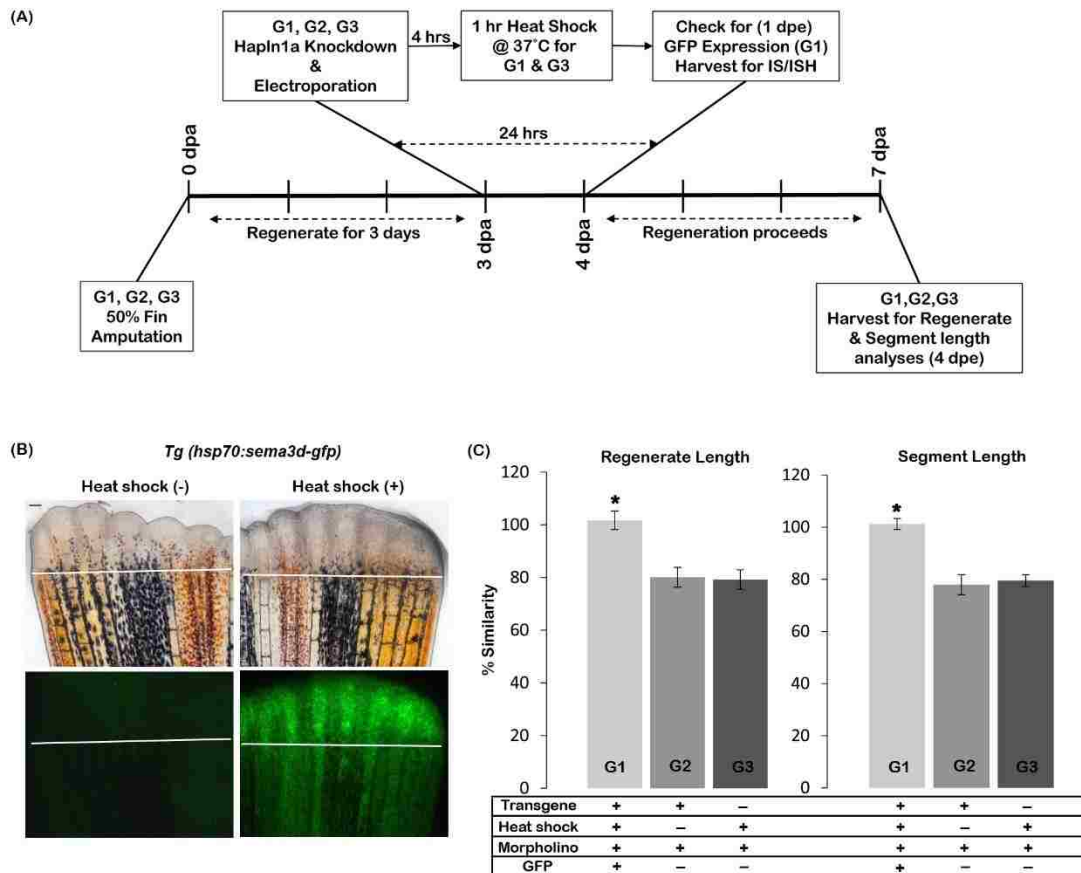


Figure 3.10: Sema3d overexpression rescues *hapln1a* knockdown phenotypes. (A) Experimental design. Three groups of fish were analysed: G1, G2 and G3. Fins from all three groups were amputated at 50% level. On 3 dpa all animals (G1, G2 and G3) were treated for *hapln1a* knockdown. Four hours post knockdown, G1 and G3 animals were heat shocked for 1hr at 37°C. G2 animals were not treated for heat shock. The following day, 1 dpe, G1 animals were selected for GFP positive fins. For GFP detection, immunostaining (IS) and in situ hybridization experiments (ISH), fins were harvested 1 dpe and for regenerate and segment length analyses fins were harvested at 4 dpe. (B) Heat shock induces Sema3d-GFP (green) expression in *Tg(hsp70:sema3d-gfp)*. GFP is not detected in the absence of heat shock. The white line indicates the amputation plane. Scale bar represents 50µm. (C) Following *hapln1a* knockdown the experimental group (G1) that is positive for both transgene and heat shock alone shows rescue for the phenotypes (i.e., shows high percent similarity compared to the un-injected side) whereas the control

groups either negative for heat shock (G2) or negative for transgene (G3) fail to show rescue (i.e., shows reduced percent similarity compared to the un-injected side). Students t-test was performed ($p < 0.05$) to determine significance, and the error bars indicate standard error of mean.

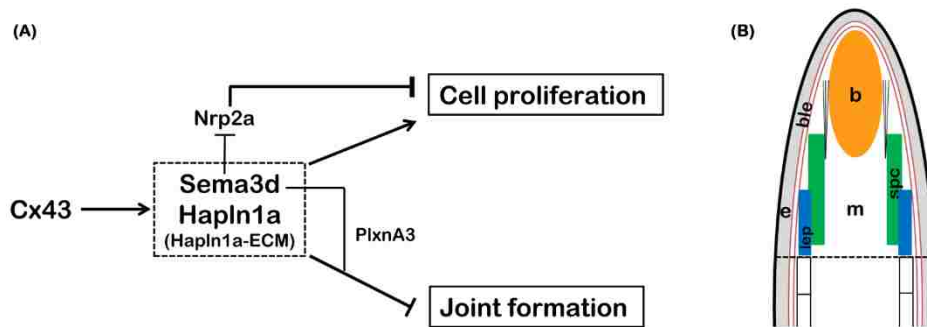


Figure 3.11: Hapln1a and Sema3d function in a common pathway to mediate Cx43 function during fin regeneration. (A) Proposed pathway showing interactions of Hapln1a-ECM and Sema3d proteins in skeletal growth and patterning. The Hapln1a dependent ECM stabilizes Sema3d protein and permits Sema3d dependent signaling events through its putative receptors, Nrp2a to promote cell proliferation (growth) and PlxnA3 to inhibit joint formation (patterning), to mediate Cx43 functions. (B) Speculative model showing co-operative functioning of Hapln1a-ECM and Sema3d protein. Hapln1a-ECM components HA and Hapln1a are expressed in the blastema (orange), mesenchyme (white), epidermis (grey) and by the skeletal precursor cells (green) in the lateral compartment. Acan is expressed both in the blastema and surrounding the lepidotrichia (blue). The *sema3d* mRNA is produced in the lateral skeletal precursor cells (green) (Ton and Iovine, 2012), while Sema3d protein is secreted. The Hapln1a-ECM stabilizes the secreted Sema3d protein and may facilitate its proper diffusion to promote signaling events via its receptors (the *nrp2a* mRNA is expressed in the medial mesenchyme while the *plxna3* mRNA is expressed in the lateral skeletal precursor cells, [15]). The black dotted line represents the plane of amputation, b, blastema; ble, basal layer of epithelium; e, epidermis; m, mesenchyme; lep, lepidotrichia; spc, skeletal precursor cells.

3.7 Tables

Gene	Primer Sequence for ISH	Morpholino Sequence
<i>hapln1a</i>	F-ggttctccgcttggcagcg	MO-gccacagaaaacagagcaatcatct
	RT7- taatacgactcactataggg gcccatccctgcctaagacc	MM-gccagacaaaagagaccaatgatct
<i>sema3d</i>	F-cgaagtgtagtaccatttacg	MO-tgtccggctcccctgcagtcttcat
	RT7- taatacgactcactataggg tatgaggatcatatgtcc	MM-tgtgccgctgccctccactcttcat
<i>has1</i>	F-gaaatttgtctctgtgcccagc	MO-tctttaagactggcttgaggccat
	RT7- taatacgactcactataggg gacctaaagggccgc	MM-tcttaaacagtggcttcacgtccat
<i>has2</i>	F-gttgggacgacactgttcgg	MO-gctgaccgctttatcacatctcatc
	RT7- taatacgactcactataggg ctcgattgtcagatggcgg	MM-gctcacccttaacagatgtcatc
<i>has3</i>	F-ggtgcggatcttcatcaccacc	
	RT7- taatacgactcactataggg ggtctggtgtaccagggc	
<i>acana</i>	F-cttcaggacaacacagtcaacg	
	RT7- taatacgactcactataggg cttcatcgctgtttcagagtagc	
<i>acانب</i>	F-cccattgctctgacactaccg	MO-acagcaggagccaaatcaaagacat
	RT7- taatacgactcactataggg catagcggccagattcagc	
<i>vcana</i>	F-cctaccagtttgtctacgcagc	
	RT7- taatacgactcactataggg gctgttctgatgtagcaatggtcg	
<i>vcانب</i>	F-gaacttcacacaagctcagcagg	
	RT7- taatacgactcactataggg aatcacactctccggagtctcc	

The RNA polymerase T7 binding site in reverse primers is highlighted in bold. F = Forward primer; RT7 = Reverse primer; MO = Targeting morpholino; MM = Control morpholino with 5 mismatch pairs to target sequence

Table 3.1: Primer and Morpholino Sequence

3.8 References

1. Paznekas WA, Boyadjiev SA, Shapiro RE, Daniels O, Wollnik B, et al. (2003) Connexin 43 (GJA1) mutations cause the pleiotropic phenotype of oculodentodigital dysplasia. *Am J Hum Genet* 72: 408-418.
2. Flenniken AM, Osborne LR, Anderson N, Ciliberti N, Fleming C, et al. (2005) A Gja1 missense mutation in a mouse model of oculodentodigital dysplasia. *Development* 132: 4375-4386.
3. Iovine MK, Higgins EP, Hindes A, Coblitz B, Johnson SL (2005) Mutations in connexin43 (GJA1) perturb bone growth in zebrafish fins. *Dev Biol* 278: 208-219.
4. Wei CJ, Xu X, Lo CW (2004) Connexins and cell signaling in development and disease. *Annu Rev Cell Dev Biol* 20: 811-838.
5. Batra N, Kar R, Jiang JX (2012) Gap junctions and hemichannels in signal transmission, function and development of bone. *Biochim Biophys Acta* 1818: 1909-1918.
6. Goodenough DA, Goliger JA, Paul DL (1996) Connexins, connexons, and intercellular communication. *Annu Rev Biochem* 65: 475-502.
7. Sohl G, Willecke K (2004) Gap junctions and the connexin protein family. *Cardiovasc Res* 62: 228-232.

8. Jones SJ, Gray C, Sakamaki H, Arora M, Boyde A, et al. (1993) The incidence and size of gap junctions between the bone cells in rat calvaria. *Anat Embryol (Berl)* 187: 343-352.
9. Lecanda F, Warlow PM, Sheikh S, Furlan F, Steinberg TH, et al. (2000) Connexin43 deficiency causes delayed ossification, craniofacial abnormalities, and osteoblast dysfunction. *J Cell Biol* 151: 931-944.
10. McGonnell IM, Green CR, Tickle C, Becker DL (2001) Connexin43 gap junction protein plays an essential role in morphogenesis of the embryonic chick face. *Dev Dyn* 222: 420-438.
11. Law LY, Lin JS, Becker DL, Green CR (2002) Knockdown of connexin43-mediated regulation of the zone of polarizing activity in the developing chick limb leads to digit truncation. *Dev Growth Differ* 44: 537-547.
12. Hoptak-Solga AD, Klein KA, DeRosa AM, White TW, Iovine MK (2007) Zebrafish short fin mutations in connexin43 lead to aberrant gap junctional intercellular communication. *FEBS Lett* 581: 3297-3302.
13. Hoptak-Solga AD, Nielsen S, Jain I, Thummel R, Hyde DR, et al. (2008) Connexin43 (GJA1) is required in the population of dividing cells during fin regeneration. *Dev Biol* 317: 541-548.
14. Sims K, Jr., Eble DM, Iovine MK (2009) Connexin43 regulates joint location in zebrafish fins. *Dev Biol* 327: 410-418

15. Ton QV, Iovine M (2012) Semaphorin3d mediates Cx43-dependent phenotypes during fin regeneration. *Dev Biol* 366: 195-203.
16. Govindan J, Iovine MK (2014) Hapln1a is required for connexin43-dependent growth and patterning in the regenerating fin skeleton. *PLoS One* 9: e88574.
17. Watanabe H, Yamada Y (1999) Mice lacking link protein develop dwarfism and craniofacial abnormalities. *Nat Genet* 21: 225-229.
18. Ghatak S, Misra S, Toole BP (2005) Hyaluronan constitutively regulates ErbB2 phosphorylation and signaling complex formation in carcinoma cells. *J Biol Chem* 280: 8875-8883.
19. Jiang D, Liang J, Noble PW (2007) Hyaluronan in tissue injury and repair. *Annu Rev Cell Dev Biol* 23: 435-461.
20. Misra S, Toole BP, Ghatak S (2006) Hyaluronan constitutively regulates activation of multiple receptor tyrosine kinases in epithelial and carcinoma cells. *J Biol Chem* 281: 34936-34941.
21. Mercer SE, Odelberg SJ, Simon HG (2013) A dynamic spatiotemporal extracellular matrix facilitates epicardial-mediated vertebrate heart regeneration. *Dev Biol* 382: 457-469.
22. Kim SH, Turnbull J, Guimond S (2011) Extracellular matrix and cell signalling: the dynamic cooperation of integrin, proteoglycan and growth factor receptor. *J Endocrinol* 209: 139-151.

23. Hynes RO (2014) Stretching the boundaries of extracellular matrix research. *Nat Rev Mol Cell Biol* 15: 761-763.
24. Westerfield M (1993) *The Zebrafish Book: A guide for the laboratory use of zebrafish (Brachydanio rerio)*. University of Oregon Press, Eugene, OR.
25. Thummel R, Bai S, Sarras MP, Jr., Song P, McDermott J, et al. (2006) Inhibition of zebrafish fin regeneration using in vivo electroporation of morpholinos against *fgfr1* and *msxb*. *Dev Dyn* 235: 336-346.
26. Iovine MK, Johnson SL (2000) Genetic analysis of isometric growth control mechanisms in the zebrafish caudal Fin. *Genetics* 155: 1321-1329.
27. Bhadra J, Iovine MK (2015) Hsp47 mediates Cx43-dependent skeletal growth and patterning in the regenerating fin. *Mech Dev*. In Press.
28. Du SJ, Frenkel V, Kindschi G, Zohar Y (2001) Visualizing normal and defective bone development in zebrafish embryos using the fluorescent chromophore calcein. *Dev Biol* 238: 239-246.
29. Munch J, Gonzalez-Rajal A, de la Pompa JL Notch regulates blastema proliferation and prevents differentiation during adult zebrafish fin regeneration. *Development* 140: 1402-1411.
30. Govindan J, Iovine MK (2015) Dynamic remodeling of the extra cellular matrix during zebrafish fin regeneration. *Gene Expr Patterns*. In Press.

31. Ghokale JRPaB, A.L (2001) *The Biochemistry of Bone. Osteoporosis*. San Diego: Academic Press. pp. 82.
32. Recklies AD, White C, Melching L, Roughley PJ (2001) Differential regulation and expression of hyaluronan synthases in human articular chondrocytes, synovial cells and osteosarcoma cells. *Biochem J* 354: 17-24.
33. Spicer AP, Nguyen TK (1999) Mammalian hyaluronan synthases: investigation of functional relationships in vivo. *Biochem Soc Trans* 27: 109-115.
34. Camenisch TD, Spicer AP, Brehm-Gibson T, Biesterfeldt J, Augustine ML, et al. (2000) Disruption of hyaluronan synthase-2 abrogates normal cardiac morphogenesis and hyaluronan-mediated transformation of epithelium to mesenchyme. *J Clin Invest* 106: 349-360.
35. Salbach J, Rachner TD, Rauner M, Hempel U, Anderegg U, et al. (2012) Regenerative potential of glycosaminoglycans for skin and bone. *J Mol Med (Berl)* 90: 625-635.
36. Toole BP (2009) Hyaluronan-CD44 Interactions in Cancer: Paradoxes and Possibilities. *Clin Cancer Res* 15: 7462-7468.
37. Toole BP, Gross J (1971) The extracellular matrix of the regenerating newt limb: synthesis and removal of hyaluronate prior to differentiation. *Dev Biol* 25: 57-77.
38. De Cat B, David G (2001) Developmental roles of the glypicans. *Semin Cell Dev Biol* 12: 117-125.

39. Ruoslahti E, Yamaguchi Y (1991) Proteoglycans as modulators of growth factor activities. *Cell* 64: 867-869.
40. Liu Y, Berndt J, Su F, Tawarayama H, Shoji W, et al. (2004) Semaphorin3D guides retinal axons along the dorsoventral axis of the tectum. *J Neurosci* 24: 310-318.
41. Matsumoto K, Li Y, Jakuba C, Sugiyama Y, Sayo T, et al. (2009) Conditional inactivation of Has2 reveals a crucial role for hyaluronan in skeletal growth, patterning, chondrocyte maturation and joint formation in the developing limb. *Development* 136: 2825-2835.
42. Wirrig EE, Snarr BS, Chintalapudi MR, O'Neal J L, Phelps AL, et al. (2007) Cartilage link protein 1 (Crtl1), an extracellular matrix component playing an important role in heart development. *Dev Biol* 310: 291-303.
43. Wight TN (2002) Versican: a versatile extracellular matrix proteoglycan in cell biology. *Curr Opin Cell Biol* 14: 617-623.
44. Snow HE, Riccio LM, Mjaatvedt CH, Hoffman S, Capehart AA (2005) Versican expression during skeletal/joint morphogenesis and patterning of muscle and nerve in the embryonic mouse limb. *Anat Rec A Discov Mol Cell Evol Biol* 282: 95-105.
45. Li H, Schwartz NB, Vertel BM (1993) cDNA cloning of chick cartilage chondroitin sulfate (aggrecan) core protein and identification of a stop codon in the aggrecan gene associated with the chondrodystrophy, nanomelia. *J Biol Chem* 268: 23504-23511.

46. Wai AW, Ng LJ, Watanabe H, Yamada Y, Tam PP, et al. (1998) Disrupted expression of matrix genes in the growth plate of the mouse cartilage matrix deficiency (cmd) mutant. *Dev Genet* 22: 349-358.
47. Watanabe H, Kimata K, Line S, Strong D, Gao LY, et al. (1994) Mouse cartilage matrix deficiency (cmd) caused by a 7 bp deletion in the aggrecan gene. *Nat Genet* 7: 154-157.
48. Bastow ER, Byers S, Golub SB, Clarkin CE, Pitsillides AA, et al. (2008) Hyaluronan synthesis and degradation in cartilage and bone. *Cell Mol Life Sci* 65: 395-413.
49. Roughley PJaM, P (2013) The role of HA and Has2 in the Dvelopment and Function of the skeleton. *Extracellular matrix in development: Springer-Verlag Berlin Heidelberg*. pp. 219-247.
50. Li XY, Guo X, Wang LX, Geng D, Kang LL, et al. (2007) [Serum hyaluronic acid, tumor necrosis factor -alpha, vascular endothelial growth factor, NO, and Se levels in adult patients with Kashin-Beck disease]. *Nan Fang Yi Ke Da Xue Xue Bao* 27: 941-944.
51. Weigel PH, Hascall VC, Tammi M (1997) Hyaluronan synthases. *J Biol Chem* 272: 13997-14000.
52. Shyjan AM, Heldin P, Butcher EC, Yoshino T, Briskin MJ (1996) Functional cloning of the cDNA for a human hyaluronan synthase. *J Biol Chem* 271: 23395-23399.

53. Watanabe K, Yamaguchi Y (1996) Molecular identification of a putative human hyaluronan synthase. *J Biol Chem* 271: 22945-22948.
54. Spicer AP, Seldin MF, Olsen AS, Brown N, Wells DE, et al. (1997) Chromosomal localization of the human and mouse hyaluronan synthase genes. *Genomics* 41: 493-497.
55. Bakkers J, Kramer C, Pothof J, Quaedvlieg NE, Spaink HP, et al. (2004) Has2 is required upstream of Rac1 to govern dorsal migration of lateral cells during zebrafish gastrulation. *Development* 131: 525-537.
56. Yoshida M, Itano N, Yamada Y, Kimata K (2000) In vitro synthesis of hyaluronan by a single protein derived from mouse HAS1 gene and characterization of amino acid residues essential for the activity. *J Biol Chem* 275: 497-506.
57. Itano N, Sawai T, Yoshida M, Lenas P, Yamada Y, et al. (1999) Three isoforms of mammalian hyaluronan synthases have distinct enzymatic properties. *J Biol Chem* 274: 25085-25092.
58. Hiscock DR, Caterson B, Flannery CR (2000) Expression of hyaluronan synthases in articular cartilage. *Osteoarthritis Cartilage* 8: 120-126.
59. Nishida Y, Knudson CB, Nietfeld JJ, Margulis A, Knudson W (1999) Antisense inhibition of hyaluronan synthase-2 in human articular chondrocytes inhibits proteoglycan retention and matrix assembly. *J Biol Chem* 274: 21893-21899.

60. Moffatt P, Lee ER, St-Jacques B, Matsumoto K, Yamaguchi Y, et al. (2011) Hyaluronan production by means of Has2 gene expression in chondrocytes is essential for long bone development. *Dev Dyn* 240: 404-412.
61. Thorogood PV, Hinchliffe JR (1975) An analysis of the condensation process during chondrogenesis in the embryonic chick hind limb. *J Embryol Exp Morphol* 33: 581-606.
62. Koshier RA, Savage MP, Walker KH (1981) A gradation of hyaluronate accumulation along the proximodistal axis of the embryonic chick limb bud. *J Embryol Exp Morphol* 63: 85-98.
63. Singley CT, Solursh M (1981) The spatial distribution of hyaluronic acid and mesenchymal condensation in the embryonic chick wing. *Dev Biol* 84: 102-120.
64. Contreras EG, Gaete M, Sanchez N, Carrasco H, Larrain J (2009) Early requirement of Hyaluronan for tail regeneration in *Xenopus* tadpoles. *Development* 136: 2987-2996.
65. Calve S, Odelberg SJ, Simon HG A transitional extracellular matrix instructs cell behavior during muscle regeneration. *Dev Biol* 344: 259-271.
66. Casini P, Nardi I, Ori M Hyaluronan is required for cranial neural crest cells migration and craniofacial development. *Dev Dyn* 241: 294-302.
67. Kreuger J, Perez L, Giraldez AJ, Cohen SM (2004) Opposing activities of Dally-like glypican at high and low levels of Wingless morphogen activity. *Dev Cell* 7: 503-512.

68. Kirkpatrick CA, Dimitroff BD, Rawson JM, Selleck SB (2004) Spatial regulation of Wntless morphogen distribution and signaling by Dally-like protein. *Dev Cell* 7: 513-523.

Chapter 4

Dynamic remodeling of the extra cellular matrix during
zebrafish fin regeneration

Gene Expression Patterns, [doi:10.1016/j.gep.2015.06.001](https://doi.org/10.1016/j.gep.2015.06.001)

4.1 Abstract

Extracellular matrix plays a dynamic role during the process of wound healing, embryogenesis and tissue regeneration. Caudal fin regeneration in zebrafish is an excellent model to study tissue and skeletal regeneration. We have analyzed the expression pattern of some of the well characterized ECM proteins during the process of caudal fin regeneration in zebrafish. Our results show that a transitional matrix analogous to the one formed during newt skeletal and heart muscle regeneration is synthesized during fin regeneration. Here we demonstrate that a provisional matrix rich in hyaluronic acid, tenascin C, and fibronectin is synthesized following amputation. Additionally, we observed that the link protein Hapln1a dependent ECM, consisting of Hapln1a, hyaluronan and proteoglycan aggrecan, is upregulated during fin regeneration. Laminin, the protein characteristic of differentiated tissues, showed only modest change in the expression pattern. Our findings on zebrafish fin regeneration implicates that changes in the extracellular milieu represent an evolutionarily conserved mechanism that proceeds during tissue regeneration, yet with distinct players depending on the type of tissue that is involved.

4.2 Introduction

The Extra Cellular Matrix (ECM) is secreted by cells and is composed of a wide variety of components that broadly include proteins, carbohydrates and proteins modified by sugar moieties termed proteoglycans (PG). Together these components form a complex meshwork that provides both structural and functional information to the cells. Initially, the ECM was thought to play only passive roles as a

space filling material between cells and tissues. More recent work suggests that in addition to providing structural stability, the ECM also acts to sequester and store growth factors, present growth factors to their receptors and sense and transduce mechanical signals [1,2]. Therefore, the biochemical and the mechanical cues provided by the ECM play critical roles in regulating cell behaviors including migration, shape, survival, differentiation, and proliferation. Moreover, remodeling of the ECM occurs during normal development, morphogenesis, wound healing and during the mediation of disease states such as cancer [3,4]. Also, ECM remodeling has recently been shown to contribute to epimorphic regeneration of newt skeletal muscle and heart, *Xenopus* tadpole tails, and zebrafish heart [5-8].

Although mounting evidence suggests the importance of the ECM on cellular functions critical for morphogenesis, development, wound healing, tissue repair and regeneration, only a handful of studies address the role of ECM and its components during epimorphic regeneration. Several studies substantiate the establishment of a common transitional matrix rich in hyaluronic acid (HA), fibronectin (FN) and tenascin C (TNC) during epimorphic regeneration [7-9] and down regulation of ECM proteins that are characteristic of differentiated skeletal tissues like laminin (LAM) and collagen type I [10,11]. Moreover, numerous studies have identified important roles for the polyanionic high molecular weight compound hyaluronic acid (HA). HA is upregulated in matrices undergoing remodeling, during regenerative repair mechanisms [4,7,8,12], and has been demonstrated to modulate signal transduction pathways such as EGFR/ErbB, TGF β and BMP [13-15]. HA is a linear non-sulfated glycosaminoglycan (GAG) of

repeating disaccharide units of [D-glucuronic acid (1- β -3) and Nacetyl-D-glucosamine (1- β -4)]_n and plays a principal role in organizing PG aggregates like aggrecan (Acan) and versican (Vcan). HAPG aggregates are stabilized by link proteins, which bring PGs to a backbone of HA [16,17]. The PG family is a heterogeneous group consisting of a core protein with GAG side chains attached covalently. As opposed to HA, the GAGs in PGs are frequently sulfated. Acan is distinct from Vcan in that Acan has ~100 keratin and chondroitin sulfate GAG chains attached to the core protein, whereas Vcan has only ~12-15 chondroitin sulfate GAG chains [18,19]. These poly-anionic macromolecular aggregates provide the required structural organization and flexibility and bind to several cationic proteins involved in signaling that aid the progression of regeneration [20].

Our lab was the first to demonstrate the functional consequences of reduced HA during zebrafish fin regeneration [21]. For example, we found that the link protein Hapln1a (Hyaluronan and Proteoglycan Link Protein 1a) is required for cell proliferation and fin ray joint formation. Hapln1a belongs to the family of link proteins that play a critical role in stabilizing the ECM by linking the aggregates of HA and PGs. We define Hapln1a and the associated HA and PGs as Hapln1a-ECM. We have shown that reduction in Hapln1a levels leads to reduction in HA levels that might contribute to the observed skeletal phenotypes in the regenerating fins [21]. Together, data from our study and other studies highlight the importance of ECM components (HA and PGs) stabilized by Hapln1a during skeletal growth and patterning [12,22].

To achieve a better understanding about how the ECM is remodeled during zebrafish fin regeneration, we looked at components of the ECM over time. We focused on the expression pattern of Hapln1a-ECM components (i.e. Hapln1a, HA, Acan, Vcan), as well as the other components of the putative transitional matrix i.e. FN and TNC [7,8,10,11]. In addition, we included LAM, which is characteristic of differentiated tissues. We find that all components of the transitional matrix (HA, FN and TNC) are also upregulated during fin regeneration. Moreover, we find that Hapln1a and Acan expression patterns change extensively over the time course, while Vcan pattern is less dynamic. In contrast, LAM expression pattern showed modest changes from ontogeny to regenerating fins. These findings provide the first examination of ECM remodeling during skeletal regeneration of zebrafish fin.

4.3 Materials and Method

Statement on the ethical treatment of animals

This study was carried out in strict accordance with the recommendations in the Guide for the Care and Use of Laboratory Animals of the National Institutes of Health. The protocols used for this manuscript were approved by Lehigh's Institutional Animal Care and Use Committee (IACUC) (protocol identification #128, approved 11/16/2014). Lehigh University's Animal Welfare Assurance Number is A-3877-01. All experiments were performed to minimize pain and discomfort.

Housing and husbandry

Zebrafish are housed in a re-circulating system built by Aquatic Habitats (now Pentair). Both 3L tanks (up to 12 fish/tank) and 10 L tanks (up to 30 fish / tank) are used. The fish room has a 14:10 light:dark cycle and room temperature (RT) varies from 27-29°C [23]. Water quality is automatically monitored and dosed to maintain conductivity (400-600 µS) and pH (6.95-7.30). Nitrogen levels are maintained by a biofilter. A 10 % water change occurs daily. Recirculating water is filtered sequentially through pad filters, bag filters, and a carbon canister before circulating over UV lights for sterilization. Fish are fed three times daily, once with brine shrimp (hatched from INVE artemia cysts) and twice with flake food (Aquatox AX5) supplemented with 7.5 % micropellets (Hikari), 7.5 % Golden Pearl (300-500 micron, Brine Shrimp direct), and 5 % Cyclo-Peeze (Argent).

Animal procedures

The wild-type C32 zebrafish (*Danio rerio*) strain was used in this study. Fish were anaesthetized in 0.1% tricaine and caudal-fin amputations were performed at 50 % level. Fin regeneration was then allowed to proceed until the desired time period (3, 5 or 7 days post amputation [dpa]) and the regenerated fins were harvested from anaesthetized fish. Fins were processed for immunohistochemistry as described below. A minimum of 5 different fins for each time point were sectioned and approximately 15-20 sections per fin were analyzed for each of the ECM component under study.

Fixing conditions and cryosectioning

Prior to immunostaining, ontogenic fins (i.e. unamputated) and regenerating fins (3, 5 and 7 dpa) were fixed overnight (O/N) with 4% PFA in PBS (for detection of HA, Hapln1a, Fibronectin, Tenascin-C and Laminin). After a brief methanol wash, fins were dehydrated in 100% methanol and stored at -20°C until use. Before sectioning, fins were sequentially rehydrated in a methanol-PBS series of washes and then were embedded in 1.5% agarose/5% sucrose in PBS and equilibrated in 30% sucrose in PBS. For detection of Acan and Vcan, fins were fixed for 10 min with 2% PFA at RT followed by three 10 min washes with 1X PBS, and were next embedded in 1.5% agarose/5% sucrose in PBS and equilibrated in 30% sucrose in PBS. Following that embedded fins were mounted in OCT and cryosectioned (15 μm sections) using a Reichertâ Jung 2800 Frigocut cryostat. Sections were collected on Superfrost Plus slides (Fisher) and allowed to air dry O/N at RT. Sections can be stored at -20°C for up to a year. The slides were stored at -20°C for at least one day before starting the experiment.

Immunofluorescence

First, the slides were brought to RT for at least one hour. Sections were circled using a marking pen (ImmEdge Pen H-4000; PAP pen, VWR Laboratories). For Hapln1a and Vcan immunostaining, the sections were rehydrated twice for 10 min in PBS followed by two washes with block (2% BSA, 0.1% TritonX 100 in PBS). Then, sections were blocked for another one hour at RT and then incubated in respective primary antibodies. The following primary antibodies were used: Mouse anti-Hapln1a antibody (MD Bioproducts, 1:500) and Rabbit anti-versican (H-56) (Santa Cruz Biotechnology-SC-25831) O/N at 4°C .

For FN, TNC and LAM the sections were rehydrated twice for 10 min in PBS followed by a brief Trypsin-EDTA treatment (1:1 diluted with PBS) (Gibco-Life Technologies #25300-054) for 3 min at RT and then washed with PBS twice for 10 min. Following that, slides were washed with block for 10 min at RT. Then, sections were blocked for another one hour at RT, incubated in respective primary antibodies O/N at 4°C. The following primary antibodies were used: Rabbit anti-human fibronectin (Sigma-F3648, 1:100); Rabbit anti-chicken tenascin (US Biological-T2550-23, 1:500) and Rabbit anti-rat laminin (Thermo scientific-RB-082-A1, 1:100).

For Acan immunostaining, the sections were rehydrated twice for 10 min in PBS at RT, followed by antigen unmasking by digestion with chondroitinase. First, the slides were incubated with the chondroitinase treatment buffer (50mM Tris, 60mM sodium acetate, 0.02% BSA, pH 8.0) at 37°C for 5 min, followed by deglycosylation using chondroitinase ABC enzyme (Sigma-C2905, final concentration 0.05U in the treatment buffer) for 2 h at 37°C. Following that, slides were washed with block for 10 min at RT. Then, sections were blocked for another one hour at RT, incubated with Mouse anti-aggrecan (BC-3) (Thermo Scientific-MA3-16888) primary antibody O/N at 4°C.

Following incubation with primary antibodies, sections were washed three times in block (15 min each), incubated at RT for one hour with secondary antibody goat anti-mouse Alexa-488 (Invitrogen, 1:200, pre-absorbed for one hour, at RT with fixed zebrafish fins to reduce background staining) and washed again three times in block (15 min each). Sections were next incubated with propidium iodide (final concentration 0.01mg/ml in block) for 30 min at RT, followed by a quick wash with distilled water.

Then the slides were blotted dry and mounted for imaging. Confocal microscopy was used to image the sections using a 40×/1.3 numerical aperture objective on an inverted microscope (Axiovert 200 M; Carl Zeiss, Jena, Germany) equipped with an LSM510 META scan head (Carl Zeiss). Argon ion and 543 HeNe lasers were used to generate the 488 and 543 lines used for excitation, and pinholes were typically set to 1–1.5 Airy units. Images were exported as TIFF files and printed using Photoshop.

Histo-chemical analysis of HA

HA was detected as described [21]. Briefly the sections were rehydrated twice for 10 min in PBS followed by two washes with block. Then, sections were blocked for another 1 h at RT, incubated with biotinylated hyaluronic acid binding protein (bHABP-Calbiochem-385911, 1:100) O/N at 4°C. The sections were washed three times in block (15 min each), incubated at RT for one hour with streptavidin-Alexa-546 conjugate, (Invitrogen, 1:200) and washed again three times in block (15 min each). Sections were next incubated with propidium iodide (final concentration 0.01mg/ml in block) for 30 min at RT, followed by a quick wash with distilled water. Then the slides were blotted dry and mounted for imaging as described above.

Semi-quantitative analysis for protein expression during the time course of regeneration

Semi quantitation of fluorescence staining for expression of each protein under study, over the time course of regeneration was performed using ImageJ software. Briefly, the tissue sections for each time point was selected using the freeform drawing tool and converted to RGB stack. Then using the analyze menu, the measurements were

set to obtain the values for area, integrated density and mean gray values for Alexa 488 fluorescence. To account for the background, three unstained regions surrounding the tissue were selected and the values were obtained as before. To calculate the corrected total fluorescence pixel intensity for each section the following formula was used. Corrected total fluorescence = Integrated Density – (Area of selected tissue X Mean fluorescence of the back ground). This was repeated for each time point, for each of the protein under study and the average and standard deviation were calculated and plotted as Average total pixel intensity on the Y-axis. For ontogeny Acan fin sections, since the staining is localized to the joints, the area around the joints was selected instead of the whole section and the corrected total fluorescence was calculated as before.

4.4 Results and Discussion

Previous studies on newt skeletal muscle and heart regeneration have shown that upon tissue injury, ECM remodeling results in the synthesis of a regeneration specific transitional matrix rich in HA, TNC and FN [5-8,12,24,25]. These components are considered as the fundamental ECM components during embryonic development [22,26-28] and wound healing [29-31]. The spatial and temporal expression and the concentration of these components influence the type of response that is elicited upon tissue injury. Comparative gene ontology analysis has shown that the up regulation of this transitional matrix is an evolutionarily conserved response between species during tissue regeneration, as opposed to repair mechanisms that result in scarring [8]. Importantly, during early stages of repair, HA provides a highly hydrated environment and TNC generates anti-adhesive effects thereby promoting the undifferentiated state.

Concomitant with the up regulation of this transitional matrix, several studies have shown that the components of differentiated tissues, like collagen type I and LAM, are suppressed by the action of matrix metallo proteases (MMP's). Together, these changes lead to significant changes in the local environment that prevent scarring and instead are conducive for regeneration to proceed [10,11,32]. We have demonstrated in this study that the components of the transitional matrix are also expressed during zebrafish caudal fin regeneration. To our knowledge, this is the first study to describe the expression pattern of these ECM proteins in a time course during fin regeneration.

The zebrafish caudal fin is made up of 16-18 segmented bony fin rays (lepidotrichia) that are connected by soft inter ray tissue that is devoid of any skeleton. The lepidotrichia are made of two concave hemi-rays that are lined by bone secreting osteoblasts [33,34]. Lepidotrichia surround blood vessels, nerves, fibroblasts and pigment cells and are covered by a multilayered epidermis. Following amputation, a wound epidermis derived from the stump epithelium closes the wound. Formation of a multilayered epidermis has been shown to be an important requirement for blastema establishment and proliferation of cells [35]. Just beneath the wound epidermis and distal to each fin ray, a blastema is formed that consists of de-differentiated and highly proliferative cells [36-39]. The longitudinal section of a fin ray reveals a simple architecture with a central mesenchyme separated from the multilayered outer epidermis by a single layer of epithelial cells termed the basal layer of epithelium (BLE) (Fig. 1). During regeneration, just beneath the BLE, collagenous fibers called the actinotrichia are synthesized that serve to support the fin folds [40,41]. Osteoblasts and joint forming

cells, collectively termed the skeletal precursor cells (SPC's), reside between the actinotrichia and BLE [42,43]. The formation of the blastema and the regenerative outgrowth is characterized by cell division and cell differentiation to replace all lost tissues of the fin.

In order to evaluate changes in ECM components during skeletal regeneration, we examined ECM proteins in longitudinal fin sections at 0 dpa (uncut), 3 dpa, 5 dpa and 7 dpa regenerating fins. The uncut 0 dpa fin represents the ontogenic, non-regenerative state mostly consisting of well differentiated tissue. The early time point 3 dpa represents the time during which maximum rate of regeneration occurs [44,45]. Later, regenerative outgrowth and fin patterning continues up to 14 days [34]. The time points of 5 and 7 dpa were chosen to evaluate the expression patterns of the ECM proteins during the outgrowth and patterning phase of fin regeneration. We further paired immunohistochemical analyses with semi-quantitative analyses in order to validate the qualitative interpretation of overall changes in expression levels.

Hapln1a dependent ECM undergoes transient dynamic modification during regeneration

In a recent study, we showed that the ECM protein Hapln1a plays critical roles during skeletal growth and patterning by influencing cell proliferation, joint formation and the distribution of HA in the regenerating fin (Govindan and Iovine, 2014). Here we evaluate expression and localization of the link protein Hapln1a, the PGs Acan and Vcan, and HA during the time course for regeneration. Hapln1a and HA exhibit similar expression patterns during all time points of regeneration (Fig. 2A and B). In ontogeny

fins, both Hapln1a and HA were low in the epidermis. In the mesenchyme, Hapln1a was almost absent but HA was observed. HA appeared to be tightly associated with epidermal cells and may be associated in a pericellular manner (Knudson et al., 2002; Toole, 2004). By 3 dpa, Hapln1a and HA were predominantly upregulated in mesenchyme and epidermis (Fig. 2A and B). The proximal end of the mesenchymal compartment showed more expression compared to the proliferative blastema. Additionally, HA was also strongly upregulated in the mesenchyme of the stump tissue (Figure S1). At 5 dpa, Hapln1a and HA were seen throughout the mesenchymal compartment and in the epidermis. During 7 dpa, the Hapln1a staining was more like the ontogeny fin where the epidermal staining was reduced significantly, but there was moderate staining in the mesenchyme. HA appeared to go down at 7 dpa compared to 3 and 5 dpa but was still moderately expressed throughout the mesenchyme (Fig. 2A and B).

The similar expression pattern of Hapln1a and HA during regeneration is expected as these two components are dependent on each other to associate with the PG aggregates. In particular, HA by itself is known to play a crucial role during matrix remodeling. It is well documented that HA synthesis and HA dependent signaling play a critical role during tissue regeneration, implying that it could be an evolutionarily conserved process that takes place in response to tissue loss to promote regeneration. The HA expression pattern in the regenerating zebrafish fin strongly corroborates with newt skeletal muscle and *Xenopus* tail regeneration studies where HA is expressed strongly in the distal stump and proximal blastema, as compared to the distal end of the

regenerate. This, in turn is thought to regulate the proliferative state of mesenchymal cells in the regenerating tissue by modulating the distance between the cells [7,12,28,46,47]. Also, the immediate up regulation of HA proximal to the amputation plane and in the distal stump could play an important role to promote smooth migration of the progenitor cells into the regenerating blastema. For example in vitro studies using newt myoblasts have shown that myoblasts in an HA rich environment show reduced fusion and differentiation and a significant increase in migration [7]. In contrast, the comparatively reduced expression of HA in the blastema could facilitate cell proliferation [7,20,48,49].

The aggregating PGs Acan/Vcan are present surrounding the bones and are important for matrix organization, cell motility and growth and are effective inhibitors of mineral deposition because of their ability to sequester calcium and impose steric hindrance [50]. Furthermore, changes in GAG composition are now considered a signature event during various physiological and pathological remodeling processes, such as bone formation, regeneration, scarring, osteoarthritis, and cancer metastasis [51,52]. We have analyzed the expression pattern of both Acan and Vcan in regenerating fins.

Acan expression shows a distinct pattern in each of the different stages during fin regeneration. In ontogeny fins, Acan strongly localized to the mature joints and was poorly expressed in the mesenchyme and epidermis (Fig. 2C). On 3 dpa, we observed a moderate up regulation of Acan expression surrounding the mesenchymal cells, and around the stump bone matrix. Epidermal staining was reduced compared to the

mesenchyme. Around 5 dpa, Acan expression was very strongly associated with lepidotrichia consisting of SPC's and, to a lesser extent with actinotrichia and mesenchyme. Acan expression goes down by 7 dpa, but was still observed in the lepidotrichia and to a lesser extent surrounding the mesenchymal cells (Fig. 2C). Even though the skeletal elements in fin rays are considered to be of dermal origin and formed by intramembranous ossification [53,54], studies have shown the expression of chondrogenic markers that are specific to cartilage, implying that the fin skeleton could be an intermediate between intramembranous and endochondral type of bone [55-57]. There is evidence showing that Acan contributes to functional properties such as mechanical stiffness, and to the normal development and growth of membranous bones [20,58]. These data are consistent with our findings. In 5 dpa sections, Acan is expressed in the area of lepidotrichia where the bone forming osteoblasts reside. This suggests that the fin skeleton requires relatively higher Acan expression levels at specific tissue compartments as part of a coordinated program of ECM synthesis and remodeling during skeletal regeneration.

We next evaluated the expression of Vcan, another major PG that forms aggregates with HA and is expressed during bone development [59]. We found that, in ontogeny fin sections, Vcan staining was minimal in the mesenchyme, but was prominent in the epidermis (Fig. 2D). During 3 dpa and 5 dpa, Vcan was slightly upregulated in the expanded mesenchyme and also was found associated with the cells of BLE and epidermis. At 7 dpa, the Vcan levels in the mesenchyme were reduced to ontogeny levels while appearing slightly upregulated in the epidermis. Overall, the Vcan

expression pattern did not show robust changes compared to the other components of the Hapln1a ECM during regeneration. Vcan was found mostly associated with the epidermis during ontogeny and the later time point 7 dpa, but was slightly upregulated in the mesenchyme during the earlier time points of regeneration (Fig. 2D). Even though previous studies have shown Vcan expression in mesenchymal condensations of chick limb cartilage [60,61], epiphyseal ends of long bones [62] and in mouse presumptive joints [63], the exact role of Vcan is not clearly known. It has been suggested that the ternary stable complex of Vcan-HA-Link protein has anti-adhesive effects, creating a highly hydrated environment conducive for cell migration [64-66]. Further studies are required to elucidate the functional role of Vcan during fin regeneration.

A semi-quantitative analysis of Hapln1a-ECM components during the time course of regeneration shows that all components exhibit a change in the expression pattern during early regeneration compared to the ontogeny state (Fig. 2E). In particular, Hapln1a and HA show more robust changes than Vcan. Acan showed distinct temporal and spatial expression patterns and was maximal at 5 dpa. Moreover, by 7 dpa the overall Acan expression levels appear reduced compared to earlier time points. Thus, it is possible that components of the Hapln1a-ECM contribute more to the earlier stages of skeletal regeneration versus later stages.

TNC, FN and LAM show distinct expression patterns during fin regeneration

Earlier studies in zebrafish fin regeneration have used TNC as a counter stain, to evaluate the integrity of the mesenchyme [35,39,67,68], and to define and demarcate the distal mesenchymal region of the regenerating vertebrate appendages [35,67,68].

Here, we show that TNC exhibits a dynamic expression pattern during fin regeneration and, hence, could play a combined role with other components in defining the regeneration specific matrix. In ontogeny fins, TNC was expressed poorly (Fig. 3A). During 3 dpa, extensive staining was seen just beneath the BLE, in the blastema, and in the mesenchyme throughout the regenerating fin tissue. At 5 dpa, the expression still seemed very strong and was similar to 3 dpa. At the later time point 7 dpa, the pattern still resembled 3 and 5 dpa, but the strength of staining was lower than 5 dpa showing that it is down regulated during the later time point of regeneration (Fig. 3A). During all regenerative time points that were under study, TNC expression was found to be present and clearly demarcate the mesenchyme from the epidermis. TNC is known to be upregulated in injured tissue sites where the outcome is regeneration rather than scarring [69,70]. Previous studies on newt muscle and heart regeneration have shown that TNC in the regeneration specific transitional matrix promotes cell migration and suppresses differentiation by coordinating function with HA and creating a hydrated environment to facilitate cell motility. Further, in vitro studies using newt myoblasts and in vivo studies in regenerating newt heart and muscles have shown that TNC promotes cell cycle re-entry thereby promoting cell proliferation [7,8]. Moreover, TNC alone has been shown to be sufficient to induce cardiomyocyte proliferation in vitro suggesting that ECM derived signals can induce cell proliferation during regeneration [8]. During zebrafish fin regeneration we observed an initial up regulation of HA and TNC. Based on the previous studies, we hypothesize that the initial up regulation of

these components can be an important event for progenitor cell migration and the down regulation at later time points could be a required step to promote differentiation.

FN is another ECM component that is shown to be specifically upregulated in the transitional matrix that is formed during regeneration of newt heart and skeletal muscle [7,8] and in zebrafish heart [71]. FN promotes tissue regeneration in multiple ways. It is known to be involved in clearing the tissue debris at the site of injury and influences both cell proliferation and differentiation by serving as a scaffold for cell adhesion and migration [72]. We observed that FN is expressed during zebrafish fin regeneration (Fig. 3B). In both epidermis and mesenchyme, FN expression was minimal in ontogeny fins. During 3 dpa, FN expression was upregulated in the mesenchymal compartment and remained low in the epidermis. At 5 dpa, the expression was much stronger and was observed strongly in the blastema and, to a lesser extent, in the epidermis up to the apical tip of the fin. At 7 dpa, the expression of FN appeared to go down and was more like the ontogeny pattern (Fig. 3B). Compared to TNC and HA which are upregulated throughout the regenerative time course, FN exhibited a more transient and modest temporal up regulation followed by a decrease in expression during later time points of fin regeneration. Previous *in vivo* and *in vitro* studies have shown that FN promotes differentiation and also might be playing a combined role with TNC to promote DNA synthesis and proliferation [7,8]. Loss of function experiments have shown that FN is essential for proper heart regeneration and could play a role in signaling during cardiomyocyte migration [71]. Expression of FN in regenerating fins

is intriguing and further studies will help us to understand the role of FN expression during fin regeneration.

In addition to the above mentioned ECM proteins, we also looked at the expression of the protein LAM that is characteristic of differentiated tissues. LAM is one among several glycoproteins present in the basement membranes that self assembles to form the basal laminae or BLE, adjacent to the epithelial layers of the epidermis. In ontogeny fins, LAM was expressed both in mesenchyme and epidermis throughout the fin section, typical of a differentiated tissue (Fig. 3C). During 3 dpa and 5 dpa, we observed prominent expression of LAM surrounding the cells of BLE and importantly reduced and dispersed expression in mesenchyme and epidermis. At the later time point 7 dpa, specific expression surrounding BLE disappeared and the pattern resembled ontogeny fin sections (Fig. 3C). Overall, we observed only a modest change in the expression of LAM during the time course of fin regeneration. BLE has several functions, including boundary formation to separate and connect several tissue types, providing a mechanical scaffold and molecular information to regulate cell migration and proliferation [73,74]. Additional *in vitro* and *in vivo* studies will reveal the importance and functional roles of specific up regulation of LAM expression surrounding the BLE during regeneration.

A semi-quantitative analysis of the overall expression levels of TNC, FN and LAM during the time course of regeneration shows robust up regulation of TN and FN during the earlier time points compared to the ontogeny state (Fig. 3D). In contrast, LAM expression shows minimal changes between ontogeny and regeneration and

during the time course of regeneration. These findings suggest that TNC and FN are functionally more important during earlier stages of fin regeneration. Since LAM is present at relatively constant levels, LAM may not provide a specific functional requirement for regenerating tissue.

4.5 Conclusions

Adult mammals have very limited regeneration capacity following tissue injury. In contrast, some animals like axolotls, newts and zebrafish possess an unlimited and remarkable level of tissue regenerative ability. Recent studies have highlighted the importance of dynamic extracellular modifications that occur during newt heart and skeletal muscle and zebrafish heart regeneration. In this study, we have shown that zebrafish fin regeneration also recapitulates a similar response following fin amputation. This indeed provides additional evidence for the evolutionarily conserved ECM alterations that take place during tissue repair and regeneration. Future work will be directed towards understanding the mechanism of how the involved players contribute individually and function together to regulate cell behavior. For example, combined *in vivo* and *in vitro* studies will provide new insights into how the biochemical properties of the changing ECM plays a role in regulating proliferation and differentiation during the fin skeletal tissue regeneration.

4.6 Figures

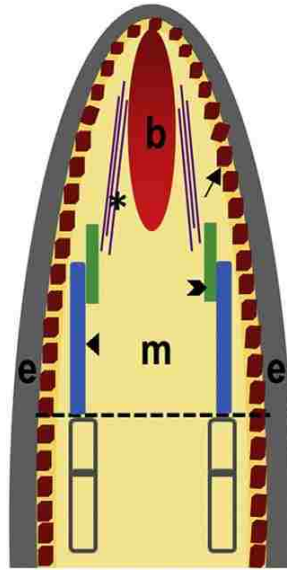


Figure 4.1: Cartoon of a longitudinal section illustrating the different compartments in a regenerating fin ray. The dotted line (black) represents the amputation plane. Upon amputation, a wound epidermis (e) (gray) is formed. The arrow points to the basal layer of epithelium (brown cuboidal cells) just beneath the epidermis (e) (gray) separating it from the central mesenchyme (m) (cream). Following that, blastema (b) (red) is established that contains two zones, the distal blastema, containing relatively slowly proliferating cells that direct regenerative outgrowth, and proximal blastema, containing rapidly proliferating cells that differentiate into other cell types. The closed arrowhead points to the newly formed bony rays-lepidotrichia (blue), open arrowhead points to the skeletal precursor cells (green) and the asterix (*) denotes the actinotrichia (purple lines) extending towards the tip of the fin.

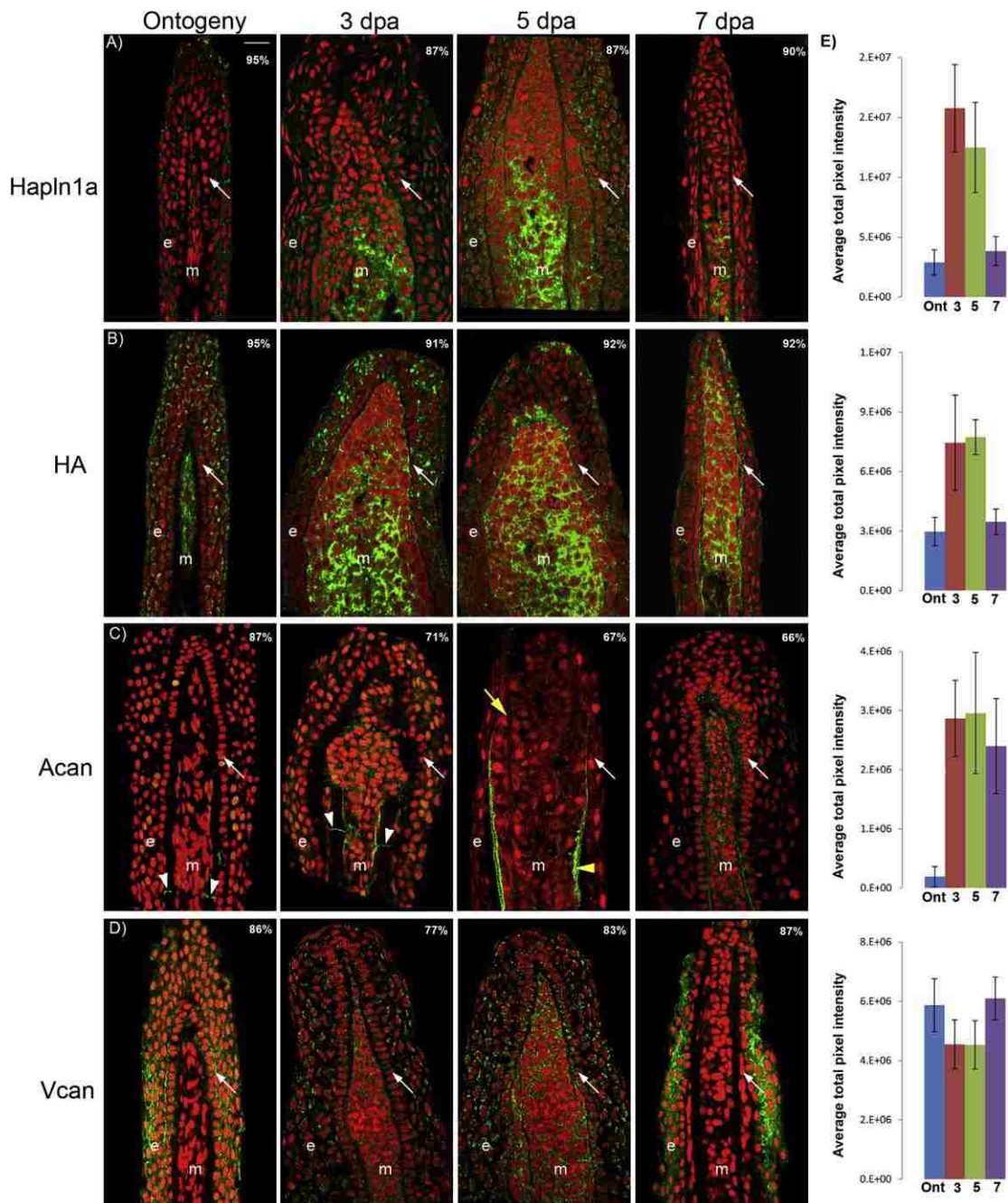


Figure 4.2: Immunostaining and histochemistry for Hapln1a-ECM components during the time course of regeneration. Longitudinal fin sections were treated with the respective primary antibodies and detected using the corresponding secondary antibody conjugated with Alexa Fluore 488 (green). Propidium iodide (nuclei) is used as the counter stain (red). For each time point the percentage of sections

showing similar expression pattern is denoted in each panel (n=40-65 sections). (A) Immunostaining for Hapln1a; (B) histochemical detection of HA using biotin-HA binding protein; (C) immunostaining for Acan, the arrowhead identifies the joints and (D) immunostaining for Vcan. (E) The graph illustrates the overall change in the expression level during the time course of regeneration for each component. Efforts to compare expression levels between components were not completed. Arrows identify the basal layer of epithelium (BLE); yellow arrowhead identifies lepidotrichia and yellow arrow identifies actinotrichia; m, mesenchyme; e, epidermis; dpa, days post amputation. Scale bar is 20 μm .

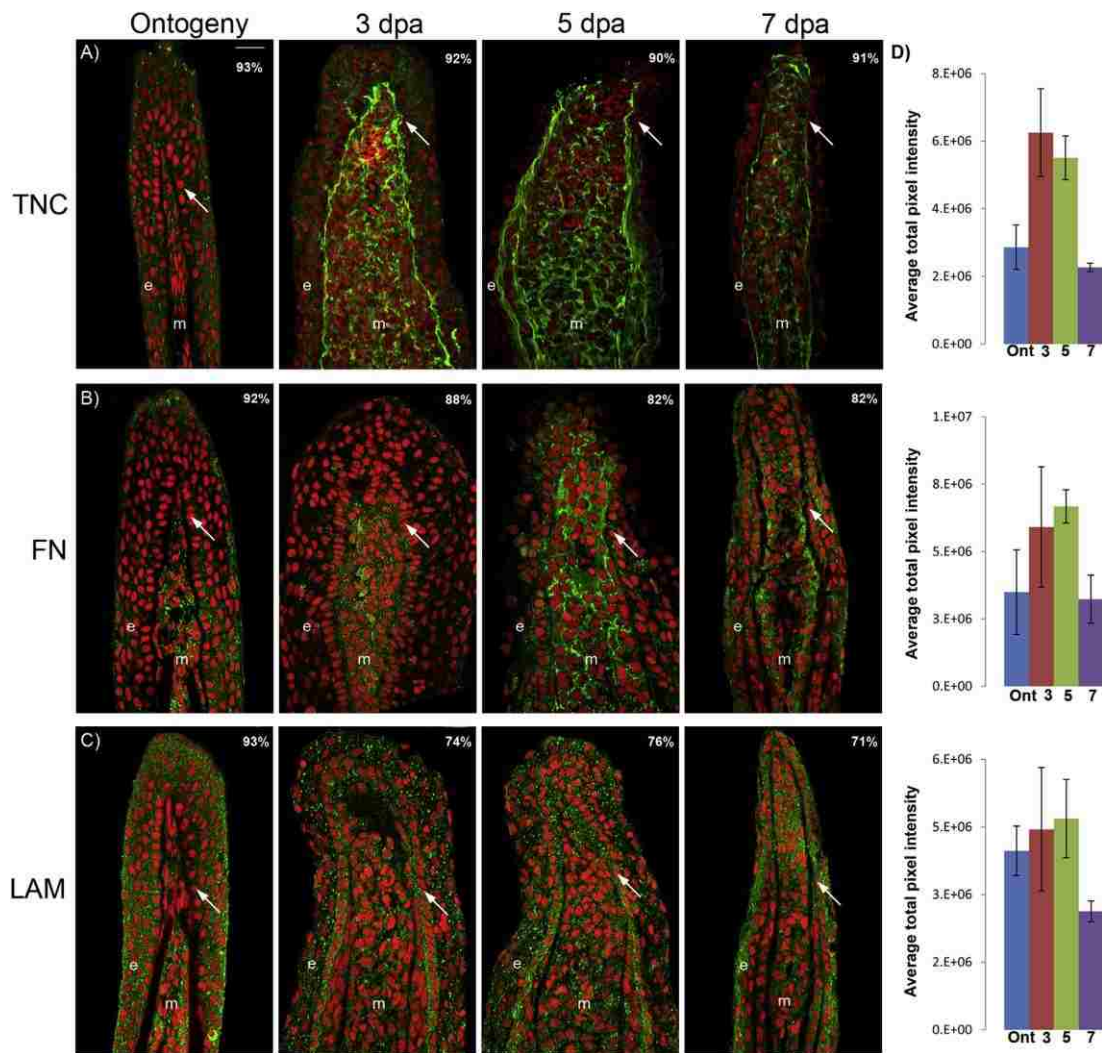


Figure 4.3: Immunostaining for TNC, FN and LAM during the time course of regeneration. Longitudinal fin sections were treated with the respective primary antibodies and detected using the corresponding secondary antibody conjugated with Alexa Fluore 488 (green). Propidium iodide (nuclei) is used as the counter stain (red). For each time point under study the percentage of sections showing similar expression pattern is denoted in each panel (n=40-65 sections). (A) Immunostaining for TNC; (B) immunostaining for FN and (C) immunostaining for LAM. (D) The graph illustrates the overall changes in the expression levels of each of the component under study during the time course of regeneration. Efforts to compare expression levels between

components were not completed. Arrows identify the basal layer of epithelium (BLE); m, mesenchyme; e, epidermis dpa, days post amputation. Scale bar is 20 μ m.

4.7 References

1. Hynes RO (2014) Stretching the boundaries of extracellular matrix research. *Nat Rev Mol Cell Biol* 15: 761-763.
2. Kim SH, Turnbull J, Guimond S (2011) Extracellular matrix and cell signalling: the dynamic cooperation of integrin, proteoglycan and growth factor receptor. *J Endocrinol* 209: 139-151.
3. Daley WP, Yamada KM (2013) ECM-modulated cellular dynamics as a driving force for tissue morphogenesis. *Curr Opin Genet Dev* 23: 408-414.
4. Tolg C, McCarthy JB, Yazdani A, Turley EA (2014) Hyaluronan and RHAMM in wound repair and the "cancerization" of stromal tissues. *Biomed Res Int* 2014: 103923.
5. Toole BP, Gross J (1971) The extracellular matrix of the regenerating newt limb: synthesis and removal of hyaluronate prior to differentiation. *Dev Biol* 25: 57-77.
6. Tassava RA, Nace JD, Wei Y (1996) Extracellular matrix protein turnover during salamander limb regeneration. *Wound Repair Regen* 4: 75-81.
7. Calve S, Odelberg SJ, Simon HG (2010) A transitional extracellular matrix instructs cell behavior during muscle regeneration. *Dev Biol* 344: 259-271.
8. Mercer SE, Odelberg SJ, Simon HG (2013) A dynamic spatiotemporal extracellular matrix facilitates epicardial-mediated vertebrate heart regeneration. *Dev Biol* 382: 457-469.

9. Mercer SE, Cheng CH, Atkinson DL, Krcmery J, Guzman CE, et al. (2012) Multi-tissue microarray analysis identifies a molecular signature of regeneration. *PLoS One* 7: e52375.
10. Mailman ML, Dresden MH (1976) Collagen metabolism in the regenerating forelimb of *Notophthalmus viridescens*: synthesis, accumulation, and maturation. *Dev Biol* 50: 378-394.
11. Gulati AK, Zalewski AA, Reddi AH (1983) An immunofluorescent study of the distribution of fibronectin and laminin during limb regeneration in the adult newt. *Dev Biol* 96: 355-365.
12. Contreras EG, Gaete M, Sanchez N, Carrasco H, Larrain J (2009) Early requirement of Hyaluronan for tail regeneration in *Xenopus* tadpoles. *Development* 136: 2987-2996.
13. Bourguignon LY, Singleton PA, Zhu H, Zhou B (2002) Hyaluronan promotes signaling interaction between CD44 and the transforming growth factor beta receptor I in metastatic breast tumor cells. *J Biol Chem* 277: 39703-39712.
14. Peterson RS, Andhare RA, Rousche KT, Knudson W, Wang W, et al. (2004) CD44 modulates Smad1 activation in the BMP-7 signaling pathway. *J Cell Biol* 166: 1081-1091.
15. Ghatak S, Misra S, Toole BP (2005) Hyaluronan constitutively regulates ErbB2 phosphorylation and signaling complex formation in carcinoma cells. *J Biol Chem* 280: 8875-8883.

16. Hardingham T (1998) Chondroitin sulfate and joint disease. *Osteoarthritis Cartilage* 6 Suppl A: 3-5.
17. Hardingham TE (1979) The role of link-protein in the structure of cartilage proteoglycan aggregates. *Biochem J* 177: 237-247.
18. Poole AR, Matsui Y, Hinek A, Lee ER (1989) Cartilage macromolecules and the calcification of cartilage matrix. *Anat Rec* 224: 167-179.
19. Lee I, Ono Y, Lee A, Omiya K, Moriya Y, et al. (1998) Immunocytochemical localization and biochemical characterization of large proteoglycans in developing rat bone. *J Oral Sci* 40: 77-87.
20. Spicer AP, Tien JY (2004) Hyaluronan and morphogenesis. *Birth Defects Res C Embryo Today* 72: 89-108.
21. Govindan J, Iovine MK (2014) Hapln1a is required for connexin43-dependent growth and patterning in the regenerating fin skeleton. *PLoS One* 9: e88574.
22. Matsumoto K, Li Y, Jakuba C, Sugiyama Y, Sayo T, et al. (2009) Conditional inactivation of Has2 reveals a crucial role for hyaluronan in skeletal growth, patterning, chondrocyte maturation and joint formation in the developing limb. *Development* 136: 2825-2835.
23. Westerfield M (1993) *The Zebrafish Book: A guide for the laboratory use of zebrafish (Brachydanio rerio)*. University of Oregon Press, Eugene, OR.

24. Repesh LA, Fitzgerald TJ, Furcht LT (1982) Changes in the distribution of fibronectin during limb regeneration in newts using immunocytochemistry. *Differentiation* 22: 125-131.
25. Calve S, Simon HG (2012) Biochemical and mechanical environment cooperatively regulate skeletal muscle regeneration. *FASEB J* 26: 2538-2545.
26. Chiquet M, Eppenberger HM, Turner DC (1981) Muscle morphogenesis: Evidence for an organizing function of exogenous fibronectin. *Dev Biol* 88: 220-235.
27. Chiquet M, Fambrough DM (1984) Chick myotendinous antigen. I. A monoclonal antibody as a marker for tendon and muscle morphogenesis. *J Cell Biol* 98: 1926-1936.
28. Kosher RA, Savage MP, Walker KH (1981) A gradation of hyaluronate accumulation along the proximodistal axis of the embryonic chick limb bud. *J Embryol Exp Morphol* 63: 85-98.
29. Longaker MT, Chiu ES, Adzick NS, Stern M, Harrison MR, et al. (1991) Studies in fetal wound healing. V. A prolonged presence of hyaluronic acid characterizes fetal wound fluid. *Ann Surg* 213: 292-296.
30. Whitby DJ, Ferguson MW (1991) The extracellular matrix of lip wounds in fetal, neonatal and adult mice. *Development* 112: 651-668.
31. Ghosh P, Shimmon S, Whitehouse MW (2006) Arthritic disease suppression and cartilage protection with glycosaminoglycan polypeptide complexes (Peptacans)

derived from the cartilage extracellular matrix: a novel approach to therapy. *Inflammopharmacology* 14: 155-162.

32. Vinarsky V, Atkinson DL, Stevenson TJ, Keating MT, Odelberg SJ (2005) Normal newt limb regeneration requires matrix metalloproteinase function. *Dev Biol* 279: 86-98.

33. Akimenko MA, Mari-Beffa M, Becerra J, Geraudie J (2003) Old questions, new tools, and some answers to the mystery of fin regeneration. *Dev Dyn* 226: 190-201.

34. Tal TL, Franzosa JA, Tanguay RL (2009) Molecular signaling networks that choreograph epimorphic fin regeneration in zebrafish - a mini-review. *Gerontology* 56: 231-240.

35. Chablais F, Jazwinska A (2010) IGF signaling between blastema and wound epidermis is required for fin regeneration. *Development* 137: 871-879.

36. Knopf F, Hammond C, Chekuru A, Kurth T, Hans S, et al. (2011) Bone regenerates via dedifferentiation of osteoblasts in the zebrafish fin. *Dev Cell* 20: 713-724.

37. Sousa S, Afonso N, Bensimon-Brito A, Fonseca M, Simoes M, et al. (2011) Differentiated skeletal cells contribute to blastema formation during zebrafish fin regeneration. *Development* 138: 3897-3905.

38. Tu S, Johnson SL (2011) Fate restriction in the growing and regenerating zebrafish fin. *Dev Cell* 20: 725-732.

39. Stewart S, Stankunas K (2012) Limited dedifferentiation provides replacement tissue during zebrafish fin regeneration. *Dev Biol* 365: 339-349.
40. Thorogood P (1991) The development of the teleost fin and implications for our understanding of tetrapod limb evolution. *Developmental patterning of the vertebrate limb*: Springer. pp. 347-354.
41. Sordino P, van der Hoeven F, Duboule D (1995) Hox gene expression in teleost fins and the origin of vertebrate digits. *Nature* 375: 678-681.
42. Grandel H, Schulte-Merker S (1998) The development of the paired fins in the zebrafish (*Danio rerio*). *Mech Dev* 79: 99-120.
43. Ton QV, Iovine MK (2013) Identification of an *evx1*-dependent joint-formation pathway during FIN regeneration. *PLoS One* 8: e81240.
44. Lee Y, Grill S, Sanchez A, Murphy-Ryan M, Poss KD (2005) Fgf signaling instructs position-dependent growth rate during zebrafish fin regeneration. *Development* 132: 5173-5183.
45. Hoptak-Solga AD, Nielsen S, Jain I, Thummel R, Hyde DR, et al. (2008) Connexin43 (GJA1) is required in the population of dividing cells during fin regeneration. *Dev Biol* 317: 541-548.
46. Thorogood PV, Hinchliffe JR (1975) An analysis of the condensation process during chondrogenesis in the embryonic chick hind limb. *J Embryol Exp Morphol* 33: 581-606.

47. Singley CT, Solursh M (1981) The spatial distribution of hyaluronic acid and mesenchymal condensation in the embryonic chick wing. *Dev Biol* 84: 102-120.
48. Knudson CB, Knudson W (1993) Hyaluronan-binding proteins in development, tissue homeostasis, and disease. *FASEB J* 7: 1233-1241.
49. Lee JY, Spicer AP (2000) Hyaluronan: a multifunctional, megaDalton, stealth molecule. *Curr Opin Cell Biol* 12: 581-586.
50. Ghokale JRPaB, A.L (2001) *The Biochemistry of Bone. Osteoporosis*. San Diego: Academic Press. pp. 82.
51. Toole BP (2009) Hyaluronan-CD44 Interactions in Cancer: Paradoxes and Possibilities. *Clin Cancer Res* 15: 7462-7468.
52. Salbach J, Rachner TD, Rauner M, Hempel U, Anderegg U, et al. (2012) Regenerative potential of glycosaminoglycans for skin and bone. *J Mol Med (Berl)* 90: 625-635.
53. Haas HJ (1962) Studies on mechanisms of joint and bone formation in the skeleton rays of fish fins. *Dev Biol* 5: 1-34.
54. Geraudie J, Landis WJ (1982) The fine structure of the developing pelvic fin dermal skeleton in the trout *Salmo gairdneri*. *Am J Anat* 163: 141-156.
55. Johnson SL, Weston JA (1995) Temperature-sensitive mutations that cause stage-specific defects in Zebrafish fin regeneration. *Genetics* 141: 1583-1595.

56. Padhi BK, Joly L, Tellis P, Smith A, Nanjappa P, et al. (2004) Screen for genes differentially expressed during regeneration of the zebrafish caudal fin. *Dev Dyn* 231: 527-541.
57. Smith A, Avaron F, Guay D, Padhi BK, Akimenko MA (2006) Inhibition of BMP signaling during zebrafish fin regeneration disrupts fin growth and scleroblasts differentiation and function. *Dev Biol* 299: 438-454.
58. Wong M, Lawton T, Goetinck PF, Kuhn JL, Goldstein SA, et al. (1992) Aggrecan core protein is expressed in membranous bone of the chick embryo. Molecular and biomechanical studies of normal and nanomelia embryos. *J Biol Chem* 267: 5592-5598.
59. Nakamura M, Sone S, Takahashi I, Mizoguchi I, Echigo S, et al. (2005) Expression of versican and ADAMTS1, 4, and 5 during bone development in the rat mandible and hind limb. *J Histochem Cytochem* 53: 1553-1562.
60. Yamagata M, Yamada KM, Yoneda M, Suzuki S, Kimata K (1986) Chondroitin sulfate proteoglycan (PG-M-like proteoglycan) is involved in the binding of hyaluronic acid to cellular fibronectin. *J Biol Chem* 261: 13526-13535.
61. Shinomura T, Jensen KL, Yamagata M, Kimata K, Solursh M (1990) The distribution of mesenchyme proteoglycan (PG-M) during wing bud outgrowth. *Anat Embryol (Berl)* 181: 227-233.
62. Shibata S, Fukada K, Imai H, Abe T, Yamashita Y (2003) In situ hybridization and immunohistochemistry of versican, aggrecan and link protein, and histochemistry of hyaluronan in the developing mouse limb bud cartilage. *J Anat* 203: 425-432.

63. Snow HE, Riccio LM, Mjaatvedt CH, Hoffman S, Capehart AA (2005) Versican expression during skeletal/joint morphogenesis and patterning of muscle and nerve in the embryonic mouse limb. *Anat Rec A Discov Mol Cell Evol Biol* 282: 95-105.
64. Lee GM, Zhang F, Ishihara A, McNeil CL, Jacobson KA (1993) Unconfined lateral diffusion and an estimate of pericellular matrix viscosity revealed by measuring the mobility of gold-tagged lipids. *J Cell Biol* 120: 25-35.
65. Yamagata M, Kimata K (1994) Repression of a malignant cell-substratum adhesion phenotype by inhibiting the production of the anti-adhesive proteoglycan, PG-M/versican. *J Cell Sci* 107 (Pt 9): 2581-2590.
66. Yamagata M, Shinomura T, Kimata K (1993) Tissue variation of two large chondroitin sulfate proteoglycans (PG-M/versican and PG-H/aggrecan) in chick embryos. *Anat Embryol (Berl)* 187: 433-444.
67. Jazwinska A, Badakov R, Keating MT (2007) Activin-betaA signaling is required for zebrafish fin regeneration. *Curr Biol* 17: 1390-1395.
68. Onda H, Poulin ML, Tassava RA, Chiu IM (1991) Characterization of a newt tenascin cDNA and localization of tenascin mRNA during newt limb regeneration by in situ hybridization. *Dev Biol* 148: 219-232.
69. Murphy-Ullrich JE (2001) The de-adhesive activity of matricellular proteins: is intermediate cell adhesion an adaptive state? *Journal of Clinical Investigation* 107: 785.

70. Harty M, Neff AW, King MW, Mescher AL (2003) Regeneration or scarring: an immunologic perspective. *Dev Dyn* 226: 268-279.
71. Wang J, Karra R, Dickson AL, Poss KD (2013) Fibronectin is deposited by injury-activated epicardial cells and is necessary for zebrafish heart regeneration. *Dev Biol* 382: 427-435.
72. Stoffels JM, Zhao C, Baron W (2013) Fibronectin in tissue regeneration: timely disassembly of the scaffold is necessary to complete the build. *Cell Mol Life Sci* 70: 4243-4253.
73. Webb AE, Sanderford J, Frank D, Talbot WS, Driever W, et al. (2007) Laminin alpha5 is essential for the formation of the zebrafish fins. *Dev Biol* 311: 369-382.
74. Godwin J, Kuraitis D, Rosenthal N (2014) Extracellular matrix considerations for scar-free repair and regeneration: insights from regenerative diversity among vertebrates. *Int J Biochem Cell Biol* 56: 47-55.

Chapter 5

Summary and Future Directions

5.1 Summary

Studies using different model systems provide evidence that Cx43 function during skeletal morphogenesis is highly conserved. However, very little is known about the molecular changes that occur downstream of Cx43. One way to understand this is by looking at *cx43* dependent changes in gene expression that influence skeletal growth and patterning. Several putative genes have been identified by a novel microarray analysis that could possibly function in a *cx43* dependent way. One of the genes identified by this analysis is *hapln1a* that codes for an ECM protein. This dissertation has revealed some of the important findings about the mechanistic roles of Hapln1a in mediating Cx43 function during skeletal regeneration of zebrafish caudal fin.

To summarize, we have shown that Hapln1a is molecularly and functionally downstream of Cx43 and transient knockdown of *hapln1a* destabilizes the interaction between HA and PGs leading to reduced levels of HA [1] and Acan (Chapter 3). We observed that morpholino mediated reduction in HA, or reduction in Acan can mediate Hapln1a phenotypes, namely reduced cell proliferation (i.e., growth) and reduced segment length (i.e., affects patterning). We observed that HA had a stronger effect on cell proliferation and Acan had a stronger effect on segment length, but neither could completely recapitulate *hapln1a* knockdown phenotypes. This suggests that there might be other players contributing to Hapln1a function or, Hapln1a could have other additional functions (Chapter3). This opens up the question whether Hapln1a has other roles, other than stabilizing the HA and Acan interaction during skeletal regeneration. Moreover, we have shown that Hapln1a dependent ECM and the microenvironment

provided by the Hapln1a-ECM is crucial for stabilization of Sema3d protein (another molecule known to function downstream of Cx43) and they function together to mediate Cx43 dependent skeletal phenotypes. This shows that Hapln1a-ECM is important for proper function of signaling molecules, at least Sema3d during fin regeneration. Hence it would be interesting to know whether Hapln1a-ECM influences other signaling molecules that are required to maintain the proliferative state of the blastema. Additionally, we provide evidence that components of Hapln1a-ECM comprising of Hapln1a, HA, Acan and Vcan are expressed during fin regeneration. We have also shown that the evolutionarily conserved transitional matrix comprising of HA, TNC and FN that is formed during epimorphic regeneration of zebrafish and newt heart, and newt skeletal muscles and limbs is also conserved during zebrafish fin regeneration [2]. Our study provides the first evidence for the expression and formation of the Hapln1a-ECM and evolutionarily conserved transitional matrix and some of its functional significance during zebrafish fin skeleton regeneration. Hence determining components of the ECM (especially Hapln1a, HA, Acan, TNC and FN) that may provide regulatory cues for cell proliferation and cell differentiation during skeletal development will provide novel insights into skeletal regeneration. Overall, the work compiled in this dissertation highlights two important but previously unknown aspects of Cx43 function during skeletal regeneration. First we provide evidence that Hapln1a expression is Cx43 dependent and then we have shown that Hapln1a dependent ECM remodeling (consisting of at least HA and Acan) is crucial for and contributes to skeletal growth and patterning in regenerating fin. Further studies are required to elucidate the

biochemical function and importance of ECM during fin regeneration that was previously thought to have only structural roles. Several questions remain open and some of the future directions are summarized below.

5.2 Future Directions

(1) Determine whether Hapln1a has other roles, besides stabilizing the HA and Acan interaction during skeletal regeneration

We have shown that Hapln1a knockdown resulted in reduced HA (chapter 2) and reduced Acan (chapter 3). Experiments to check whether HA and Acan contributed to observed Hapln1a dependent phenotypes showed that reducing HA levels by knockdown of HA synthesizing enzymes, or Acan knockdown, both resulted in reduced cell proliferation and reduced segment length. However we observed that *has2* knockdown had a stronger effect on cell proliferation and *acانب* knockdown had a stronger effect on segment length. Even though it is not possible to compare two independent knockdown effects, it appears that the additive effects of reduced HA and reduced Acan are similar to the total effects of reduced Hapln1a (data in chapter 3). Several other studies also highlight the fact that HA promotes cell proliferation [3,4,5,6,7] and Acan deficiency leads to shortened limbs [8,9,10]. Hence it would be interesting to know whether double knockdown of *has2* and *acانب* can result in recapitulation of *hapln1a* knockdown phenotypes. This might provide further insights into additional roles of Hapln1a and help us answer the following questions namely, whether Hapln1a purely plays a structural role and are there any other unidentified players involved in this. Our preliminary data on double knockdown of *has2* and *acانب*

indeed show reduction in regenerate and segment length and reduced cell proliferation but do not recapitulate the effects seen in *hapln1a* knockdown (Figure 5.1). However, one of the caveats of this double knockdown is that, when we do the double knockdown the concentration of the morpholino is halved and hence it is necessary to quantify the effect of the knockdown on the protein levels to better understand the function. In addition to looking at the phenotypes i.e., cell proliferation and segment length in the *has2+acarb* double knockdown and *hapln1a* knockdown fins, quantitation and comparison of HA and Acan protein levels by histochemistry and immuno-staining will permit direct comparison of each single knockdown with the double knockdown. If HA and Acan levels are similar in both the double knockdown and *hapln1a* knockdown, and if the double knockdown can recapitulate the *hapln1a* knockdown phenotypes then it is likely that the majority of the effect of *hapln1a* knockdown phenotypes are due to destabilization of HA and Acan. Conversely, if the effect of double knockdown has lesser effect than *hapln1a* knockdown then it opens up new possibilities that will require further analysis.

(2) How does Hapln1a influence the evolutionarily conserved transitional matrix during fin regeneration?

In chapter 4, we have shown that establishment of a common transitional matrix rich in hyaluronic acid (HA), fibronectin (FN) and tenascin C (TNC) during epimorphic regeneration [7,11,12] of various organs in different model systems, is also established during zebrafish fin regeneration. All the components of this transitional matrix are known to have an effect on cell proliferation or cell migration or differentiation

[7,11,12]. We studied the changes in ECM composition from non-regenerative to regenerative fin. Numerous studies have identified important roles for HA in matrices undergoing remodeling and during regenerative repair mechanisms [6,7,12,13], and has been demonstrated to modulate signal transduction pathways such as EGFR/ErbB, TGF β and BMP [14,15,16]. We have shown that *hapln1a* knockdown results in reduced HA (one of the components of the conserved transitional matrix) that in turn leads to reduced cell proliferation and segment length (Chapter 3). To further understand the role of Hapln1a during regeneration and to assess how the conserved transitional ECM changes during *hapln1a*-knockdown, a similar strategy could be utilized to see the effect of *hapln1a* knockdown on other two transitional matrix components namely TNC and FN. Immuno-staining analysis for FN and TNC could be performed on *hapln1a*-knockdown regenerating fins and compared with *hapln1a*- mismatch treated (negative control) regenerating fins. Several studies have shown down regulation of ECM proteins that are characteristic of differentiated skeletal tissues like laminin (LAM) and collagen type I [17,18]. In chapter 4 we provide evidence that LAM expression shows modest change in expression pattern over the time course of regeneration. Hence performing immunostaining analysis for LAM in *hapln1a* knockdown regenerating fins and comparing with *hapln1a* mismatch treated (negative control) regenerating fins could serve as a control for these experiments. Those ECM components that vary in the *hapln1a* knockdown fins might play a role and mediate relevant cellular behaviors such as cell proliferation and cell differentiation (i.e. the two major cellular behaviors influenced by *cx43*-dependent pathways) which could be tested further by in vitro

assays. Overall, the result from these experiments will provide insight into how Hapln1a dependent ECM contributes to the Cx43 dependent skeletal phenotypes.

(3) Determining components of the ECM that may provide regulatory cues for cell proliferation and cell differentiation during skeletal development.

Skeletal development depends upon appropriate cell proliferation and cell differentiation. The fact that *hapln1a* knockdown causes reduced cell proliferation and reduced segment length provides evidence that the Hapln1a based ECM components HA and Acan influence these cellular behaviors. However, it is not clear how mutations and defects in ECM proteins cause skeletal disorders. Not much is known about the role of Hapln1a/HA/Acan or other major ECM components during zebrafish fin regeneration. In chapter 4 we provide evidence that ECM components comprising the transitional matrix, namely FN, TNC and HA are expressed in a regenerating fin. In addition we also provide evidence for the expression of other ECM components namely LAM and the PGs- Acan and Vcan [2]. Further experiments to evaluate and understand their ability to influence cellular behaviors will provide novel insights into how these components can influence cellular behavior. Tissue culture polystyrene dishes coated with different ECM components have been successfully used to study muscle regeneration [7]. Results from the experiments mentioned in the previous section can provide ideas to design tissue culture experiments for the ECM components that are up-regulated during regeneration or show a difference in *hapln1a* knockdown fins. However, the use of ECM components that are not up-regulated or that do not show any change upon *hapln1a* knockdown will provide an important internal control for the

analyses. These ECM components can be coated individually on polystyrene tissue culture dishes as described [7]. Cells from a zebrafish fin cell line (adult fin fibroblast, AB9) can be plated over each ECM component and Hapln1a mediated cellular behaviors namely, cell proliferation and joint formation, can be evaluated. Cell proliferation can be monitored by measuring the incorporation of BrdU (i.e. an analog of one of the 4 bases that comprise DNA) into cell nuclei. BrdU-positive cells will be counted over time, and the ability of different ECM components to induce cell proliferation can be evaluated. The ability of different ECM components to induce differentiation of bone-forming cells or joint-forming cells can be monitored either by staining for established bone and joint markers (i.e. alkaline phosphatase for bone, matrix metalloproteases for joints), or by the detection of genes up-regulated in bone cells (i.e., *runx2*, *osx*) or joint cells (*evx1*). Completion of these experiments will help in defining the ECM components that are up-regulated during regeneration and the ECM components that depend on Hapln1a for their continued expression and will provide information if the same ECM components facilitate cell proliferation and/or cell differentiation. Results from these experiments will play a critical role to predict which ECM proteins are most relevant during growth and patterning of the skeleton. These findings will be crucial for establishing evidence-based hypotheses for how the ECM may regulate cell proliferation and cell differentiation, the two major cellular behaviors impacted by reduced Hapln1a.

(4) Elucidate the role of HA signaling during fin skeletogenesis

The Hapln1a based ECM is largely composed of hyaluronic acid (HA) and proteoglycan (PG) network that is cross linked and stabilized by Hapln1a. Our studies show that knockdown of *hapln1a* results in reduced HA levels as evaluated by histochemical HABP staining. HA is an abundant component of ECM and is enriched in matrices undergoing remodeling [19] such as in case of tissue injury, and functional studies to evaluate its role in zebrafish fin regeneration have shown that HA influences cell proliferation and joint formation (Chapter 3). Studies reveal that any treatment influencing the synthesis or degradation of the HA polymer causes defects in bone size, shape, and growth in animal model systems [20,21,22]. These data provide compelling evidence that HA contributes significantly to skeletogenesis. Moreover, HA receptors like CD44 and RHAMM can transduce signals thereby activating a variety of intracellular signaling cascades like ERK1/2, PKC, FAK and Rho1 [23], and it is possible that, by altering the HA levels, Hapln1a is indirectly affecting one or many of the signaling pathways. Attempts to look at the expression of HA receptors CD44 and RHAMM, revealed that RHAMM is expressed in regenerating fins (Figure 5.2). Interestingly in situ hybridization for *rhamm* in 5 dpa regenerating fins of WT, *sof*^{b123} and *alf*^{dy86} showed that compared to WT, *rhamm* is much upregulated in *alf*^{dy86} and downregulated in *sof*^{b123} (a pattern similar to *cx43* expression) suggesting an exciting possible role for *rhamm* in Cx43 pathway. Further studies are required to understand whether HA interacts with RHAMM during fin regeneration and contributes to Cx43 dependent functions.

(5) Elucidating the effect of Hapln1a-ECM on secreted signaling molecules

Previous findings from our lab have revealed that the secreted signaling molecule Sema3d coordinates growth and patterning of the vertebrate skeleton through interactions with two distinct cell surface receptors. The receptor Nrp2a mediates skeletal growth/cell proliferation and receptor PlxnA3 mediates joint formation/patterning [24]. Using transgenic Sema3d over expression line, we have shown that HA/Hapln1a-ECM is required for stabilization of Sema3d to mediate the skeletal phenotypes (Chapter 3). Another independent study by mass spectroscopy analysis as an attempt to identify the co-receptors for Nrp2a revealed RHAMM as a potential Nrp2a interacting factor (data unpublished). Together these studies suggest that the HA receptor RHAMM may be required to mediate Sema3d-Nrp2a interactions. Further studies are required to prove and understand this mechanism. Also, several studies provide evidence for the expression and the critical need of various signaling molecules during the process of fin regeneration. Knowing that Hapln1a-ECM plays an important role in stabilizing Sema3d, it is intriguing to understand the effect of Hapln1a-ECM on other signaling molecules especially Activin β A and Notch which play an important role in maintaining the proliferative state of the blastema [25,26]. Further studies will provide evidence for the dependence of signaling molecules on Haplna-ECM.

(6) Zebrafish regenerating fin as a model for osteoarthritis research

Degenerative joint disease is a leading source of morbidity resulting in significant social and economic impact. One to 5% of the population under the age of 45 and 15-

85% of older individuals suffer from some form of degenerative joint disease, mainly osteoarthritis [60,61] Osteoarthritis is characterized by the slow progressive deterioration of articular cartilage. Current therapeutic regimens address mainly pain but not degeneration (RE Mitchell et al 2013). A better understanding of the distinct micro-environment of articular cartilage and the complex interactions that exist between cell and surrounding extracellular matrix (ECM) is critical so that strategies can be directed towards treating degenerative joint disease.

Cartilage is composed of the cells named chondrocytes and the ECM produced by these cells. The biochemical properties of cartilage and the physical function of joints are critically dependent on the integrity of the matrix. The ECM molecules in cartilage include proteoglycans, hyaluronan (also called hyaluronic acid or HA), type II collagen, glycoproteins and various mixtures of elastic fibers. Most of the proteoglycans exist as aggregates formed by the non-covalent association of proteoglycan with HA and link protein (WightTN 1992, Kiani et al 2002). Among the components of ECM molecules, the most crucial to the proper functioning of articular cartilage is the large aggregating chondroitin sulfate proteoglycan aggrecan and hyaluronic acid.

It is well documented that HA and Acan play crucial roles in maintaining the articular cartilage and their functions are perturbed in osteoarthritic joints [60,61] and one of the major drawbacks in osteoarthritic research is the availability of a suitable model system. This dissertation provides evidence that the ECM component HA is upregulated, and Acan is expressed in a distinct pattern and indeed contributes to skeletal phenotypes during zebrafish fin regeneration. Even though the articular

cartilage is not exactly the same as what is seen in lepidotrichia of zebrafish fin, the regenerating fin could serve as a model for studying various signaling pathways that are perturbed during osteoarthritic disease state.

One of the interesting findings from this study is the distinct expression pattern (data in chapter 4) of the cartilage PG- Acan that is expressed during fin regeneration. Previous studies have described that the skeletal elements in fin rays are of dermal origin and are formed by intramembranous ossification [27,28]. Even though fish fins are made of dermal bones several studies have shown the expression of both chondrogenic markers such as *sox9a*, *sox9b*, *ihha*, *col10a1*, *col2a1* that are considered to be strictly associated with endochondral bone formation and genes associated with intramembranous ossification such as *runx2a*, *runx2b*, *osteonectin* and *colla1* in regenerating fins [29,30,31,32,33]. Independently we have also shown the expression of the chondrogenic markers *sox9a* and *sox9b* (Figure 5.3). These observations have posed an important question about the nature of bone in zebrafish fin rays suggesting that it could be an intermediate between endochondral and intramembranous type and it is complicated to define it purely as an intramembranous type. The expression of Acan in regenerating fins in our study is an important cartilage marker [34,35] and thus supports the fin characteristics to be an intermediate between endochondral and intramembranous type. The results obtained for Acan expression were unexpected because intramembranous bones normally develop from the direct deposition of bone matrix by the mesenchymal cells and does not involve a cartilage intermediate which is an important requirement for endochondral bone formation.

To our knowledge this is the first study to analyze the expression pattern of the PG Acan during in vivo fin tissue regeneration. In ontogeny fins, Acan strongly localized to the mature joints and was poorly expressed in the mesenchyme and epidermis. On 3 dpa, we observed a moderate up regulation of Acan expression surrounding the mesenchymal cells, and around the stump bone matrix. Epidermal staining was very much lower compared to the mesenchyme. On 5 dpa, Acan expression was very strongly associated with lepidotrichia consisting of SPC's and to a lesser extent with actinotrichia and mesenchyme. Acan expression goes down by 7dpa but was still observed in the lepidotrichia and to a lesser extent surrounding the mesenchymal cells [2]. The cartilage contains chondrocytes that secrete an ECM rich in HA, Acan and type II collagen [36]. Even though our current findings on Acan expression in dermal fin skeleton was surprising, there is molecular and biochemical evidence for Acan expression in membranous bones by osteoblasts in chick embryos. Based on the studies on nanomelia chick embryos that contain a mutation that affect the transcriptional regulation of the Acan core protein, it has been suggested that Acan contributes to the functional properties especially mechanical stiffness and to the normal development and growth of membranous bones [37,38]. This clearly agrees with our current data and we observe in 5 dpa sections that Acan is expressed in the area of lepidotrichia where the bone forming osteoblasts reside. This shows that the development of fin skeleton requires relatively higher Acan expression levels at tissue specific sites transiently as part of a coordinated program of ECM synthesis and remodeling. Also, it is well known that Acan expression is regulated by BMPs [39,40] and BMP signaling has been shown to be required for fin

regeneration that regulates both chondrogenic and osteogenic gene expression during fin regeneration [29]. This opens up the possibility that Acan expression could be downstream of BMP signaling in regenerating fins that needs to be investigated.

Analyses of several signaling pathways suggest that lepidotrichia behave similar to the main skeletal tissues, at least under experimental studies using inducing factors. For example, *shh* signaling is able to ectopically induce any skeletal tissue, bone or cartilage. In fins, absence of *shh* signaling affects lepidotrichia and leads to outgrowth arrest during fin regeneration [41]. Retinoic acid is a potent repressor of cartilage formation [42,43], whereas it induces both terminal chondrocyte [44,45] and osteoblast differentiation [42,46]. Several studies highlight that retinoic acid participates in both ray pattern formation and differentiation [47,48]. Another signaling molecule Indian hedgehog (*ihh*) couples chondrogenesis and osteogenesis by repressing hypertrophic chondrocyte formation [49,50] and promoting osteoblast lineage commitment [49]. Studies on zebrafish ontogeny and fin regeneration [30] suggest that *ihh* is expressed in developing and regenerating fins during scleroblast differentiation. Fibroblast growth factors (FGFs) are able to induce all types of skeletal tissues [51,52,53,54,55]. Several studies suggest that FGF could be necessary for lepidotrichia formation. The inhibition of FGF signaling pathway stops fin outgrowth [56] and modulation of the FGF signaling regulates the rate of fin outgrowth [57,58]. *wnt* genes are also involved in the regulation of chondro-osteogenesis differentiation in mammals and *wnt3a*, *wnt5*, and *β -catenin* genes are expressed during fin regeneration [59].

From an evolutionary point of view, dermal fin rays are not homologous to the tetrapod limb. Furthermore, morphological and molecular evidence suggests that lepidotrichia is a special type of skeletal tissue different from any main skeletal tissue. Despite this recognized peculiarity of the lepidotrichia, the above-mentioned explanations and evidences suggest a close similarity between the main skeletal tissues in vertebrates and lepidotrichia (i.e., regenerating fins) and hence could be of interest in preclinical studies of osteoarthritic research and therapies. HA and Acan show distinct expression pattern and several chondro and osteogenic markers are expressed in a regenerating fin making it an attractive model for osteoarthritis research.

5.3 Figures

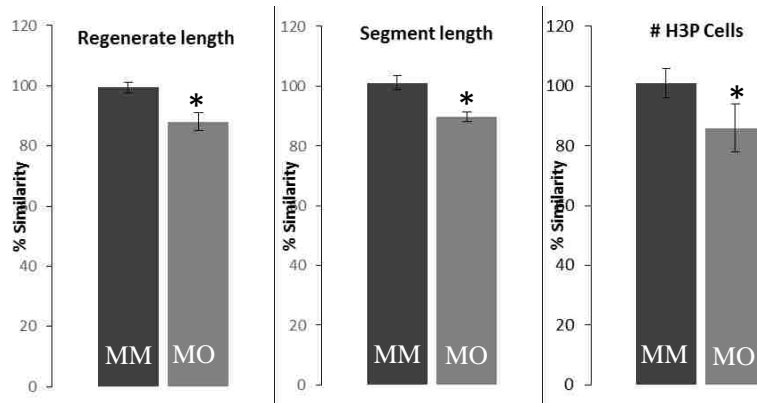


Figure 5.1: Double knockdown of *has2* and *acanb* contribute to Hapln1a phenotypes. Bar graph shows that regenerate length, segment length and cell proliferation is significantly reduced upon double knockdown. The mean of percent similarity for the MO treated experimental group and the corresponding MM treated control group were estimated and compared. Statistical significance was determined using the student's *t*-test ($P < 0.05$) and the error bars represent standard error of mean.



Figure 5.2: ISH for *rhamm*. In situ hybridization for the HA receptor *rhamm* in 5 dpa regenerating fins of WT, *sof*^{b123} and *alf*^{dty86}.



Figure 5.3: ISH for *sox9a* and *sox9b*. In situ hybridization showing the expression of the chondrogenic progenitors *sox9a* and *sox9b* in WT 5 dpa regenerating fins.

5.4 References

1. Govindan J, Iovine MK (2014) Hapln1a is required for connexin43-dependent growth and patterning in the regenerating fin skeleton. *PLoS One* 9: e88574.
2. Govindan J, Iovine MK (2015) Dynamic remodeling of the extra cellular matrix during zebrafish fin regeneration. *Gene Expr Patterns*.
3. Thorogood PV, Hinchliffe JR (1975) An analysis of the condensation process during chondrogenesis in the embryonic chick hind limb. *J Embryol Exp Morphol* 33: 581-606.
4. Kosher RA, Savage MP, Walker KH (1981) A gradation of hyaluronate accumulation along the proximodistal axis of the embryonic chick limb bud. *J Embryol Exp Morphol* 63: 85-98.
5. Singley CT, Solursh M (1981) The spatial distribution of hyaluronic acid and mesenchymal condensation in the embryonic chick wing. *Dev Biol* 84: 102-120.
6. Contreras EG, Gaete M, Sanchez N, Carrasco H, Larrain J (2009) Early requirement of Hyaluronan for tail regeneration in *Xenopus* tadpoles. *Development* 136: 2987-2996.
7. Calve S, Odelberg SJ, Simon HG (2010) A transitional extracellular matrix instructs cell behavior during muscle regeneration. *Dev Biol* 344: 259-271.
8. Li H, Schwartz NB, Vertel BM (1993) cDNA cloning of chick cartilage chondroitin sulfate (aggrecan) core protein and identification of a stop codon in the aggrecan gene associated with the chondrodystrophy, nanomelia. *J Biol Chem* 268: 23504-23511.

9. Wai AW, Ng LJ, Watanabe H, Yamada Y, Tam PP, et al. (1998) Disrupted expression of matrix genes in the growth plate of the mouse cartilage matrix deficiency (cmd) mutant. *Dev Genet* 22: 349-358.
10. Watanabe H, Kimata K, Line S, Strong D, Gao LY, et al. (1994) Mouse cartilage matrix deficiency (cmd) caused by a 7 bp deletion in the aggrecan gene. *Nat Genet* 7: 154-157.
11. Mercer SE, Cheng CH, Atkinson DL, Krcmery J, Guzman CE, et al. (2012) Multi-tissue microarray analysis identifies a molecular signature of regeneration. *PLoS One* 7: e52375.
12. Mercer SE, Odelberg SJ, Simon HG (2013) A dynamic spatiotemporal extracellular matrix facilitates epicardial-mediated vertebrate heart regeneration. *Dev Biol* 382: 457-469.
13. Tolg C, McCarthy JB, Yazdani A, Turley EA (2014) Hyaluronan and RHAMM in wound repair and the "cancerization" of stromal tissues. *Biomed Res Int* 2014: 103923.
14. Bourguignon LY, Singleton PA, Zhu H, Zhou B (2002) Hyaluronan promotes signaling interaction between CD44 and the transforming growth factor beta receptor I in metastatic breast tumor cells. *J Biol Chem* 277: 39703-39712.
15. Ghatak S, Misra S, Toole BP (2005) Hyaluronan constitutively regulates ErbB2 phosphorylation and signaling complex formation in carcinoma cells. *J Biol Chem* 280: 8875-8883.

16. Peterson RS, Andhare RA, Rousche KT, Knudson W, Wang W, et al. (2004) CD44 modulates Smad1 activation in the BMP-7 signaling pathway. *J Cell Biol* 166: 1081-1091.
17. Mailman ML, Dresden MH (1976) Collagen metabolism in the regenerating forelimb of *Notophthalmus viridescens*: synthesis, accumulation, and maturation. *Dev Biol* 50: 378-394.
18. Gulati AK, Zalewski AA, Reddi AH (1983) An immunofluorescent study of the distribution of fibronectin and laminin during limb regeneration in the adult newt. *Dev Biol* 96: 355-365.
19. Jiang D, Liang J, Noble PW (2007) Hyaluronan in tissue injury and repair. *Annu Rev Cell Dev Biol* 23: 435-461.
20. Casini P, Nardi I, Ori M Hyaluronan is required for cranial neural crest cells migration and craniofacial development. *Dev Dyn* 241: 294-302.
21. Li XY, Guo X, Wang LX, Geng D, Kang LL, et al. (2007) [Serum hyaluronic acid, tumor necrosis factor -alpha, vascular endothelial growth factor, NO, and Se levels in adult patients with Kashin-Beck disease]. *Nan Fang Yi Ke Da Xue Xue Bao* 27: 941-944.
22. Moffatt P, Lee ER, St-Jacques B, Matsumoto K, Yamaguchi Y, et al. (2011) Hyaluronan production by means of Has2 gene expression in chondrocytes is essential for long bone development. *Dev Dyn* 240: 404-412.

23. Turley EA, Noble PW, Bourguignon LY (2002) Signaling properties of hyaluronan receptors. *J Biol Chem* 277: 4589-4592.
24. Ton QV, Iovine M (2012) Semaphorin3d mediates Cx43-dependent phenotypes during fin regeneration. *Dev Biol* 366: 195-203.
25. Jazwinska A, Badakov R, Keating MT (2007) Activin-betaA signaling is required for zebrafish fin regeneration. *Curr Biol* 17: 1390-1395.
26. Munch J, Gonzalez-Rajal A, de la Pompa JL Notch regulates blastema proliferation and prevents differentiation during adult zebrafish fin regeneration. *Development* 140: 1402-1411.
27. Haas HJ (1962) Studies on mechanisms of joint and bone formation in the skeleton rays of fish fins. *Dev Biol* 5: 1-34.
28. Geraudie J, Landis WJ (1982) The fine structure of the developing pelvic fin dermal skeleton in the trout *Salmo gairdneri*. *Am J Anat* 163: 141-156.
29. Smith A, Avaron F, Guay D, Padhi BK, Akimenko MA (2006) Inhibition of BMP signaling during zebrafish fin regeneration disrupts fin growth and scleroblasts differentiation and function. *Dev Biol* 299: 438-454.
30. Avaron F, Hoffman L, Guay D, Akimenko MA (2006) Characterization of two new zebrafish members of the hedgehog family: atypical expression of a zebrafish indian hedgehog gene in skeletal elements of both endochondral and dermal origins. *Dev Dyn* 235: 478-489.

31. Padhi BK, Joly L, Tellis P, Smith A, Nanjappa P, et al. (2004) Screen for genes differentially expressed during regeneration of the zebrafish caudal fin. *Dev Dyn* 231: 527-541.
32. Johnson SL, Weston JA (1995) Temperature-sensitive mutations that cause stage-specific defects in Zebrafish fin regeneration. *Genetics* 141: 1583-1595.
33. Bhadra J, Iovine MK Hsp47 mediates Cx43-dependent skeletal growth and patterning in the regenerating fin. *Mech Dev*.
34. Watanabe H (2004) [Cartilage proteoglycan aggregate: structure and function]. *Clin Calcium* 14: 9-14.
35. Watanabe H, Yamada Y, Kimata K (1998) Roles of aggrecan, a large chondroitin sulfate proteoglycan, in cartilage structure and function. *J Biochem* 124: 687-693.
36. Kiani C, Chen L, Wu YJ, Yee AJ, Yang BB (2002) Structure and function of aggrecan. *Cell Res* 12: 19-32.
37. Wong M, Lawton T, Goetinck PF, Kuhn JL, Goldstein SA, et al. (1992) Aggrecan core protein is expressed in membranous bone of the chick embryo. Molecular and biomechanical studies of normal and nanomelia embryos. *J Biol Chem* 267: 5592-5598.
38. Spicer AP, Tien JY (2004) Hyaluronan and morphogenesis. *Birth Defects Res C Embryo Today* 72: 89-108.

39. Li J, Yoon ST, Hutton WC (2004) Effect of bone morphogenetic protein-2 (BMP-2) on matrix production, other BMPs, and BMP receptors in rat intervertebral disc cells. *J Spinal Disord Tech* 17: 423-428.
40. Grunder T, Gaissmaier C, Fritz J, Stoop R, Hortschansky P, et al. (2004) Bone morphogenetic protein (BMP)-2 enhances the expression of type II collagen and aggrecan in chondrocytes embedded in alginate beads. *Osteoarthritis Cartilage* 12: 559-567.
41. Quint E, Smith A, Avaron F, Laforest L, Miles J, et al. (2002) Bone patterning is altered in the regenerating zebrafish caudal fin after ectopic expression of sonic hedgehog and *bmp2b* or exposure to cyclopamine. *Proc Natl Acad Sci U S A* 99: 8713-8718.
42. Allen SP, Maden M, Price JS (2002) A role for retinoic acid in regulating the regeneration of deer antlers. *Dev Biol* 251: 409-423.
43. De Luca F, Uyeda JA, Mericq V, Mancilla EE, Yanovski JA, et al. (2000) Retinoic acid is a potent regulator of growth plate chondrogenesis. *Endocrinology* 141: 346-353.
44. Koyama E, Golden EB, Kirsch T, Adams SL, Chandraratna RA, et al. (1999) Retinoid signaling is required for chondrocyte maturation and endochondral bone formation during limb skeletogenesis. *Dev Biol* 208: 375-391.
45. Kirimoto A, Takagi Y, Ohya K, Shimokawa H (2005) Effects of retinoic acid on the differentiation of chondrogenic progenitor cells, ATDC5. *J Med Dent Sci* 52: 153-162.

46. Song HM, Nacamuli RP, Xia W, Bari AS, Shi YY, et al. (2005) High-dose retinoic acid modulates rat calvarial osteoblast biology. *J Cell Physiol* 202: 255-262.
47. Santamaria JA, Mari-Beffa M, Becerra J (1992) Interactions of the lepidotrichial matrix components during tail fin regeneration in teleosts. *Differentiation* 49: 143-150.
48. Suzuki T, Haga Y, Takeuchi T, Uji S, Hashimoto H, et al. (2003) Differentiation of chondrocytes and scleroblasts during dorsal fin skeletogenesis in flounder larvae. *Dev Growth Differ* 45: 435-448.
49. Kronenberg HM, Chung U (2001) The parathyroid hormone-related protein and Indian hedgehog feedback loop in the growth plate. *Novartis Found Symp* 232: 144-152; discussion 152-147.
50. Vortkamp A, Lee K, Lanske B, Segre GV, Kronenberg HM, et al. (1996) Regulation of rate of cartilage differentiation by Indian hedgehog and PTH-related protein. *Science* 273: 613-622.
51. Whitehead GG, Makino S, Lien CL, Keating MT (2005) fgf20 is essential for initiating zebrafish fin regeneration. *Science* 310: 1957-1960.
52. Tsutsumi S, Shimazu A, Miyazaki K, Pan H, Koike C, et al. (2001) Retention of multilineage differentiation potential of mesenchymal cells during proliferation in response to FGF. *Biochem Biophys Res Commun* 288: 413-419.

53. Ornitz DM, Marie PJ (2002) FGF signaling pathways in endochondral and intramembranous bone development and human genetic disease. *Genes Dev* 16: 1446-1465.
54. Iseki S, Wilkie AO, Heath JK, Ishimaru T, Eto K, et al. (1997) *Fgfr2* and osteopontin domains in the developing skull vault are mutually exclusive and can be altered by locally applied FGF2. *Development* 124: 3375-3384.
55. Sarkar S, Petiot A, Copp A, Ferretti P, Thorogood P (2001) FGF2 promotes skeletogenic differentiation of cranial neural crest cells. *Development* 128: 2143-2152.
56. Poss KD, Shen J, Nechiporuk A, McMahon G, Thisse B, et al. (2000) Roles for Fgf signaling during zebrafish fin regeneration. *Dev Biol* 222: 347-358.
57. Thummel R, Bai S, Sarras MP, Jr., Song P, McDermott J, et al. (2006) Inhibition of zebrafish fin regeneration using in vivo electroporation of morpholinos against *fgfr1* and *msxb*. *Dev Dyn* 235: 336-346.
58. Lee Y, Grill S, Sanchez A, Murphy-Ryan M, Poss KD (2005) Fgf signaling instructs position-dependent growth rate during zebrafish fin regeneration. *Development* 132: 5173-5183.
59. Poss KD, Shen J, Keating MT (2000) Induction of *lef1* during zebrafish fin regeneration. *Dev Dyn* 219: 282-286.

60. Petrella RJ (2005) Hyaluronic acid for the treatment of knee osteoarthritis: long-term outcomes from a naturalistic primary care experience. *Am J Phys Med Rehabil* 84: 278-283; quiz 284, 293.

61. Roughley PJ, Geng Y, Mort JS The non-aggregated aggrecan in the human intervertebral disc can arise by a non-proteolytic mechanism. *Eur Cell Mater* 28: 129-136; discussion 136.

Education

Ph.D Molecular Biology - 09/2010 to present
Lehigh University – PA (**GPA-3.99**)
Advisor: M Kathryn Iovine
Expected Graduation: Jan 2016

Master of Philosophy in Applied Microbiology, Dec 2003
Bharathiar University – India (**GPA-4.00**)

Master of Science in Industrial Microbiology, May 2002
University of Madras – India (**GPA-4.00**)

Bachelor of Science in Microbiology, May 2000
Bharathiar University – India (**GPA-4.00**)

Experience

Teaching Assistant - 09/2010 to 05/2015
Lehigh University - Bethlehem, PA
Instruct undergraduate and graduate students (lab courses) within the areas of cellular or molecular biology and biochemistry and provide guidance to students to plan and execute short term independent projects.
BioS 377: Biochemistry Laboratory
BioS 346: Molecular genetics Laboratory
BioS 196-010-SP12: SEA -HHMI sponsored Phage lab

Research Assistant - 01/2011 to 03/2012
Lehigh University - Bethlehem, PA
Project title: The role of the Fin protein in the switch from sigma F to sigma G in the developing *Bacillus subtilis* spore.

- Developed several Fin protein mutants of *B.subtilis* by site directed mutagenesis and check the effect of mutation by luciferase reporter assay.
- Epitope tagged Fin protein (Flag, His tags) for assaying by Western blot.

Trainee Microbiologist - 01/2005 to 01/2006
V.G.Hospital - Coimbatore, India

- Examine physiological, morphological, and cultural characteristics, using microscope, to identify and classify microorganisms in clinical samples.

- Isolate and maintain cultures of bacteria or other microorganisms in prescribed or developed media.
- Culture and Antibiotic sensitivity tests.
- Performance of rapid assay and Elisa technique for H-pylori, Anti-TB IgG & IgM, HCV, HBsAg, PSA and HIV.
- Turbimetric analysis of RA factor, ASO and CRP (Turbimetric analyzer-TULIP)
- Serological tests- WIDAL, RPR, ASO, Leptospiral antibody, Dengue IgG & IgM and demonstration of malarial parasite in peripheral blood.
- Exposure to usage of automated immunoassay analyzer (Mini VIDAS) for assay of hormones such as T3, T4, TSH, HCG

Faculty - 12/2003 to 12/2004

Sathyabama University - Chennai, India

- Courses taught: Basic Microbiological Techniques and Introduction to Molecular biology.
- Prepare course materials such as syllabi, homework assignments, and handouts and supervise undergraduate teaching, internship, and research work.
- Maintain student attendance records, grades, and other required records and advise students on academic and vocational curricula and on career issues.

Honors and Awards

1. Independent external research support awarded by National Academy of Science Grant-In-Aid of Research (GIAR) administered by Sigma Xi – October 2014.
2. Nemes Fellowship award, Lehigh University, Biological Sciences, Spring-Summer 2014. Awarded for outstanding research merit.
3. Personal interview, Sigma Xi - Meet your fellow companion – Jayalakshmi Govindan, published in 'American Scientist', 2014, Vol 102, Number 3, 240. Complete interview <https://www.sigmaxi.org/news/meet-your-fellow-companions/jayalakshmi-govindan>
4. Independent external research support awarded by National Academy of Science Grant-In-Aid of Research (GIAR) administered by Sigma Xi – March 2013.
5. Master of Science, University of Madras - Awarded University First Rank, 2002.
6. Bachelor of Science, Bharathiar University - Awarded University First Rank, Gold Medalist, 2000.

Manuscripts

1. **Govindan J**, Iovine MK. HA-Hapln1a ECM and Sema3d interact genetically to influence Cx43 dependent skeletal phenotypes during Zebrafish fin regeneration. (Submitted)
2. **Govindan J**, Iovine MK (2015) Dynamic remodeling of the extra cellular matrix during zebrafish fin regeneration. Gene Expression Patterns. doi:10.1016/j.gep.2015.06.001
3. **Govindan J**, Iovine MK (2014) Hapln1a Is Required for Connexin43-Dependent Growth and Patterning in the Regenerating Fin Skeleton. PLoS ONE 9(2): e88574.
4. Pope WH, Bowman CA, Russell DA, Jacobs-Sera D, Asai DJ, **Science Education Alliance Phage Hunters Advancing Genomics and Evolutionary Science (SEA-**

PHAGES), Phage Hunters Integrating Research and Education (PHIRE), Mycobacterial Genetics Course, Cresawn SG, Jacobos WR, Hendrix RW, Lawrence JG, Hatfull GF. (2015) Whole genome comparison of a large collection of mycobacteriophages reveals a continuum of phage genetic diversity. doi: 10.7554/eLife.06416 (*eLife*)

*** Co-author, Contributed as part of my Graduate Teaching Assistantship through a HHMI-sponsored course at Lehigh University**

Poster and Oral Presentations

1. Govindan J, Iovine MK. (Mar 2015). Dynamic remodeling of the extra cellular matrix during zebrafish fin regeneration. Mid-Atlantic SDB Regional Meeting, Princeton University, Princeton, NJ.
2. Govindan J, Iovine MK. (Nov 2014). Hapln1a is required for Cx43 dependent growth and patterning in the regenerating zebrafish fin. Mid-Atlantic Regional Zebrafish Meeting, Temple University, Philadelphia.
3. Govindan J, Iovine MK. (Jun 2014). Discerning the role of the HA-Hapln1a ECM in the regenerating fin skeleton. International Zebrafish Meeting, University of Madison, Wisconsin.
4. Govindan J, Iovine MK. (Feb 2014). Discerning the role of Hapln1a during skeletogenesis of the zebrafish fin & Tips on writing a successful Sigma Xi-GIAR proposal. Lehigh Chapter of Sigma Xi, Public Lecture and Reception. **(Oral)**
5. Govindan J, Iovine MK. (Dec 2013). Hapln1a is required for Cx43 dependent growth and patterning in the regenerating fin skeleton. Mid-Atlantic Regional Zebrafish Meeting, UMBC, Baltimore. **(Oral)**
6. Govindan J, Iovine MK. (Aug 2013). Hapln1a and Sema3d interact genetically to influence Cx43 dependent skeletal phenotypes during Zebrafish fin regeneration. Frontier Bioscience Young Researchers 2013 Retreat, Osaka University, JAPAN. Abstract No. 42
7. Govindan J, Iovine MK. (Apr 2013). Elucidating the role of Hapln1a during skeletal patterning in regenerating caudal fin. Mid-Atlantic SDB Regional Meeting, Virginia.

References

Dr. M. Kathryn Iovine
Associate Professor
Dept. of Biological Sciences
111 Research Drive, B217
Bethlehem, PA 18015
Phone: 610-758-6981
Email: mki3@lehigh.edu

Dr. Michael Kuchka,
Associate Professor

Dept. of Biological Sciences
111 Research Drive, B220
Bethlehem, PA 18015
Phone: 610-758-3687
Email: mrk5@lehigh.edu

Dr. Jutta Marzillier,
Adjunct Professor
Cedar Crest College, PA
Phone: 484-707-5677
Email: jmarzillier@gmail.com